SUITABILITY OF BIOFUELS AND PLASTIC OIL BLENDED WITH DIESEL IN CRDI ENGINE

Thesis
Submitted in partial fulfillment of the requirements for the Degree of

DOCTOR OF PHILOSOPHY

by

VENKATESH T. LAMANI

DEPARTMENT OF MECHANICAL ENGINEERING
NATIONAL INSTITUTE OF TECHNOLOGY KARNATAKA,
SURATHKAL, MANGALORE – 575025
OCTOBER, 2017

SUITABILITY OF BIOFUELS AND PLASTIC OIL BLENDED WITH DIESEL IN CRDI ENGINE

Thesis

Submitted in partial fulfillment of the requirements for the Degree of

DOCTOR OF PHILOSOPHY

by

VENKATESH T. LAMANI

Under the guidance of

Dr. AJAY KUMAR YADAV   **Dr. KUMAR G. N.**

DEPARTMENT OF MECHANICAL ENGINEERING
NATIONAL INSTITUTE OF TECHNOLOGY KARNATAKA,
SURATHKAL, MANGALORE – 575025
OCTOBER, 2017

DECLARATION

I hereby declare that the research thesis entitled **"SUITABILITY OF BIOFUELS AND PLASTIC OIL BLENDED WITH DIESEL IN CRDI ENGINE"** which is being submitted to the **National Institute of Technology Karnataka, Surathkal** in partial fulfillment of the requirements for the award of the degree of **Doctor of Philosophy** in **Mechanical Engineering** is a *bonafide report of the research work carried out by me*. The material contained in this research thesis has not been submitted to any other Universities or Institutes for the award of any degree.

Register Number: **135023ME13F11**

Name of the Research Scholar: **VENKATESH T. LAMANI**

Signature of the Research Scholar:

Department of Mechanical Engineering

Place: NITK, Surathkal

Date:

CERTIFICATE

This is to certify that the research thesis entitled **"SUITABILITY OF BIOFUELS AND PLASTIC OIL BLENDED WITH DIESEL IN CRDI ENGINE"** submitted by **Mr. VENKATESH T. LAMANI (Register Number: 135023ME13F11)** as the record of the research work carried out by him, *is accepted as the research thesis submission* in partial fulfillment of the requirements for the award of the degree of **Doctor of Philosophy.**

Dr. AJAY KUMAR YADAV   **Dr. KUMAR G. N.**

Research Guide   Research Guide

Date: Date:

Chairman, DRPC

Date:

Dedicated

to

My Beloved Parents

and

Teachers

GURUVANDANA

I consider myself on extremely fortunate student of **Dr. Ajay Kumar Yadav** and **Dr. Kumar G.N.** Their unstinted support, motivation & immaculate guidance enabled me to overcome all the impediments during my research work. I would like to place my profound gratitude & respectful salutations to them for introducing me to the fascinating area of CFD and internal combustion engine technology & imbibing in me a sense of utmost self-confidence and academic discipline. Their unrestrained trail of original ideas and sustained encouragement in all research work pursuits was all highly refreshing & stimulating experience .Which will be cherished by me throughout my life.

ACKNOWLEDGMENT

ABSTRACT

Nitrogen oxides and smoke are the substantial emissions for the diesel engines. Fuels comprising high-level oxygen content can have low smoke emission and higher efficiency due to better combustion. The objective of this research is to assess the potential to employ oxygenated fuels such as dimethyl ether, ethanol and butanol, and waste plastic oil in direct injection engine as alternative fuels for diesel. To reduce NO_X, exhaust gas recirculation technology for various fuels is studied. Computational fluid dynamics (CFD) studies on combustion and emission characteristics of common rail direct injection (CRDI) engines using oxygenated fuel-diesel blends are less developed and still under intense study. In view of that detailed CFD simulation is carried out in present study and also validated with experimental results.

Ethers are favourable alternative for diesel engine due to their chemical structure. Presence of more oxygen, absence of carbon-carbon (C-C) bond in chemical structure, and high cetane number of dimethyl ether (DME), cause less pollution in DME operated engine compared to diesel engine. Study emphasizes the effect of various EGR rates (0-20%) and DME-diesel blends (0-20%) on combustion characteristics and exhaust emissions of CRDI engine using CFD simulation. Results show that, due to better combustion characteristics of DME, indicated thermal efficiency (ITE) increases with the increase in DME- diesel blends.

Ethanol is an attractive alternative fuel because it is oxygenated, renewable and bio-based resource; thereby it has potential to reduce smoke emissions in compression-ignition engines. CFD simulation is carried out to study the effect of EGR and injection timing on the performance, combustion and exhaust emission characteristics of CRDI engine fuelled with bioethanol-diesel blends. The results indicate that the mean CO formation and ignition delay increase whereas mean NO_X formation and in-cylinder temperature decrease with increase in the EGR rate. Further, CFD simulation is carried out to find optimum injection timing for bioethanol-diesel blends (0-30% ethanol). Optimum injection timing is obtained for maximum ITE. Obtained CFD results are validated with experimental data available in literature and found good agreements.

Several second generation biofuels (e.g., n-butanol) are also promising alternative to diesel fuel. The experimental and CFD simulation is carried out to estimate the performance, combustion and exhaust emission characteristics of n-butanol-diesel blends (0 to 30%) for various injection timings and various EGR rates using modern twin-cylinder, four-stroke, CRDI engine. Experimental results reveal the increase in brake thermal efficiency (BTE) for n-butanol-diesel blends.

Attention is also focused to counter plastic waste disposal problem and to find alternate fuel to diesel by waste to energy retrieval. Present range of investigation evaluates the prospective use of waste plastic oil (WPO) as an alternative fuel for diesel engine. Experiments are conducted for various injection timings and for different EGR rates. Combustion, performance and tail pipe emissions of CRDI engine are studied. The NOx, CO and soot emissions for waste plastic oil-diesel blends are found more than neat diesel. To reduce NOx, EGR is employed which results in reduction of NOx considerably. Brake thermal efficiency (BTE) of blends is found to be higher compared to diesel. The higher NOx emitted by engine operated with WPO-Diesel blends are treated by multiple injection strategies. Experiments are carried out for various pilot injection timings and different main injection timings. The remarkable reduction in nitrogen oxide is observed by retarding main injection timing and injecting more fuel in pilot injection compared to single injection.

Key words: CRDI, EGR, CFD, Biofuel, Waste Plastic Oil, Combustion, Emission

CONTENTS **Page No.**

NOMENCLATURE

ATDC	After top dead centre
BTDC	Before top dead centre
B.S	Bharat stage
bsfc	Brake specific fuel consumption
BTE	Brake thermal efficiency
Bu	Butanol
CFD	Computation fluid dynamics
CO	Carbon monoxide
CI	Compression ignition
CPCB	Central pollution control board
CRDI	Common rail direct injection
DEE	Diethyl ether
DF	Diesel fuel
DOC	Diesel oxidation catalyst
DPF	Diesel particulate filter
D_t	Diffusion coefficient
E_a	Activation energy
ECFM3Z	Extended coherent flame model three zone
ECU	Electronic control unit
EDU	Electronic driver unit
EGR	Exhaust gas recirculation
EGT	Exhaust gas temperature
EVC	Exhaust valve closing
EVO	Exhaust valve opening
F	Correction factor
FIP	Fuel injection pressure
FTIR	Fourier Transform Infrared spectroscopy

HC	Hydrocarbon
HRR	Heat release rate
IDI	Indirect injection
IMAP	Intake manifold air pressure
IMAT	Intake manifold air temperature
IVC	Inlet valve closing
IVO	Inlet valve opening
LNT	Lean NO_X trap
$M_{air + EGR}$	Mean molar mass of the unmixed air + EGR gases
M_{Fu}	Molar mass of fuel
M_{Fu}	Molar mass of fuel
M^M	Mean molar mass of the gases in the mixed area
M_{NO}	molar mass
NHR	Net heat release
NO_2	Nitrogen dioxide
NO_X	Nitrogen oxides
P30	70% diesel + 30% waste plastic oil (volume basis)
P50	50% diesel + 50% waste plastic oil (volume basis)
PCV	Pressure control valve
PM	Particulate matter
ppm	Parts per million
ppmv	Parts per million per volume
PVC	Polyvinyl chloride
q	Heat flux
R	Universal gas constant
RME	Rapeseed oil methyl ester
rpm	Revolutions per minute
S_c and S_{ct}	Laminar and turbulent Schmidt numbers
SFC	Specific fuel consumption

SOI	Start of injection
SO_x	Sulphur oxides
T	Absolute temperature
TDC	Top dead centre
u	Velocity vector
UBHC	Unburned hydrocarbons
V_k	Diffusive velocity of the kth species
VGT	Variable-geometry turbochargers
VVT	Variable valve timing
WPO	Waste plastic oil
Y_k	Species concentration of kth species

Greek letters

$\tilde{\dot{E}}_{Fu}^{F\to M}$	Unmixed fuel source term
$\tilde{\dot{E}}_{O_2}^{A\to M}$	Unmixed oxygen source term
$\bar{s}_{NO}$	Mean nitric oxide source term
$\tilde{u}$	Density-weighted average velocity
$\bar{\dot{\omega}}_x$	Average combustion source term
ζ	Transformed coordinate system
$\left.\bar{\rho}^u\right|_u$	Density of the unburned gases
ϕ_s	Soot mass fraction
$\bar{\rho}$	Reynolds averaged fuel density
$\tilde{Y}_{NO}$	Mean mass fraction of NO_x
x_i	Cartesian coordinates
$\dfrac{dc_{NO\ prompt}}{dt}$	Prompt mechanism
$\dfrac{dc_{NO\ thermal}}{dt}$	Thermal mechanisms

$\tilde{Y}_x$	Averaged mass fraction of species x
$\bar{\rho}$	Mean density
$\tilde{Y}_{O_2}^{\infty}$	Oxygen mass fraction
$\tilde{Y}_{TO_2}$	Oxygen tracer
$\tilde{Y}_{TFu}$	Fuel tracer
ε	Dissipation rate
ϕ	Equivalence ratio
μ	Dynamic viscosity
τ_d	Ignition delay
τ_m	Mixing time
μ_t	Turbulent viscosity
ρ	Density
ω_k	Production rate of the kth species

CHAPTER 1

INTRODUCTION

1.1 Background

Energy has been globally recognized as one of the most supreme inputs for socio-economic development. There is a firm correlation between economic growth and energy consumption. On one hand, growth of an economy with its universal competitiveness hinges on the availability of cost-effective and environmentally benign energy sources, and on the other hand, the level of economic growth has been witnessed to be reliant on the energy demand. Strong growth prospects for the Indian economy will drive energy demand across different sectors, although the energy consumption per capita (per industry estimates) is one-third of the global average. Hence, access to adequate and reliable sources of energy becomes vital, particularly when one-quarter of the population lacks access to electricity**.**

India is the third-largest importer of crude oil after the United States and China and continues to rely largely on imports. Over the last four years, import volumes grew modestly from 240 billion litres to 278 billion litres as shown in Fig 1.1. Additionally, India is the fourth largest consumer of primary energy at 24.9 quadrillion British thermal unit (BTU) following China, United States and Russia. It is also the eighth largest energy producer at 14.18 quadrillion BTU. As a result, despite notable fossil fuel resources, India is increasingly dependent on energy imports (Aradhey 2017). Fig 1.2 shows the India crude oil imports sources during 2015. Dependence on imported crude oil has led Indian energy companies to diversify their supply sources (EIA report 2016). To this end, Indian national oil companies have purchased equity stakes in overseas oil and natural gas fields in South America, Africa, Southeast Asia, and the Caspian Sea region to acquire reserves and production capability. However, most crude oil is imported from the Middle East, where Indian companies have little direct access to investment.
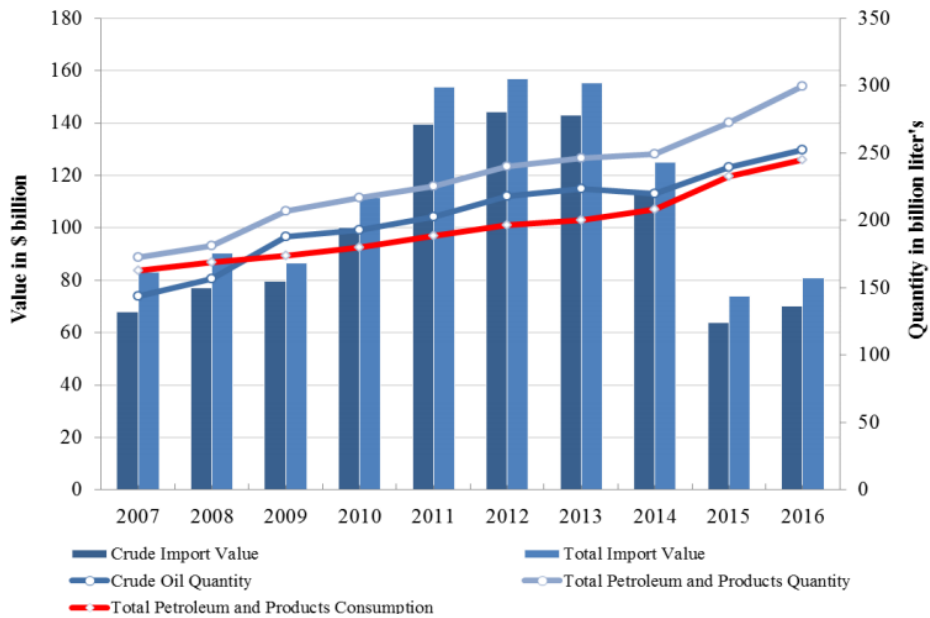
Fig. 1.1 India: Import of crude oil, petroleum products and consumption
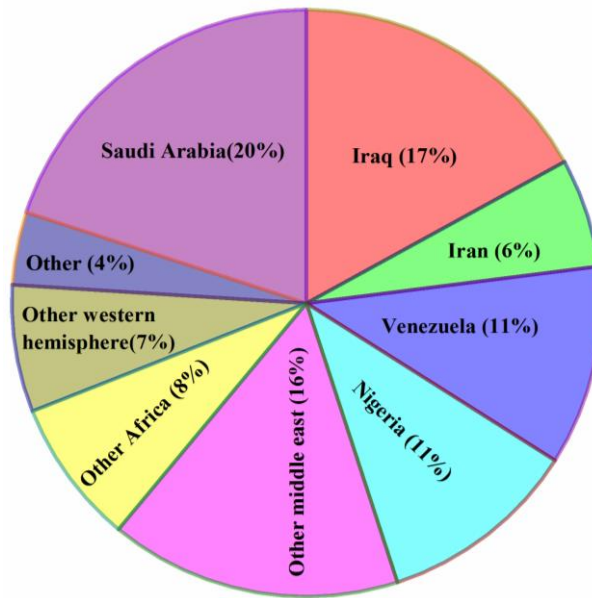
Fig. 1.2 India crude oil imports from different countries in 2015

(Courtesy: EIA report 2016, Country Analysis Brief: India)

(http://www.eia.gov/countries/analysisbriefs/India/india.pdf)

At present, about two-thirds of global energy demand is met by liquid fossil fuels because of their accessibility and suitability of use in present design of several prime movers such as internal combustion engines (Lakshminarayanan and Aghav 2010). It is well known fact that fossil fuels are exhaustible in nature and depleting very fast in worldwide. Hence, finding alternate fuel which satisfies stringent emission regulations and substitutes fossil fuel resources presently is inevitable for internal combustion engines. The prominent alternative fuel for diesel engine on which research is going on at present includes Ethers (Dimethyl ether), Alcohols (Ethanol, Butanol), Plastic oil etc.

1.2 Fuel injection system of common rail direct injection (CRDI) engine

With growing application of diesel engine, there are some limitations in the conventional fuel injection system. They are cam driven and injection pressure is proportional to engine speed. In general, it means that the peak injection pressure can only be attained at the highest engine speed, and maximum attainable injection pressure drops as engine speed decreases. CRDI engine is broadly accepted design for diesel engines in recent years. With CRDI technology a lesser fuel is consumed in view of the fact that the fuel inside the common rail is set at ultra-high pressure which helps for better atomization of fuel which results in improved mixing with air enhancing the combustion.

In common rail systems, a high-pressure pump accumulates fuel at elevated pressure. The term common rail implies that all of the fuel injectors are distributed by a common rail which acts as a pressure accumulator where the fuel is collected at high pressure. This accumulator consists of multiple injectors which inject fuel with high-pressure into the combustion chamber. The fuel injectors are controlled by electronic control unit (ECU) as shown in Fig 1.3. Since the injectors are electrically activated, the injection pressure remains constant from beginning to the end of the combustion process which is closer to the pressure in the common rail (accumulator). If the

accumulator, pump and plumbing are sized properly, the injection pressure and rate will be the same for each of the multiple injection events also.
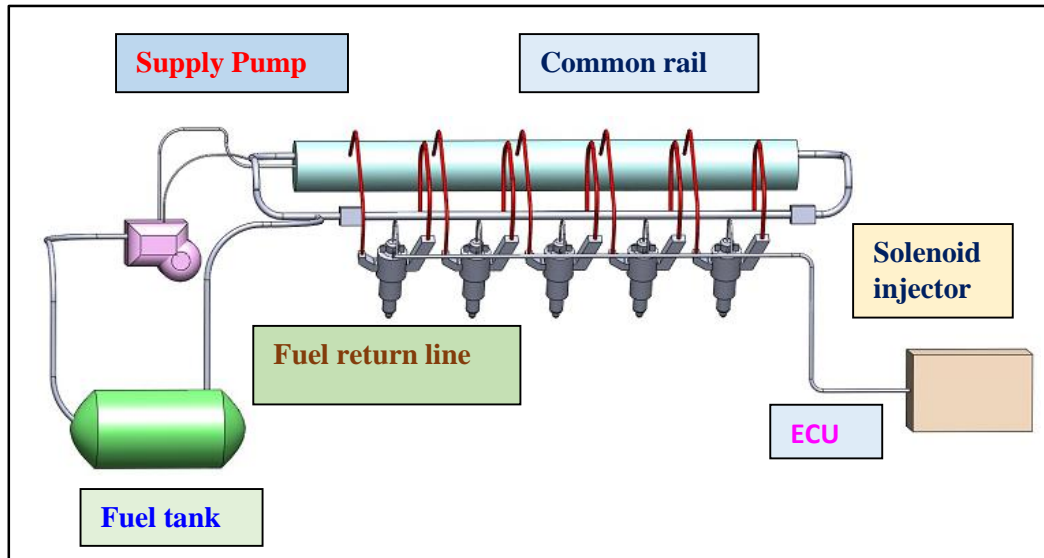
Fig.1.3 Schematic diagram of CRDI technology

Higher injection pressures with finer sprays, smaller fuel orifice sizes and sac volume, flexible injection timing, multiple injection, exhaust gas recirculation and electronic control unit are the main features of modern direct injection engines. The modern direct injection engines are compact, reliable, smooth and sturdy.

Advantages:

- High injection pressures around 10-15 times higher than conventional direct injection systems.
- Better fuel atomization throughout the injection duration to a constant rail pressure.
- Exact choice of injection timing and duration due to electronic controls.
- Pilot injection flexibility (reduce noise, particulates and NO_x emissions).
- Reduced need for swirl intensity at low engine speed due to high turbulence energy of the spray.

4

Disadvantages:

It is expensive than the conventional diesel engine. The list also comprises high degree of engine maintenance and expensive spare parts.

1.3 Emission norms in India

Bharat stage emission standards (BSES) are introduced by the Government of India (GOI) to regulate the output of air pollutants from internal combustion (IC) engines. The standards and the timeline for execution are regulated by the Central Pollution Control Board (CPCB) under the Ministry of Environment and Forests and climate change of GOI.

The standards based on European regulations were first introduced in 1991. Progressively stringent norms have been implemented since then. All new vehicles manufactured after the implementation of the norms have to be compliant with the regulations. Since October 2010, Bharat Stage (BS) III norms have been enforced across the country. In 13 major cities, Bharat Stage IV emission norms have been in place since April 2010 and it will be imposed for whole country from April 2017. In 2016, the Indian government announced that the country would elude the BS-V norms altogether and adopt BS-VI norms by 2020.

While the emission norms result in control of pollution levels, it also invariably increases vehicle cost due to the improved technology and higher fuel prices. However, the increase in private cost is offset by savings in health costs for the public, as there is lesser amount of disease causing particulate matter and pollution in the air. Exposure to air pollution can lead to respiratory and cardiovascular diseases, which caused 6.2 lakh early deaths in 2010, and the health maintenance cost due to air pollution in India has been assessed at 3% of its GDP. The emission standards of passenger vehicles are listed in Table 1.1.

Table 1.1: Indian emission standards for diesel vehicle (Bansal & Bandivadekar 2013).

Emission standard	Date	CO (g/km)	HC + NOx (g/km)	NOx (g/km)	PM (g/km)
India stage I	2000	2.72-6.9	0.9-1.7	-	0.14-0.25
Bharat Stage II[a]	2001	1-1.5	0.7-1.2	-	0.08-0.17
Bharat Stage III[b]	2005	0.64-0.95	0.56-0.86	0.5-0.78	0.05-0.10
Bharat Stage IV[c]	2010	0.54-0.74	0.3-0.46	0.25-0.39	0.025-0.06

[a] From April 1, 2000, in Delhi; January 1, 2001, in Mumbai; July 1, 2001, in Kolkata and Chennai; April 1, 2003, in Bangalore, Hyderabad, Ahmedabad, Pune, Surat, Kanpur, and Agra; April 1, 2005, in the rest of the country.

[b] From April 1, 2005, in Delhi, Mumbai, Kolkata, Chennai, Bangalore, Hyderabad, Ahmedabad, Pune, Surat, Kanpur, and Agra; April 1, 2010, in the rest of the country.

[c] From April 1, 2010, in Delhi, Mumbai, Kolkata, Chennai, Bangalore, Hyderabad, Ahmedabad, Pune, Surat, Kanpur, and Agra.

1.4 Need of alternative fuels

In the entire world, 85% of energy consumed for daily needs is obtained from the fossil fuels (coal, petroleum, and natural gas). However excessive consumption of fossil fuels consequence in the release of pollutants into the atmosphere and water resources eventually causing health problems as well as destruction of ecosystem. It will also create scarcity of fuel in near future due to its non- renewability. Such potential challenges and environmental damages create enormous concern on the development and utilization of alternative fuel sources or renewable energy sources. Various governments including India promoted the use of biofuels in energy sectors. In India, it has been widely introduced to Indian Railways as a parallel fuel in most of the CI

engine, also government took further step to motivate producers of such crops yielding biofuels. The key advantages of adopting the alternatives fuels are promising substitution for conventional fuel with lower emissions. By 2022, the Government of India (GOI) has planned to reduce its dependence on crude oil imports by 10% which can be achieved by increasing domestic output, promoting energy efficiency and conservation, and encouraging greater use of alternative fuels.

The benefits of using alternative fuels can be attributed to the following aspects:

- Pursuing energy sustainability through the comprehensive usage of alternative fuels derived from renewable energy sources and mitigating the apprehensions of limited fossil fuel energy.
- Improving engine efficiency and exhaust emissions with the aid of superior physical or chemical properties of alternative fuels compared to diesel.
- Relieving the unbalanced usage of conventional petroleum-based fossil fuels.
- Creates new employment opportunities in all geographical locations.
- Attract private and public investment.
- Improvement in rural income and employment generation, small-agricultural land holders could get more benefit through cooperatives.

Technologies for biomass-to-biofuel conversion are also under various stages of development. Though biomass is cheap, the costs of its processing are relatively higher. Once these challenges are overcome, alternative fuel sources will ultimately deliver inexpensive and endless energy.

1.5. Selection of fuel

Exploring alternate fuel which satisfies stringent emission regulations and substitutes fossil fuel resources for internal combustion (IC) engines is a great challenge for researchers. This research assesses the potential to employ oxygenated fuel (dimethyl ether (DME), ethanol and butanol) and waste plastic oil in direct injection engine to find alternative fuels for diesel. Along with suitability of alternate fuel, presence of chemical

bond in fuel also plays an important role during charge formation. The C-O bond energy is lower compared to C-H bond energy. Therefore, C-O bonds in fuel break more easily compared to the C-H bonds. The binding energy of various oxygenated fuels is listed in Table 1.2.

1.5.1. DME as alternative fuel

DME has been produced worldwide in quantities of 100,000-150,000 tonnes per annum from 1996 or earlier (Verbeek et al. 1996; Arcoumanis 2000) and is used as a propellant for spray cans in cosmetics instead of chloro-fluoro-carbons (CFC). It can be produced from carbonaceous feedstock, both from fossil fuels like natural gas and renewable sources like wood. Its production method most closely resembles that of methanol. De-hydrogenation of methanol and direct conversion from synthesis gas (syngas) are methods to produce DME (Mills 1994).

Table 1.2: Bond characteristics of butanol, DME and ethanol (Park et al. 2014)

| Bond Type | Binding energy (BE) (kJ/mol) | Number of bonds | | |
		Butanol	Ethanol	DME
C-C	357.7	4	1	0
C-H	410.4	9	5	6
C-O	359.0	1	1	2
O-H	452.8	1	1	0
BE (kJ/mol)		5,936.8	3,221.5	3180.4

DME properties: The key properties of DME and diesel fuel (Arcoumanis et al. 2008) are shown in Table 1.3 (Kapus et al. 1995; Sorenson et al. 1998). DME has low carbon-to-hydrogen ratio with a chemical formula of CH_3-O-CH_3. In gaseous state it is invisible under standard atmospheric conditions. When it is pressurized above 0.5 MPa, it condenses to the liquid phase. Gaseous DME is denser than air while liquid DME has a density two thirds that of water. The vapour pressure is similar to that of LPG and requires the same handling and storage precautions. It dissolves in water up to 6% by mass. However, it is not compatible with most elastomers due to its corrosiveness, so

that careful selection of materials is necessary to prevent deterioration of seals after prolonged exposure to DME. DME displays a visible blue flame when burning over a wide range of air-fuel ratios, similar to natural gas, which is an important safety characteristic. Nevertheless, the operation of DME combustion system needs the adoption of rigorous procedures for safe operation due to the wide flammability limits. The importance of the properties of DME can be identified by examining its advantages and disadvantages as a candidate fuel for replacing diesel fuel in compression-ignition (CI) engines.

Table 1.3: Properties of diesel, n-butanol DME and ethanol

Fuel properties	Diesel fuel	n-Butanol	DME	Ethanol
Density at 20°C (kg/m^3)	835	809.7	606	790
Cetane number	52	25	55-66	8
Lower calorific value (MJ/kg)	42.49	33.09	27.6	26.95
Kinematic viscosity at 40°C (mm^2/s)	2.72	2.22	0.131	1.4
Boiling point (°C)	180-360	117.5	-23	78
Latent heat of evaporation (kJ/kg)	270-375	581.4	410	840-880
Oxygen (% weight)	0	21.59	34.8	34.8
Carbon (% weight)	86.13	64.82	52	52
Hydrogen (% weight)	13.87	13.49	13	13
Stoichiometric air–fuel ratio	14.62	11.19	9.06	9.06
Molecular weight	211.7	74.12	46	46
Self-ignition temperature (ºC)	254-300	345	235	365

Advantages:

(i) High oxygen content: Together with the absence of any C-C bonds it is responsible for its smokeless combustion; low formation and high oxidation rates of particulates would therefore be expected under CI engine operation.

(ii) Low boiling point: It leads to quick evaporation when a liquid-phase DME is injected into the engine cylinder.

(iii) High cetane number: DME results in instantaneous vaporization due to low auto-ignition temperature. Teng et al., (2001) examined the high cetane number (>55) of DME from the viewpoint of its thermochemical characteristics. Its critical temperature, 400 K (127 ℃) is lower than the compressed air temperature at the later stages of the compression stroke, which allows the DME injected into the cylinder to evaporate immediately. When the temperature of DME is higher than 400 K, it becomes superheated vapour and no evaporation is associated with the mixing.

Disadvantages:

(i) Low combustion enthalpy

(ii) Low modulus of elasticity

(iii) DME Toxicity: The current literature provides sufficient information to assess the potential impacts of DME to human and ecological receptors. DME has a low order of toxicity on both an acute and chronic basis. The main physiological action of DME is that of "weak anesthesia" when inhaled at high levels. DME is extremely stable chemically and is essentially an inert chemical substance (Tier 2015).

(v) Retrofitting of fuel-injection system: The features of a fuel-injection system for DME and the characteristics of the flow in the injector nozzle are different from those for diesel fuel due to the different physical and chemical properties. Characteristics features of appropriate fuel-injection system for DME are summarized below.

Features of the fuel-injection system:

Closed pressurized fuel system: Since DME exists in gas phase under standard atmospheric conditions, it must be pressurized in a fuel system including a storage tank, and handled like a liquefied gas.

Cavitation in the fuel-injection system: The high vapour pressure of DME may cause cavitation, which may prevent stable fuel-injection operation (Arcoumanis 2000).

Low injection pressure: DME gasifies immediately during injection, due to its low boiling point, even though it is injected as a liquid.

Leakage: Due to its low viscosity, conventional fuel-injection systems are not suitable for DME due to leakage problems (Yu and Bae 2003).

Low lubricity: The lower lubricity of DME than that of diesel fuel leads to wear problems (Verbeek et al.1996).

Long injection period: The low liquid density and low calorific value require a higher volume of DME to be injected into the cylinder, compared with that for diesel fuel. In particular, 1.8 times the volume of diesel fuel is needed (to supply the same amount of energy) which necessitates a longer injection period and advanced injection timing.

Higher compression work: The compression work of the fuel pump for DME will always be higher than that for diesel fuel, because DME has lower density and higher compressibility than diesel (Teng et al. 2001).

1.5.2 Alcohol as alternative fuel

Unlike conventional gasoline and diesel, the alcohols are alternative oxygenated fuels. Compared to diesel, alcohols have less combustion energy. However, the lowest stoichiometric air to fuel ratio helps alcohol fuels to produce more power inside an engine when these fuels are burnt. Alcohol fuels show a better tendency to decrease IC engine emissions because of less carbon and sulphur content and more oxygen content (Lapuerta 2008) compared to diesel. Alcohol fuels such as methanol, ethanol, propanol and butanol etc. can be used with fossil-based fuels in various percentages for diesel engines as a clean alternative fuel source.

Ethanol as alternative fuel:

Bioethanol can be produced from agricultural products such as sugarcane, corn, sugar beet, molasses, cassava root, and barley by alcoholic fermentation process. The global ethanol production is 8.46×10^{10} liters per year.

Table 1.4: Potential feedstock for ethanol production (Zabed et al. 2017)

Sugary biomasses	Starchy crops	Lignocellulosic biomass
Sugarcane (Saccharum officinarum), Sweet sorghum (Sorghum bicolor), Sugar beet (Beta vulgaris), Watermelon (Citrullus lanatus), Dates (Phoenix dactylifera), and Molasses.	Corn (Zea mays), Wheat (Triticum aestivum), Cassava (Manihot esculenta), Barley (Hordeum vulgare), Canna (Canna edulis), Sweet potato (Ipomoea batatas), Potato (Solanum tuberosum), Yam (Dioscorea rotundata), Jerusalem artichoke (Helianthus tuberosus), Iles-iles (Amorphophalus campanulatus), Oat (Avena sativa), and Banana (Musa sp.)	Perennial grasses, aquatic plants, agricultural residues, forest biomass and waste and municipal solid waste (MSW), corn stover, corn cob, wheat straw, rice straw, sugarcane bagasse, sweet sorghum bagasse, barley straw, pine (soft wood), yellow poplar (hard wood), water hyacinth, switchgrass, cocksfoot grass (Dactylis glomerata).

Ethanol-blended fuel is widely used in Brazil, United States, and Europe. The basic steps for production of ethanol are yeast fermentation of sugars, distillation, dehydration and denaturing (Aradhey 2017). An estimated 1.65 billion liters of ethanol will be produced in 2017, almost 20 percent less than last year. Theoretically, the ethanol available is sufficient to meet the 5 percent blend target, but demand rationing, particularly from potable and industrial sectors, will limit ethanol market penetration close to 2 percent. Industry sources

indicate that the OMCs may procure additional 700 million liters in 2017. The main properties of ethanol are listed in Table 1.3 (Labeckas et al. 2014). The key feedstock for ethanol fermentations are recorded in Table 1.4. Bioethanol is a low cost oxygenate with high oxygen content of 34% by weight. Bioethanol is safer for transportation and storage due to its higher auto-ignition temperature than that of diesel (Furey et al. 1991;Naegeli et al.1997).

Advantages of Ethanol:

- Exhaust gases of ethanol are much cleaner, it burns more cleanly.
- High oxygen contains.
- Safer for transportation.
- Ethanol is considered as a renewable resource.
- It reduces the greenhouse gases.

Disadvantages of Ethanol:

The key obstacles to use bio-ethanol-diesel blends in diesel engine are as follows:

- Ethanol has limited solubility in diesel fuel. Phase separation and water tolerance in ethanol-diesel blend fuel are crucial problem.
- Ethanol fuel has low cetane number, whereas the diesel engine prefers high cetane number fuel.
- The viscosity of ethanol is lower than that of the diesel fuel, so that the lubricity is an additional concern of ethanol-diesel blend.
- Biodiversity: A large amount of land is required to grow crops, this could destroy some natural habitats.
- The food vs fuel debate: Due to lucrative prices of bioethanol, farmers start the production of biofuel which increases food price around the world.
- Carbon emission: When all elements are taken into consideration, during the production process of bioethanol a huge amount of CO_2 is released which makes ecological effectiveness close to zero.
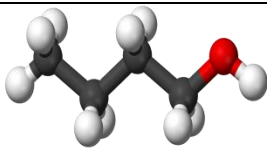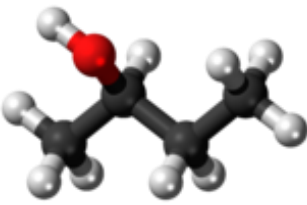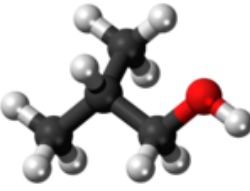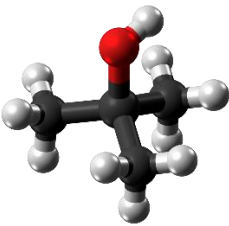
- Transportation: Ethanol is hygroscopic, and absorbs water from air thus has corrosion aggressiveness.

n-butanol as alternative fuel:

Butanol is one of the primary alcohol category which has more advantages (properties are close to diesel) than ethanol and methanol as an alternative fuel for diesel engine. Butanol has a lower auto-ignition temperature than methanol and ethanol. Therefore, butanol can be ignited easier when burned in diesel engines. Besides, butanol is less evaporative and releases more energy per unit mass than ethanol and methanol. Butanol has also a higher cetane number than ethanol and methanol, thus make it more suitable additive for diesel fuel (Szwaja et al. 2010). Ethanol, which is highly miscible with gasoline is however less miscible with diesel over a wide range of conditions. On the other hand, butanol has a higher miscibility factor with high stable characteristics in diesel without phase separation (Dogan 2011).

The different structure of butanol isomers have a direct impact on the physical properties of the biofuel (Wallner et al. 2009). It exists in the form of different isomers based on the location of the hydroxyl (OH) group and carbon chain structure. These are 1-butanol (n-butanol), 2-butanol (secondary butanol), iso-butanol and tert-butanol. The 1-butanol is a straight-chain structure with the alcohol (OH) at the terminal carbon. The 2-butanol has the hydroxyl group at an internal carbon. Iso-butanol is a branched isomer with the OH group at the terminal carbon and tert butanol refers to the branched isomer with the OH group at an internal carbon. All the above mentioned form of isomers and their some main application are described in Table 1. 5. n-butanol, iso-butanol and tert-butanol can be utilized as fuel additives, but n-butanol is the most favorable since it can be easily mixed with gasoline and diesel. (Jin et al. (2011); Chen et al. (2009); Dernotte (2010); Liu 2013).

Table 1.5: Butanol isomers: structures and applications

Butanol isomer	Molecular structure	Application
1-butanol (n-butanol)		i. Fuel additives ii. Solvents (paint industry)
2-butanol (Sec-butanol)		i. Domestic cleaning agent ii. Perfumes and artificial flavours iii. Industrial cleaner
Iso-butanol		i. Fuel additives ii. Solvents (paint industry) iii. Ink agent
Tert-butanol		i. Fuel additives ii. Paint remover iii. Octane booster

Butanol can be produced by alcoholic fermentation of the biomass feedstock such as algae, corn, and other plant materials containing cellulose that could not be used for food (Dogan 2011). Due to the low production of butanol, many research groups and biotechnology companies (Cathay Industrial Biotech, Cobalt Biofuels, Green Biologics, Metabolic Explorer, and Tetravitae Bioscience) are attempting to develop new technologies to increase the butanol yield using alternative resources like Butyl Fuel (Jin 2011). Hence it is expected that high yield of bio-butanol will probably be achieved in the near future. Some of the key physical and chemical properties of diesel and n-butanol are listed in Table 1.3 (Rakopoulos et al. 2010). Petro-butanol is obtained by the propylene hydro formylation well known as oxo route (Da Silva Trindade et al. 2017). But this method is not economical since synthetic butanol production costs are

linked to the propylene market which is strongly linked to the price of crude oil.

Advantages of n-butanol compared to ethanol:

- **Higher heating value**: Generally the heating value of alcohol rises with improved carbon content. n-butanol is a four carbon alcohol, the double in relative to ethanol and holding around 50% more energy density in a given volume. In practice, it signifies that an engine running on n-butanol is expected to present a lower fuel consumption and a better mileage compared to ethanol.

- **Lower volatility:** The volatility of alcohols drops with the rise in carbon content which indicates that n-butanol will have less affinity to vaporization. In addition to its lower volatility, it has higher flash point in relation to ethanol. These two features show that n-butanol is theoretically safer when investigating in high temperatures compare to ethanol.

- **Intersolubility**: n- butanol is highly soluble in diesel without any phase separation.

- **Higher lubricity:** n-butanol may potentially protect some components of the engine that have direct contact with fuel (like fuel pumps, fuel rails, injectors) against wear problems.

- High cetane number

Disadvantages of n-butanol compared to ethanol:

- Higher viscosity
- Less oxygen contents

1.5.3. Waste plastic oil as alternative fuel in diesel engine

The surge in plastics usage increases the extent of plastic wastes being produced. Plastic waste can be categorized into two groups i.e., municipal and industrial. Industrial plastics are usually more homogeneous whereas municipal plastics are more heterogeneous and contain extraneous materials (Buekens et al. 1998; Zhou et al.2014). The plastic waste disposal is a key environmental risk due to its non-degradability (Scott et al. 1990; Sarker et al. 2011; Ucar et al. 2005), its potential threat to aquatic and terrestrial animals

(Thompson et al. 2009), and its impact on environmental pollution (Yamamoto et al. 2001). The plastic footprint is considered more hazardous than carbon footprint. The 5 R's (Reduce, Recycle, Reuse, Recover, and Residual Management) have been regarded to be the base for waste management, and must be sternly abided in order to maintain ecological balance. Some of the solutions for plastic waste management are incineration and land filling. However, incineration contributes to pollution by producing dangerous and toxic emissions. Apart from the challenge of plastic waste disposal, another worldwide concern is the energy crisis. The core energy sources for transportation are fossil fuels. Today, these fuels are being consumed at an unsustainably high rate all over the globe. The challenges of plastic waste management and energy demand can concurrently be addressed by the production of fuel from plastics. The fuels produced from plastics can have properties comparable to fossil fuels. The absence of water content makes the fuel non-acidic and non-corrosive compared to other fuels. Therefore, conversion of these plastic wastes to usable oil is increasing and important field of study that can possibly mitigate the energy crisis as well as waste management.

Plastic consumption in India:

The overall consumption of plastics in India during the last decade is displayed in Table 1.6. As per the Central Pollution Control Board (CPCB) report, packaging and polyvinyl chloride (PVC) pipe industry grows at the rate of 16-18% per year. The use of plastic goods in our day to day practices is increasing briskly, not only for domestic purposes but also for industrial applications which is growing at a rate of 22% annually.

Table 1.6: Plastics consumption in India (Source: CPCB)

S. No.	Year	Consumption (Tons)
1	1996	61,000
2	2000	3,00,000
3	2001	4,00,000
4	2007	8,500,000

Production of waste plastic oil:

The conversion of waste plastics into lucrative oil is based on the process of pyrolysis which occurs under anaerobic conditions as illustrated in Fig 1.4. The vaporizing pressure forces the product gas from the pyrolysis reactor to flow into the alumina-based catalytic reformer. The oil burner at the bottom of the jacket surrounding the reactor heats the reactor for the thermal decomposition with the temperature controlled at 400°C, and the exhaust gas flows into the outer side jacket of the catalytic reformer, heats the reformer and then exhausted out via the vent.
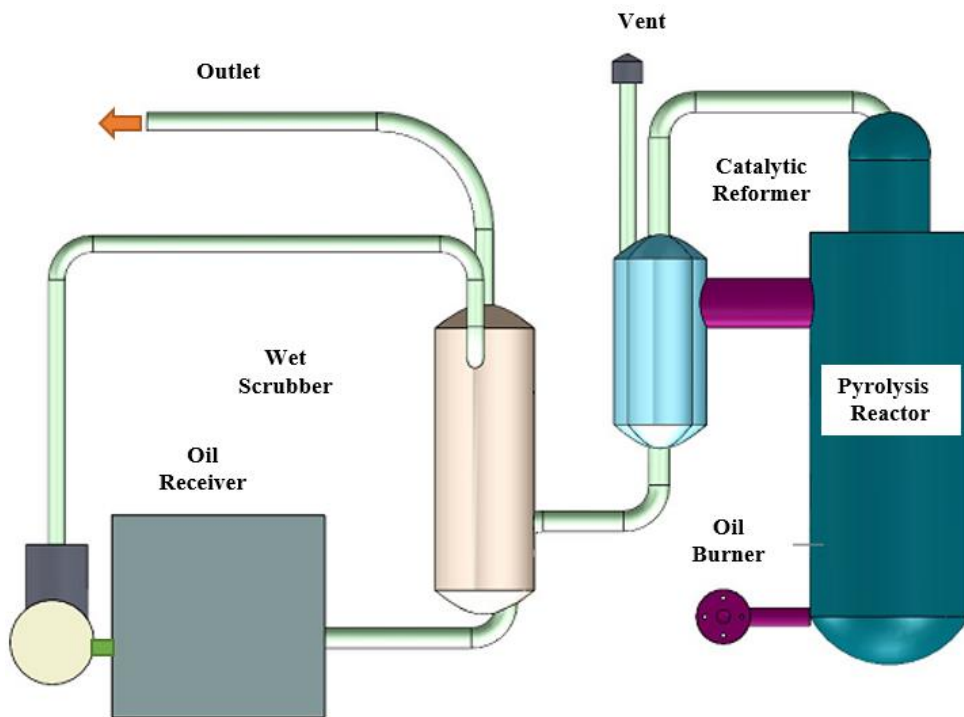
Fig. 1.4 Pyrolysis process of a plastic plant (Lee et al. 2015)

Further cracking of the product gas takes place in the catalytic reformer; after which direct scrubbing is carried out by spraying the oil. Collection of the condensed oil is done in the oil receiver. The off-gas is supplied to the incinerator next to this pyrolysis system to be completely burned. After terminating the pyrolysis reaction in the reactor, an overhead

18

crane lifts up the reactor and installs a new reactor which is already packed with the feedstock and the whole process starts again.

1.6 Diesel engine emission control strategies

Fig 1.5 shows the diesel engine tailpipe exhaust emission control techniques. Emission can be controlled by in-situ as well as after treatment methods as portrayed in Fig 1.5.
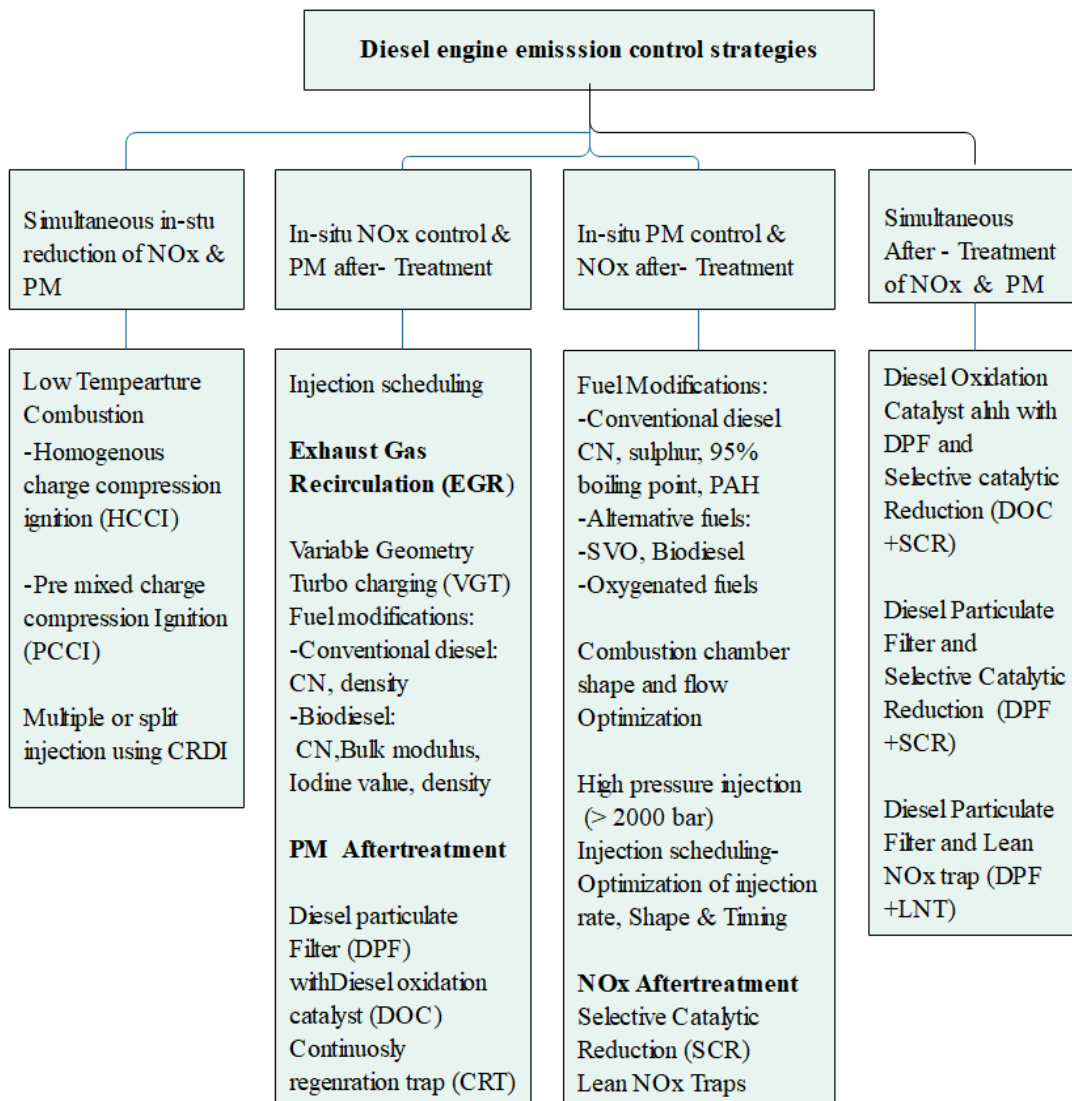
Fig. 1.5 Diesel emission controls- a summary of in-cylinder and after treatment options

1.7. Low temperature combustion (LTC)

Low temperature combustion takes place at temperatures below the formation regime of NO_X and at local equivalence ratios below the formation regime of diesel soot. These systems can be divided into two categories. Those in which the combustion phasing is decoupled from the injection timing and the kinetics of the chemical reactions dominate the combustion, are in the first category known as homogeneous charge compression ignition (HCCI) mode. In the second category, combustion phasing is closely coupled to the fuel injection event which is termed as premixed charge compression ignition (PCCI) mode. In the former category, air and fuel are thoroughly premixed in such a way that at the start of the combustion, the mixture is nearly homogeneous and characterized by an equivalence ratio, which is lower than unity everywhere. For the second category, pre-mixing occurs between the fuel injection and start of combustion, but significant regions exist where the equivalence ratio is greater than unity at the start of the combustion. Fig 1.6 shows the plot of local equivalence ratio (ϕ) vs. flame temperature (T) with different combustion mechanisms.
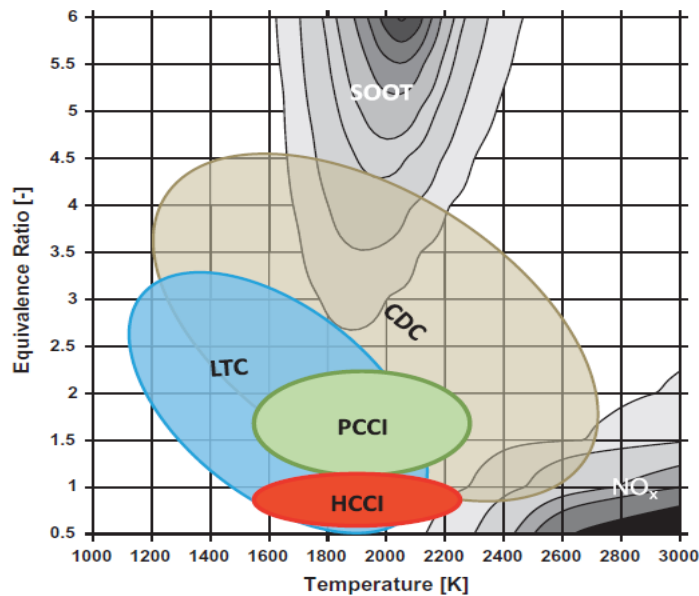
Fig. 1.6 Predominant ϕ–T working conditions for combustion modes (Benajes et al. 2014)

Conventional combustion overleaps the formation zones of NO_X and soot, but LTC techniques like HCCI and PCCI avoid these zones and reduce NO_X and soot simultaneously. Recently, a new approach of LTC, Reactivity Controlled Compression Ignition (RCCI) has been proposed by several authors (Imtenan et al. 2014). This technology has the potential to overcome some of the limitations of HCCI and PCCI. In RCCI low reactive fuel is injected at advanced injection timing and high reactive fuel near to start of combustion. Nearly homogeneous charge can be achieved with RCCI. This technique is presently in research phase, and major modification is required to implement it. Further, a simple method being widely employed to mitigate NO_X in IC engine is exhaust gas recirculation (EGR) technique. In this, a portion of engine exhaust gas is recirculated to the engine cylinders through intake manifold. Among all the LTC technique EGR is easiest to implement and control the hazardous NO_X emission from diesel engine.

Exhaust Gas Recirculation (EGR):

Recirculation of exhaust gas into cylinder is usually controlled by a solenoid valve which maintains required EGR rate. A detailed schematic diagram of engine with EGR systems is shown in Fig 1.7. The substitution of exhaust gas (which takes no further part in combustion) with air reduces the proportion of the fresh oxygen available for combustion.
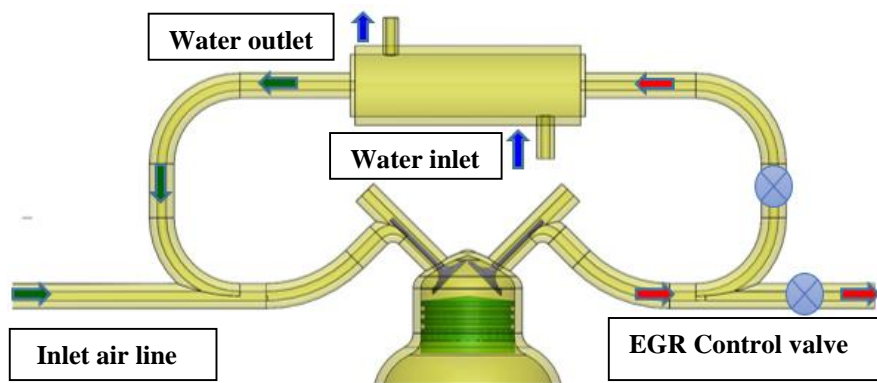
Fig.1.7 Exhaust gas recirculation system

This causes correspondingly lower heat release and peak cylinder temperature causing

reduction in formation of NOx (as temperature is the driving factor for NOx emission). Further presence of inert gases in the cylinder further limits the peak temperature. The gas to be re-circulated may also be passed through an EGR cooler to reduce the temperature before entering into cylinder. This has two benefits, one is reduction of charge temperature results in lower in-cylinder temperature and other one is the greater density of cooled EGR gas allows a higher proportion of EGR to be used. Conversely, the decrease in oxygen concentration in the combustion chamber at burning zones weakens the soot oxidation process which leads to the decrease in local combustion temperature and hence less soot oxidation rate. Consequently, the employment of EGR is related with more in exhaust smoke and particulate matter.

Effects of EGR on engine cycle:

Effect of EGR rate on driveability and emissions of IC engine are shown the Fig 1.8. Reduction in the available oxygen in the cylinder will lower the peak power obtainable from the engine which causes abnormal engine noise with penalty in fuel consumption.
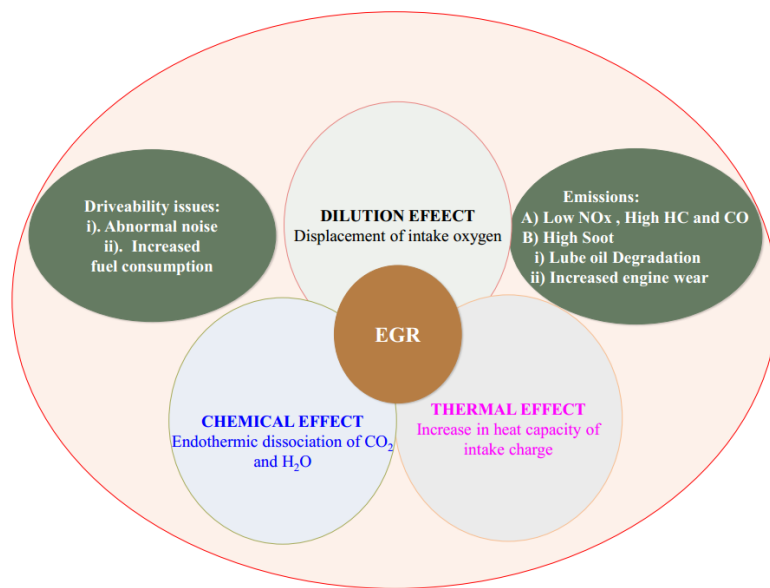
Fig. 1.8 Effect of EGR on performance and emissions

The effect of EGR on combustion characteristics is explained below (Ghazikhani et al.

2010):

i) Dilution effect- As EGR decreases the concentration of oxygen in the cylinder, the fuel spray has to diffuse further to encounter sufficient O_2 to form a stoichiometric mixture suitable for combustion. This extended flammable region contains not only stoichiometric mixture but also additional amount of CO_2, H_2O and N_2. The additional quantity of these components absorbs the released heat from the combustion and combustion temperature will be lowered. Also the reduced amount of oxygen decreases the oxygen partial pressure and it affects the kinetics of the elementary NO_x formation reaction.

ii) Ignition delay effect - The existence of diluents such as CO_2 and H_2O causes an increase in ignition delay and changes the start of combustion. As a consequence, the whole combustion process shifts further toward the expansion stroke. This causes in the products of combustion to be less exposed to high temperature conditions and accordingly less nitrogen oxides formation.

iii) Chemical effect- The recirculated CO_2 and water vapor from exhaust gases dissociate at the presence of high temperature during combustion period which can modify combustion temperature and NO_x formation. Particularly, the endothermic dissociation process of H_2O and CO_2 reduces the flame temperature.

iv) Thermal effect - Due to the higher heat capacity of CO_2 and H_2O contained in EGR in comparison with O_2 and N_2 which are normally a part of inlet air, the overall heat capacity of the in-cylinder mixture gets increased and causes low flame temperature.

Multiple injections:

Multiple injections approach is estimated as an effective tool to reduce the exhaust emissions in which the total mass of fuel is split into two or more injections per combustion event. Dividing the injection order into two events are called main and pilot (split injection). A pilot injection is also defined as an injection where 15% or less of the total mass of fuel is injected in the first injection. The effect of multiple

injection on soot emission from diesel engine is demonstrated schematically as shown in Fig 1.9. It is observed from Fig that in single injection, fuel enters with very high momentum into combustion chamber and spray penetrates to fuel rich zone. The tip of the jet is at low temperature (relative) which replenishes the rich region and forms soot. Conversely, in a multiple injection, the second injection enters into a relatively at high temperature and lean fuel region. Therefore, soot formation is considerably decreased due to the injected fuel quickly burned before soot formation. Also, duration between the injections (pilot and main) must be optimized so that soot formation zone of pilot injection should not replenish with the fresh injected fuel. The advantages of split injection is greatly dependent on quantity of fuel in each injection and dwell timings.
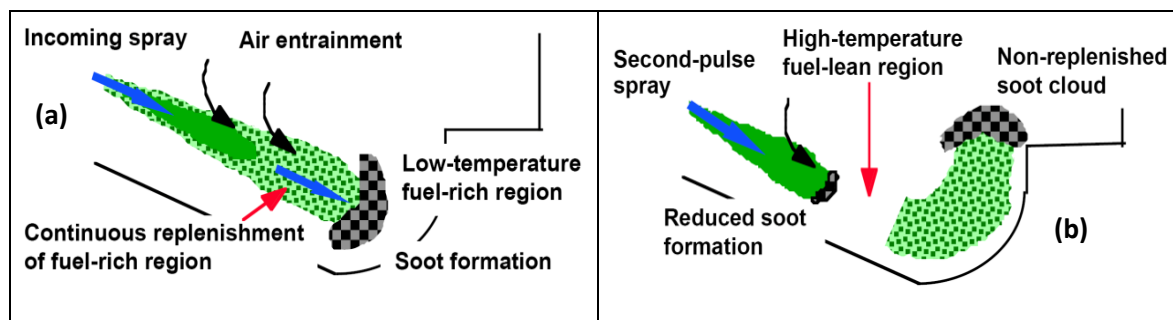
Fig. 1.9 Schematics diagram showing soot-reduction mechanisms of split injections a) Single injection (b) Split injection (Han et al. 1996).

1.8. Organization of Thesis

This thesis is organized into seven eight chapters to help the reader in understanding the nature of this work, as follows.

Chapter 1 deals with the introduction which comprises of selection criteria of alternative fuels in CRDI engine.

Chapter 2 deals with review of literature of the previous works. Based on the literature gap, objectives of the present work have been framed and mentioned in chapter 2.

Chapter 3 This chapter describes the development of experimental test rig, details of the engine instrumentation; error analysis, research methodology (experimental and computational) employed in present range of studies.

C**hapter 4** introduce the CFD simulation of combustion, emission characteristics of CRDI engine operated with DME-diesel blends.

C**hapter 5** introduce the CFD simulation of combustion, emission characteristics of CRDI engine operated with ethanol-diesel blends.

Chapter 6 presents experimental and CFD studies for engine operated with bio-butanol-diesel blends for various injection timings and EGR rates.

Chapter 7 deals with finding optimum injection timing, suitable EGR rate along with multiple injections for CRDI engine operated with WPO-diesel blends. Finally,

Chapter 8 presents concluding remarks of the present investigations and discusses the scope for future work.

CHAPTER 2

LITERATURE REVIEW

An extensive review of the literature on the performance, emission and combustion characteristics of CRDI engines for various oxygenated fuels (dimethyl ether, ethanol and butanol) and waste plastic oil blended with diesel is presented in this chapter. This review also includes computational as well as experimental studies, the effect of exhaust gas recirculation (EGR) rate, and injection strategies (injection timings, multiple injection techniques) in CRDI engine.

2.1. Oxygenated fuels in CRDI engine

DME: Youn et al. (2011) investigated the effect of DME fuel along with injection characteristics (spray behaviours) on the engine performance and the exhaust emissions of CRDI engine. Based on the experimental investigation, they found that the injection quantity of DME fuel was more than that of the ultra-low sulphur diesel (ULSD) at same operating conditions. They also remarked the higher in-cylinder peak pressure and shorter ignition delay for DME compared to ULSD. The NOx emission of DME fuel was found higher than ULSD with no soot emission. Also, hydro carbon (HC) and carbon monoxide (CO) emissions were lower than diesel.

Fuel spray characteristics and macroscopic behaviours of the DME blended with biodiesel (soybean oil) at different blends are deliberated by Bang et al. (2010). B25, B50, and B75 test fuels (B75 means 75% biodiesel and 25% DME blended fuel by weight) are considered in their study. At the same energizing period and injection pressure, it was observed that the DME fuel with higher blends need longer injection duration than that of the lower blending ratio. The higher DME blends with biodiesel also showed a low peak value of injection rate compared to the lower DME blend at the same injection time. As the blending ratio of DME fuel was increased, the effective initial velocity of neat biodiesel and lower DME blended with biodiesel increased compared to the higher DME blended.

Combustion and emission from a twin-cylinder, naturally aspirated, direct injection, four stroke air cooled CI engine fuelled with DME was investigated by Cipolat et al. (2007). They observed that for lower engine speed, NOx emission from DME is higher than diesel, whereas for higher speed NOx emissions were approximately same compared to diesel. The equivalence ratio and maximum combustion chamber pressure with DME were lower than the diesel fuelling throughout the speed range.

Park et al. (2010) explored numerically the effect of in-cylinder DME spray behaviour on the combustion and exhaust emissions characteristics of a high speed diesel engine. The peak combustion pressure, IMEP and less ISFC were observed at 30° BTDC injection timing. The HC and CO emissions from DME fuel show lower values and distributions between BTDC 25° to BTDC 10°. There was a rapid increase in HC and CO emissions with advancing injection timing with 30° BTDC.

Empirical equations based on experimental and analytical models to investigate the effect of injection parameters on a diesel engine using DME as an alternative fuel was studied by Shu et al. (2008). The atomization behaviour (macroscopic and microscopic) of experimental and empirical models for diesel and DME fuel was compared. The effect of energizing duration on the injection rate shows the injection delay of DME was shorter and the peak injection rates of diesel fuel little higher than those of DME. Diesel spray development shows that the diesel spray was wider and longer than DME under identical injection conditions.

Ethanol: Experimental investigation on performance and emission characteristics of four stroke water-cooled diesel engine was carried out by Jilin et al. (2012). They perceived that for ambient temperature above 25°C, bioethanol-diesel blend was physically stable with the single emulsifier, whereas for ambient temperature less than 25 °C phase separation was observed. They also concluded that the brake thermal efficiency gets improved and the equivalent bsfc gets reduced for engine operated with ethanol-diesel blends. Further NO_x and smoke emissions were found to be reduced for ethanol-diesel blends with marginal penalty in CO emission at low loads.

Experimental study on turbocharged four cylinder four-stroke heavy-duty CRDI engine operated with bioethanol-diesel blends was carried out by Fang et al. (2013). They observed that maximum heat release rate increases with addition of bioethanol in diesel. Further, engine tail pipe emissions (NO_x, Smoke) were reduced and BTE was improved in bioethanol compared to diesel.

Zhu et al. (2011) conducted the experiment on a naturally aspirated water-cooled 4-cylinder diesel engine. They studied the performance and emission features of engine for five different loads by using biodiesel, ethanol-biodiesel blends (BE), and Euro-V diesel fuel. They witnessed improvement in combustion characteristics and BTE at 5% ethanol-diesel blends (BE5) with reduction in NO_X and PM. They also observed increase in peak pressure, heat release rate, HC and CO emissions for higher ethanol-diesel blends.

The effect of injector configuration on the combustion and emissions characteristics of CI engine fuelled with ethanol as the main fuel and dimethyl ether as ignition promoter was analysed by Cipolat et al. (2009). It has been witnessed that engine configuration with four-hole injector produces more power, higher fuel conversion efficiency and lesser emissions (THC and NO_X) compared to three-hole injector configuration.

Effect of ethanol concentration on engine emissions was investigated in twin cylinder direct injection diesel engine (Yilmaz and Vigil 2014; Yilmaz et al. 2014). They observed that the emissions strongly depend not only on engine operating conditions, but also on fuel blends concentrations, and concluded that high concentrations of ethanol increases HC emissions.

Armas et al. (2011) carried out an experimental study to compare two different fuels properties on light duty CRDI engine at injection pressure 150 MPa. Results show that the use of the ethanol-biodiesel-diesel blend produced a similar effect on the durability of the injection pump components and on the injector nozzle as that produced by diesel fuel.

Rakopoulos et al. (2008) investigated the effects of bioethanol-diesel blends on the performance and exhaust emissions of heavy duty direct injection engine. They conducted

the experiment on Mercedes-Benz, six-cylinder, four-stroke, water-cooled turbocharged engine and observed significant reduction in smoke density. For higher percentage of ethanol in the blend, the NO_X and CO emissions remained the same or marginally reduced, whereas specific fuel consumption, BTE and HC emissions were increased.

Influence of ethanol and rapeseed oil methyl ester (RME) addition to diesel fuel was studied by Labeckas et al. (2014). They conducted the experiment on a naturally aspirated four-stroke four-cylinder diesel engine and found reduction in NOx and HC emissions for richer combustible mixtures. Further they observed that diesel with E15 and RME5 blend develops 16% higher mean effective pressure with higher bsfc compared to neat diesel.

Study on optimization of injection parameters was carried out by Beatrice et al. (2014) using design of experiments (DOE) method. Four cylinder light duty diesel engine was operated with bioethanol/rapeseed methyl ester (RME)/diesel blends. They observed reduction of smoke and NO_x in emission with marginal penalty of CO and HC at low load conditions with increase of ethanol percentage in blend.

Fraioli et al. (2014) studied the dual fuel configuration to investigate the effect of premixed ethanol in CI engine experimentally, and results were compared with numerical study. They conducted the experiments on four-cylinder CRDI Euro V engine with an external air compressor to supply pressurized intake. Bioethanol as premixed fuel, while n-heptane injected directly in combustion chamber. The test was performed at low load condition at 1500 rpm. Optical measurement and computed result suggest that presence of ethanol causes wider auto ignition area and smoothing effect on ignition of n-heptane, due to the chemical and physical effect.

Kim et al. (2008) investigated the performance and emissions of four cylinder CRDI engine for ethanol blended with three different types of ultra-low sulphur fuels. They observed that total hydrocarbon (THC) conversion efficiency with the ethanol-diesel blend reached up to 40-60%, and CO conversion efficiency reached up to 80-90%. Further smoke emissions from the use of ethanol-diesel blend fuels were slightly decreased.

n-butanol: To evaluate the effects of biobutanol-diesel blends (8% and 16% by vol.) on combustion characteristics, Rakopoulos et al. (2011) carried out experimental study on six-cylinder turbocharged (after-cooled) heavy duty direct injection engine. They found increase in ignition delay and reduction in peak in-cylinder pressures and temperature during the first part of combustion. Further, smoke opacity was reduced drastically with higher biobutanol-diesel blends.

Kumar et al. (2016) conducted an experiment to assess the effects of n-butanol and n-pentanol mixed with biodiesel (10% and 20% by volume) in a single cylinder direct injection engine. The engine was operated at a constant speed at three different loads. Compared to biodiesel, biobutanol-biodiesel blends resulted in higher BTE with increase in the bsfc by 2-4% at low and medium engine loads. Both the blended fuels witnessed a significant reduction in the particulate matter and elemental carbon emissions, with butanol being more efficient than pentanol.

The experimental investigation of n-butanol and biodiesel blended with diesel on combustion and emission characteristics of heavy duty diesel engine was carried out by Isik et al. (2016) at low load conditions. They observed that biobutanol addition to diesel and biodiesel can be considered as a suitable blend to improve the flow properties. They also observed increase in thermal efficiency, and reduction in CO and NOx under comparatively lower load conditions.

Dogan (2011) evaluated the influence of n-butanol-diesel blends (butanol 0-20%) on engine performance and exhaust emissions of a single cylinder four stroke high speed naturally aspirated direct injection engine at different loads and constant speed (2600 rpm). The experimental test results showed the reduction in smoke opacity, NO_X and CO emissions whereas increase in hydrocarbon emission was observed with increase in n-butanol-diesel blends. In addition BTE and bsfc were increased.

2.2. Exhaust gas recirculation (EGR) in CRDI engine with oxygenated fuels

It is well known fact that NO_X emission is effectively reduced by EGR (Ramos, 1989).

The review on the effect of EGR in CRDI engine with oxygenated fuel blended with diesel is presented here.

Experimental investigation of effect of cold and hot EGR rate on combustion and emission characteristics of direct injection engine was carried out by Arcoumanis et al. (1995) and Ladommatos et al. (1996). It was observed that engine operating with cool EGR improves the volumetric efficiency and inlet charge density. Hence better trade-off between NO_X and soot can be made with cool EGR.

Comprehensive experimental investigation was carried out by Ladommatos et al. (1997) to study the influence of EGR rate in a 2.5 litre four cylinder CI engine. They witnessed the escalation of ignition delay with increase in EGR rate, and combustion process gets shifted towards the expansion stroke. Further, in- cylinder temperature reaches maximum for shorter duration of time.   Hence, lower thermal NOx and increase in soot in exhaust emission were observed.

 Mattarelli et al. (2000) studied the effect of cool and hot EGR on multi valve, turbo charged 2.5 L diesel engine. Their observations demonstrated that the cooled EGR is an effective method to reduce NOx majorly for engine operated at high load conditions. They also suggested that EGR along with injection strategy may be considered for optimum results.

DME: Arcoumanis et al. (2008) studied the suitability of DME and the effect of EGR rate in diesel engine. They observed the reduction in particulate matter and marginal increase in NOx emission. Performance of DME operated engine was also comparable to diesel fuel engine. NOx emissions from DME-fuelled engines can meet future regulations with high EGR rate in combination with a lean NOx trap.

Exhaust gas recirculation in association with oxidation catalyst to premeditate the exhaust emission from a multi-cylinder DME engine was investigated by Ying et al. (2008). Experiments were conducted on a four-cylinder naturally aspirated four-stroke direct injection engine. Result indicates reduction in NOx emission about 40% at a higher EGR

rate without visible smoke, and deteriorating thermal efficiency with DME. However, CO emission was increased with the higher EGR rate. Finally, they concluded that DME engine can meet strict emission regulations with an integration system of EGR and exhaust after treatment.

Park et al. (2013) briefed an overview of a DME fuel as alternative fuel with EGR for a CI engine. They observed the ignition of DME in combustion chamber starts early compared to diesel/biodiesel fuelled CI engine. In addition, DME combustion was found soot-free due to absence of carbon-carbon bonds, and had lower HC and CO emissions than that of diesel combustion. The higher NOx emission from DME fuelled combustion can be reduced by EGR.

Park et al. (2014) reviewed the effect of EGR and DME in CI engines on combustion performance and exhaust emission characteristics. They found low HC and CO emissions in DME operated engines compared to diesel. In addition, PM emission of DME combustion was very low due to its molecular structure. They also observed reduction in NO_X at higher EGR rate without affecting soot formation. To decrease NOx emission, engine after-treatment devices, such as lean NO_X traps (LNTs), urea-selective catalytic reduction, and the combination of EGR and catalyst can be applied (Palash et al. 2013).

The effect of DME pre-mixing ratio and cooled EGR rate on combustion performance and emission characteristics of a DME-diesel dual fuel premixed charge compression ignition (PCCI) engine is pondered by Zhao et al. (2014). They observed low smoke and NO_X with increase in HC and CO emissions at higher DME pre-mixing ratio.

An experimental study to investigate the performance and combustion characteristics of four-stroke twin-cylinder naturally aspirated DME fuelled PCCI diesel engine with the port premixing was conducted by Wang et al. (2014). They observed the increase in peak pressure and temperature with an incremental DME quantity in early injection. At a constant DME quantity, the lower bsfc was observed at 7ºCA BTDC.

Auto-ignition mechanism to control combustion phasing in homogeneous charged compression ignition (HCCI) engine fuelled with DME for various EGR rate using zero dimensional model was studied by Putrasari et al. (2017). Experiments were conducted on modified single cylinder HCCI engine for various injection timing. DME fuel was injected directly into combustion chamber. The results indicate that for higher EGR rates, decomposition of hydrogen peroxide (H_2O_2) was slower, which contributes to high temperature heat release by reducing the rate of hydroxyl radical (OH). Higher EGR rate reduces the power and increases the carbon monoxide (CO).

n-butanol: Port fuel injection combined with EGR effects in direct injection engine operated with biobutanol-diesel blends was studied experimentally by Chen et al. (2013). They observed that n-butanol and EGR together affect the combustion process. Peak cylinder pressure and heat release rate were increased with increase in butanol concentration without affecting ignition delay. However, reverse trend is observed for higher EGR rate with longer combustion duration. Also, HC and CO emissions were increased with increase in butanol concentration causing higher isfc and lower indicated thermal efficiency (ITE).

Han et al. (2013) examined the effect of EGR strategies and high load test operation for diesel, n-butanol and ethanol blends in high compression ratio engines. It was observed that n-butanol appears to be a promising alternative fuel at higher injection pressure. The longer ignition delay and fuel-borne oxygen content resulted in near-zero soot emissions. The CI of n-butanol charge is an effective measure of LTC enabling and reduction of soot emissions.

Chen et al. (2014) performed an experiment on combustion and emission characteristics of biobutanol-diesel blend with 40% butanol percentage (i.e., Bu40) in a heavy-duty diesel engine. The effect of EGR rate was evaluated experimentally and compared with neat diesel. The results indicate that Bu40 has higher cylinder pressure, longer ignition delay, and faster burning rate than neat diesel. No significant variation in HC and CO emissions as well as ITE was observed with EGR until optimum conditions.

Influence of biobutanol-diesel blends and EGR rate on single-cylinder diesel engine was examined by Zheng et al. (2015). Four butanol isomers i.e., n-butanol, sec-butanol, iso-butanol and tert-butanol were blended with diesel by volume ratios of 20% and 40%. Experiments were conducted over a wide range of EGR from 0% to 65%. They found that biobutanol-diesel blends show higher in-cylinder pressure and net heat release rate compared to neat diesel. Differences in cylinder pressures and heat release rates among different biobutanol-diesel blends become larger with increase in EGR rate and blending ratio. For biobutanol-diesel blends higher thermal efficiencies were observed compared to neat diesel. They also observed that the addition of butanol isomers significantly reduces soot emission, whereas the particulate formation increases due to application of EGR.

Trade-off between smoke and NO_X emission was studied by Kumar (2016) using combine effect of EGR rate and injection timing in a direct injection engine. For the experimental study, two higher alcohol/diesel blends i.e., Bu40 (40% iso-butanol+60% diesel) and P40 (40% n-pentanol+60% diesel) blends were considered. They observed longer ignition delay, higher peak pressure and premixed heat release rate in the case of Bu40 compared to P40. They also found that Bu40 presented better smoke suppression characteristics than P40. HC emission was increased and CO emission was decreased for both blends at all EGR rates.

2.3. Injection strategies in CRDI engine

This section presents the detailed review of literature on injection strategies which includes the effect of injection timings with single and multiple injections.

Diesel: The influences of pilot injection and EGR on single cylinder diesel engine were investigated by Zhang (1999). He observed the reduction in NOx and combustion noise with penalty in soot emission for pilot injection. Additionally by reducing pilot injection quantity and increasing interval between pilot and main injection, lesser soot emission was observed.

The effects of low compression ratio (CR) and high EGR rate for various multiple injection schemes on combustion characteristics of direct injection engine were investigated by Mendez et al. (2009). They highlighted that for low CR and high EGR rates (46%), ignition delay escalates, and for pilot injection, peak heat release rate reduces. The fuel injected during pilot injection was over diffused causing very lean air fuel mixture and was never attained auto ignition. As a consequence similar HRR profile was observed for single and multiple injections which reveal that fuel for both the cases burns at same time.

It is well known fact that combustion noise during ignition and maximum HRR are generally correlated (Mendez et al. 2009), hence controlling the maximum HRR is desirable to reduce the noise. Multiple injection is promising method to reduce the maximum HRR in single peak by splitting it into two or more peaks. So that the amplitude of HRR due to split injection is lower than single injection. From Fig 2.1, it is observed that with two injections maximum HRR was decreased compared to single injection leads to 7dB reduction in combustion noise. Soot formation mainly depends on the interval between pilot and main injection, hence with optimized interval soot formation can be reduced.
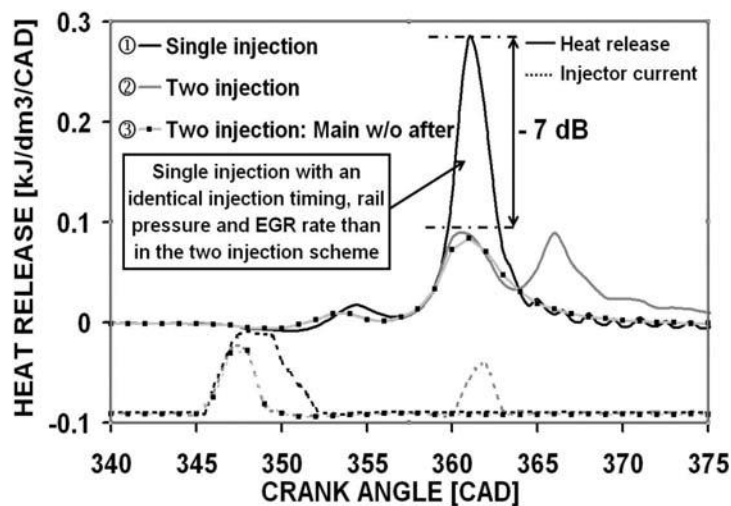
Fig. 2.1 Single and double injections heat release (Mendez et al. 2009)

Ricaud et al. (2002) conducted series of experiments to optimize the engine performance

using split injection schemes. Several combination of split injection schemes were tested (pilot +main, 2pilot+main, 2pilot+ main +post). They reported that injection timing, EGR rates, fuel quantity in pilot, and dwell period and injection timings are the key parameters for optimization. Soot and Combustion noise can be limited with multiple injection schemes. The combination of pilot, main and post injection in association with EGR rate on emission characteristics was studied by Dronniou et al. (2005). Figures 2.2 and 2.3 show reduction in soot emission for pilot and post injections.
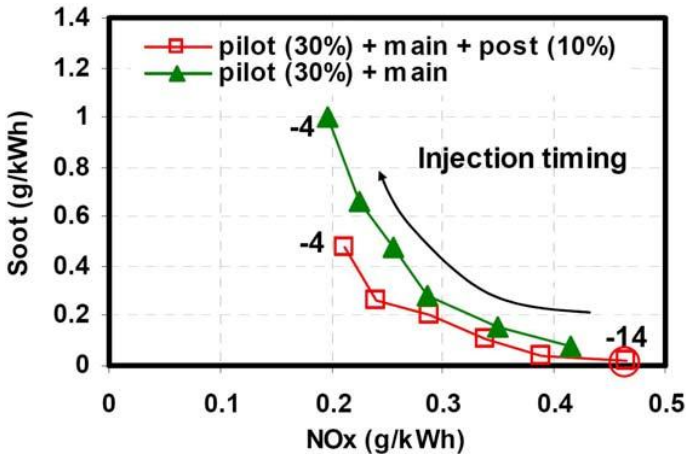
Fig. 2.2 Influence of post-injection on NO -Soot trade-off (Dronniou et al. 2005)
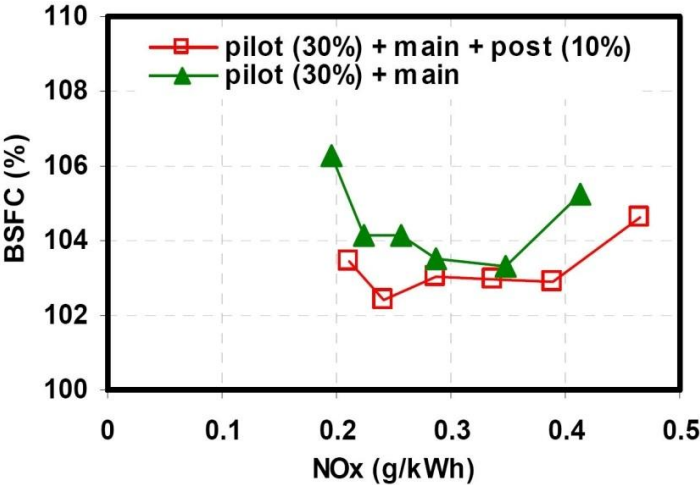
Fig. 2.3 Influence of post-injection on NOx vs bsfc (Dronniou et al. 2005)

EGR is known to be effective method to reduce NOx emissions, but usually increases particulate emissions. On the other hand, multiple injections are considered as an effective means to improve particulate emissions. Thus, it is of interest to explore the possibility of simultaneous reduction in particulate and NOx emissions with the combined use of EGR and multiple injections.

DME: Influence of DME fuel on engine performance and exhaust emission characteristics of CI engine with various injection timings was investigated by Kim et al. (2008). They witnessed the longer injection duration, higher IMEP and NOx emission with lower CO and HC emissions for DME compared to neat diesel fuel.

Comparison of conventional direct injection and PCCI combustion was experimentally studied by Ying et al. (2010) with DME for wide operating range of speeds and loads. Higher BTE and lower NO_X emission were observed for PCCI combustion compared to conventional direct injection combustion. NOx emission showed decreasing trend with increase in DME quantity in pilot injection at low loads, contrarily increasing trend observed at high loads engine operations. HC and CO emissions were found higher for PCCI operation under all DME pilot injections.

The effect of multiple injection strategies (pilot injection, split injection, and advanced + post injection) on performance and emission characteristic of CRDI engine fuelled with DME was assessed by Park et al. (2015). They observed less NO_X, HC, soot and CO emissions for the pilot injection strategy with advanced main injection. Moreover, the pilot injection strategy showed the highest imep and the lowest isfc during all test conditions.

Kim et al. (2011) conducted experimental and numerical study to investigate the impact of injection angle and advance injection timing on combustion, emission and performance characteristics in a DME fuelled CI engine. For numerical study, detailed chemical kinetic DME oxidation model was employed. They observed that most of the fuel spray and evaporation occur in wide injection angles (injected spray with narrow injection angles was impinged on the bottom wall after 60°BTDC SOI) and distributed at the crevice region for

advance injection timings. In addition, NO_X emission at the SOI of 20°BTDC and TDC was higher with negligible soot emission.

Effect of spray angle and injection strategies on the combustion characteristics, concentrations of exhaust emissions on a single-cylinder naturally aspirated direct injection diesel engine with DME as a fuel was studied by Yoon et al. (2010). The engine test was performed at 1400 rpm, and the injection timings were varied from TDC to 40° BTDC at two spray angle injectors (θ_{spray}=70° and 60°). Results were compared with the results of conventional spray angle (θ_{spray}=156°). They observed low intensities of soot emissions at all injection timings for all test injectors. The NOx emissions for narrow-angle injectors simultaneously increased with advance in injection timing upto 25° BTDC, whereas for the wide-angle injector it was 20° BTDC. With advanced timing of the first injection, narrow-angle injectors with multiple injections also achieved low NOx and soot emission similar to single-injection.

n-butanol: The effect of multiple injection strategies with exhaust gas recirculation on combustion and emission characteristics of high speed diesel engine fuelled with biobutanol-diesel blends (20% and 30% butanol blended diesel by volume) was studied experimentally by Huang et al. (2015). They observed that for all advanced pilot injection timing, the peak heat release rate decreases for pre-injection and slightly increases for the main-injection. They also observed reduction in NOx and soot emissions for pilot injection. Further, for more pilot injection quantity, they observed increase in peak value of heat release rate for pilot injection while decrease for the main-injection.

Yun et al. (2016) studied the effect of biobutanol- diesel blends (Bu10 and Bu20) on the combustion and emission characteristics in a four-cylinder CI engine exercising the pilot injection approaches. They observed longer ignition delay for higher blends than that of diesel fuel for all pilot injection timings. However, the exhaust temperature was lower than that of diesel at all injection timings. NOx, CO and soot from Bu20 were lower compared to diesel at all test conditions whereas higher HC emission was observed compared to diesel.

Cheng et al. (2016) investigated the effect of partial premixed compression ignition technique in a four-cylinder light-duty diesel engine fuelled with n-butanol-diesel blends with the help of early or late injection. The influence of injection timing and load rate on PM mass-size distribution have also been inspected. Experimental results show that both early and late injections affect the premixed duration of combustion, ultimately helping in formation of homogenous mixture and more active in reduction of soot formation. Even when the load rate is increased, the premixed combustion fraction drop directing to intense rise of soot mass due to the abrupt change in ignition delay.

Yao et al. (2010) experimentally investigated the influence of the biobutanol-diesel (0 – 15%) blend on the performance and emissions of a heavy duty direct injection engine with multi-injection technique. At constant engine speed and load, exhaust gas recirculation were regulated to maintain NO_X emission below the allowable limit. They observed that the n-butanol addition can considerably decrease the soot and CO emissions with minor effect on NOx formation with marginal impact on the bsfc and ITE. It was shown that early pilot injection decreases soot emission but consequences in an intense rise of CO emission, whereas post injection reduces soot and CO emissions effectively.

2.4. Waste plastic oil as fuel in CRDI engine

Investigation on the performance and emission characteristics of diesel engine fuelled with waste plastic oil (WPO100) was carried out by Mani et al. (2009) and reported improvement in BTE compared to diesel. Mani et al. (2010) studied the effect of WPO-diesel blends and exhaust gas recirculation (EGR) on the performance and emission of a diesel engine. They noticed that as blends and EGR rates increase the BTE and NO_x decrease with penalty in CO, HC and soot. Study of combustion characteristics of a diesel engine using waste plastic oil and its blends was experimentally carried out by Kaimal et al. (2015). They observed higher heat release rate (HRR) and peak pressure for blend compared to neat diesel operations and marginally decrease in BTE which contradicts the previous studies carried out by Mani et al. WPO-Diesel blends in combination with Diethyl

ether (DEE) was studied by Devaraj et al. (2015), and found the reduction in emission and improvement in performance with DEE combination.

2.5 Summary of the literature review

The literature review presents a broad overview of research studies hitherto carried out on CRDI engine operated with various fuels (DME, ethanol, n-butanol and WPO), injection timings, EGR and injection strategies, etc. Based on this literature survey, the following observations are made:

- Fast depleting fossil fuel reserves have alarmed to find alternate renewable fuels which could effectively replace conventional fuels and be available at lesser cost.

- DME is emerging as one of the preferred alternative fuel in diesel engine due to its favourable environmental and thermo physical properties.

- Higher oxygen content of bio-ethanol mitigates soot emission hence, it is considered as important substitute in diesel engine. Very few papers are reported on optimisation of injection timings.

- n - butanol is most preferred oxygenated fuel in diesel engine as NO_X and soot trade-off is easier due to high latent heat of evaporation fuel bound oxygen.

- Influence of multiple injection strategies in an engine cycle, have not been understood clearly.

- Waste plastic-oil with high pressure injection in CRDI engine are scant in open literature.

- Biofuels virtually decreases all regulated emissions and urgency need is to develop advanced technologies and concepts in this area to optimize the various engine parameters that will result in clean environment and more efficient diesel engines.

- Numerical simulations allow to perform conceptual studies with extreme boundary conditions, that could not be realized in experiments because of either too large or too

small length and time scales, or because a hazardous outcome prohibits the execution of the respective experiment.

2.6 Research gap

The following gaps were found from literature survey

- CFD analysis with oxygenated fuel in CRDI engine is very scant in open literature.

- Less work has been carried out with ultra-high pressure injection system and biofuel combination.

- The analysis of performance, emission and combustion characteristics for various EGR concentrations with varying biofuel blends and engine loads.

- Effect of low temperature combustion (LTC) on performance, emission and combustion characteristics of CRDI engine.

- No literature are reported with waste plastic oil in diesel engine operated with multiple injection strategy.

2.7 Objectives of the present investigation

The present study investigate the effect of biofuels and plastic oil blends with diesel, on engine performance, combustion and emissions in a twin cylinder, CRDI engine. The engine operating parameters of injection timing, EGR and multiple injection timing are varied.

The detailed objectives of the investigation are as presented below

1. To investigate the performance, emission and combustion characteristics of CRDI engine using CFD model.
2. To analyse the performance, combustion and emission characteristics of dimethyl ether-diesel blends and bioethanol-diesel blends in CRDI engine through CFD.

3. To understand the effect of n-butanol-diesel blends, injection timings and EGR rates on engine performance, emission characteristics using experimental and computational studies.

4. To investigate the effect of exhaust gas recirculation and injection strategies (single and multiple injection) in CRDI engine using plastic oil-diesel blends experimentally.

2.8 Scope of the work/ results expected

➢ Set up of an experimental test rig to analyse the combustion characteristics of biofuel-diesel blended fuel in a compression ignition engine.

➢ Biofuel blend usage in diesel engine may result in decrease of particulate matter (PM) and carbon monoxide (CO) but slight increase of nitrogen oxides (NO_x).

➢ CFD simulation of engine with EGR provides LTC mode results decrease in NO_x.

➢ Computational simulation with multiple injections mode results in simultaneous control of both NO_x and soot emissions.

CHAPTER 3

EXPERIMENTAL AND COMPUTATIONAL RESERCH METHODOLOGY

This chapter describes the components of the research engine facility, research methodology and computational fluid dynamic (CFD) code and the governing equations applied for validation to achieve the objectives framed under present research work. The discussion also includes engine modifications, experimental parameters, measurement techniques and instrumentation for the course of the research to fulfil the present study of objectives framed.

3.1 Experimental setup

Schematic diagram and representation of experimental facility are shown in Fig 3.1 (a) and (b). Twin cylinder, CRDI engine with open electronic control unit (ECU) developed by *NIRA Control AB*, is used to study the engine performance, emission, and combustion characteristics. The specifications of the engine are listed in Table 3.1. The fuel from the tank is supplied to the accumulator (common rail) by high pressure fuel pump at constant injection pressure of 100 MPa. Common rail pressure is maintained by pressure control valve (PCV) and required fuel supplied to injector is controlled by solenoid valve. Operating parameters of engine is controlled by an open ECU. Pressure versus crank angle data is measured by using piezoelectric based pressure transducer. The signal of cylinder pressure is acquired at every 1º crank angle for 100 cycles, and average value of 100 cycles is considered for combustion analysis. The pressure signal is fed into the NI USB-6210 DAQ and stored in a data acquisition card linked to the computer. Exhaust gas recirculation is activated by ECU with vaccum pump, solenoid valve and vaccum modulator. Required EGR value is set in ECU map, that monitors the vaccum pump to maintain required vaccum, and solenoid valve operates accordingly. Further, engine tail pipe emissions are measured by exhaust gas analyzer (AVL 444) with diesel probe to measure the concentrations of HC, CO, NO_X, CO_2 and O_2. The details of the engine instrumentation and range are presented in Table 3.2 and 3.3. Soot emission is measured by opacity meter (AVL 415SE).

Table 3.1: Engine specifications

Description	Type
Number of cylinders	2
Bore × Stroke, mm	83×84
Connecting rod length, mm	141
Swept volume, cm^3	909
Compression ratio	18.5
Injection Type	Common rail
Injection pressure, MPa	100
Injection timing	Variable (9°-18° BTDC)
Speed	2000 rpm
Make	Mahindra Maximmo

Table 3.2: Details of the engine instrumentation

	Instrument	Functional use	Measuring technique
i.	Saj test - Eddy dynamometer	Load	Load cell
ii.	PCB piezotronics, pressure transducer	Pressure	Piezo-electric sensor
iii.	Piezo Charge Amplifier	A/D converter	Piezo-electric sensor
iv.	Angle encoder	Crank angle	Magnetic pickup type
v.	AVL Di-gas 444 exhaust gas analyser	NO_X	Chemi-luminescence detector (CLD)
		CO	Non-dispersive infra-red (NDIR)
		HC emissions	Flame ionization detector (FID)
vi.	AVL 415SE	Soot	Opacity
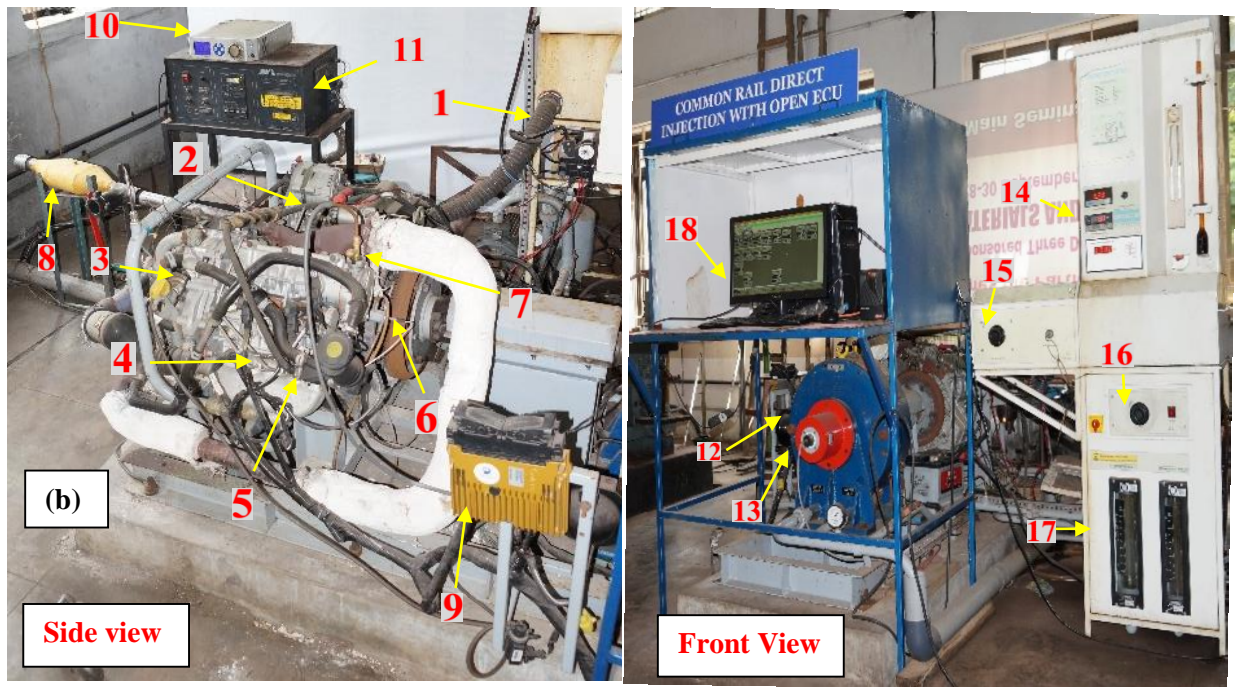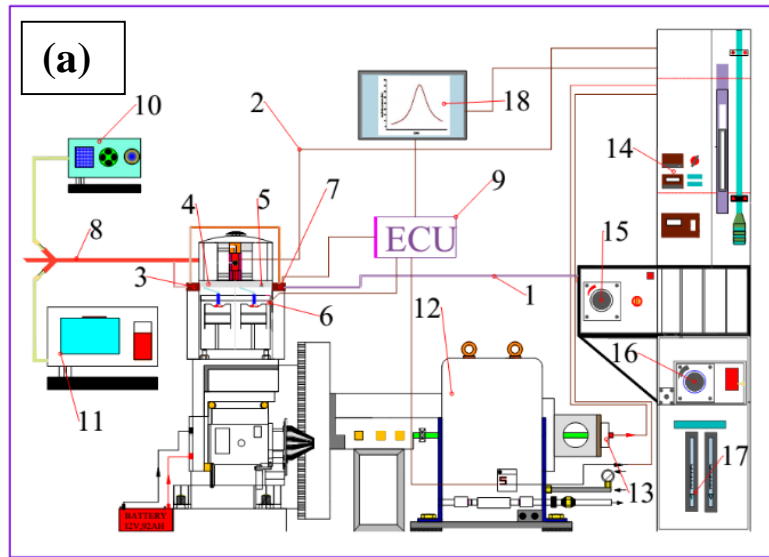
1. Airline, 2. Fuel line, 3. EGR Valve, 4. Common Rail, 5. Pressure control valve, 6. Pressure transducer, 7. Vacuum pump, 8. Exhaust line, 9. ECU, 10. Gas analyzer, 11.Smoke meter, 12. Dynamometer, 13. Encoder, 14. Speed and load display unit, 15. Throttle control unit, 16. Load control unit, 17. Rota meters, 18. Computer display

Fig. 3.1 (a) Schematic diagram and (b) experimental facility

Table 3.3: Operating range of instruments used range and % of uncertainties

Instrument	Measured quantity	Range	Uncertainties (%)
i. Dynamometer	Load	0 – 50 kg	0.1
ii. AVL Di-Gas 444 analyzer	NO$_X$	0 – 5000 ppm	0.1
	CO	0–10 vol.%	0.1
iii. Smoke opacimeter	Smoke opacity	0–100%	1.7
iv. Speed measuring Unit	Engine speed	0–9999 rpm	0.1
v. Pressure transducer	Cylinder pressure	0–345 bar	0.1
vi. Crank angle encoder	Crank angle	0–360°	0.2

3.2 Softwares used in engine setup

For the better accuracy and precision in the measurements of different engine parameter, NIRA i7r open ECU (engine control unit) is deployed in the test rig. NIRA i7r is an effective engine control unit developed by *NIRA control AB* intended to optimize performance of advanced diesel engines. NIRA i7r comes with an application tool to control loading of software program, tuning of engine data, monitoring etc. With these features, the operator gets full access to control the engine functions. Featuring support for advanced fuel injection strategies with multiple injections per stroke, NIRA i7r permits the engine tuner to attain extreme performance while retaining necessary characteristics such as quick engine response time and precise control of torque output. NIRA i7r is also designed to handle sensors and actuators related to Euro V and Tier 4 regulation including EGR and particulate filters. Further, online monitoring and recording of results obtained from the experiments conducted with different engine operating parameters are captured by IC Enginesoft software developed by *Apex Innovations*.

3.3 Error analysis

Assessment of uncertainties and error is necessary while conducting any experimental study. Uncertainties may appear because of numerous reasons like: environmental conditions, calibration, observation, instrument selection and incorrect reading. Error analysis quantifies the accuracy of the experiments being performed. The uncertainties of dependent parameters like brake power, fuel consumption are computed by partial

differentiation method using the uncertainty percentages of various instruments as shown in Table 3.3. The uncertainties for independent parameters were found by calculating the mean, standard deviation and standard error for the repeated set of 20 readings.

The total uncertainty of the experimental investigation

$=$ Square root of { (uncertainty of CO)^2 + (uncertainty of NO)^2 + (uncertainty of soot)^2 + (uncertainty of load)^2 + (uncertainty of speed)^2 + (uncertainty of time)^2 + (uncertainty of brake power)^2 + (uncertainty of fuel consumption)^2 + (uncertainty of brake thermal efficiency)^2 + (uncertainty of cylinder pressure)^2 + (uncertainty of crank angle)^2 + (uncertainty of manometer)^2 }

$$= \sqrt{ \begin{cases} (0.1)^2 + (0.6)^2 + (0.1)^2 + (1.3)^2 + (0.1)^2 + (0.2)^2 + (0.8)^2 \\ + (0.2)^2 + (0.8)^2 + (0.9)^2 + (0.1)^2 + (0.2)^2 + (0.1)^2 \end{cases} } = \pm 2.076 \text{ %}$$

3.4 Experimental Methodology

The present works, research outline is as shown in Figures 3.2 and 3.3
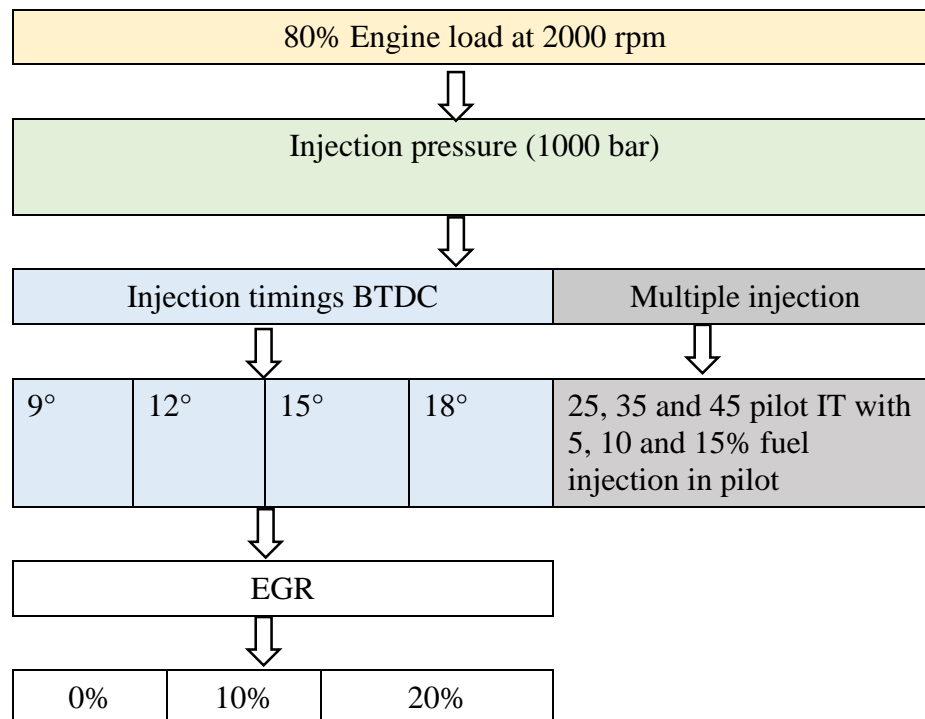
Fig. 3.2 Flow chart of experimental operating parameters

49

Alternative fuels

	Oxygenated fuels			Waste plastics
	DME	Ethanol	Butanol	WPO
Blends (%)	5, 10, 15 & 20	10, 20 & 30	10, 20 & 30	30 & 50
	CFD simulation	CFD simulation	Experimental & CFD sim.	Experimental
	EGR	EGR and IT	EGR and IT	EGR and IT with multiple injection
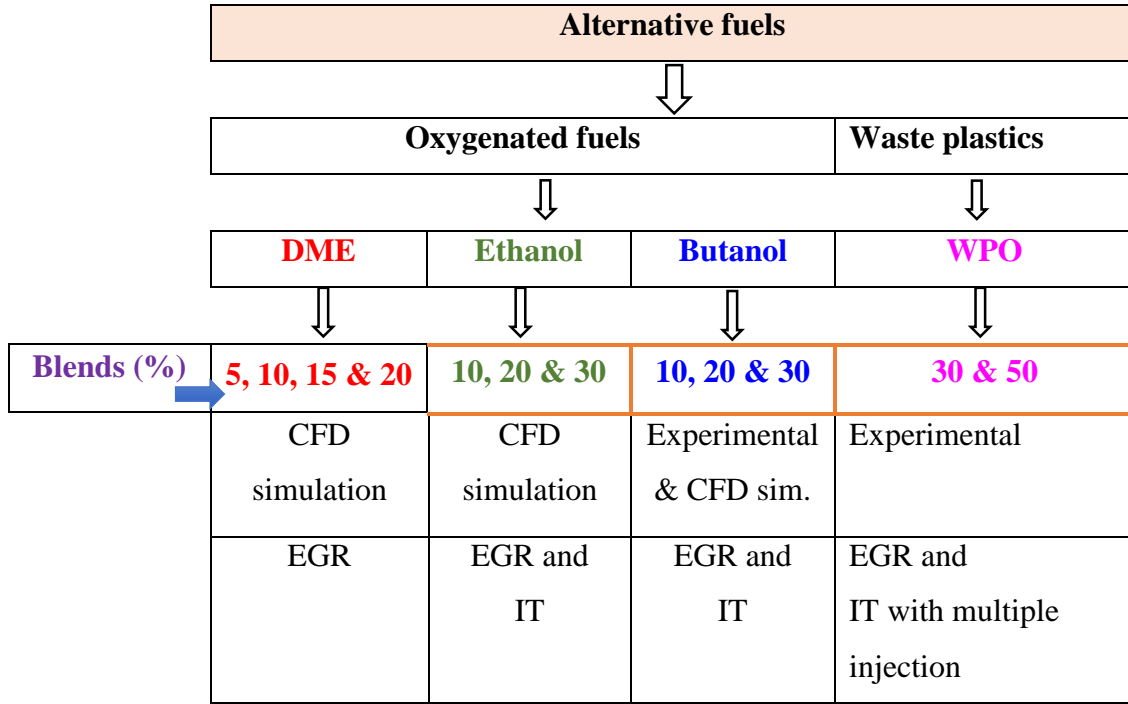
Fig. 3.3 Research strategy

3.5 Computational methodology

This section delivers an outline of the CFD workflow that has been adopted in this research work for simulating in-cylinder physical and chemical processes that govern the engine performance and emission characteristics. The workflow report including the CFD solver and modelling details on the commercial CFD code AVL FIRE is illustrated in this section.

3.6 Governing equations

The transport equations for chemical species modelled as

$$\frac{\partial(\bar{\rho}\tilde{Y}_x)}{\partial t} + \frac{\partial(\bar{u}_i\,\bar{\rho}\tilde{Y}_x)}{\partial x_i} = \frac{\partial}{\partial x_i}\left(\left(\frac{\mu}{S_c} + \frac{\mu_t}{S_{ct}}\right)\frac{\partial\tilde{Y}_x}{\partial x_i}\right) + \bar{\dot{\omega}}_x \tag{3.1}$$

The fuel transport equations are (Colin and Benkenida, 2004)

$$\frac{\partial(\bar{\rho}\tilde{Y}_{Fu}^u)}{\partial t} + \frac{\partial(\bar{\rho}\tilde{u}_i\,\bar{\rho}\tilde{Y}_{Fu}^u)}{\partial x_i} = \frac{\partial}{\partial x_i}\left(\left(\frac{\mu}{S_c} + \frac{\mu_t}{S_{ct}}\right)\frac{\partial\tilde{Y}_{Fu}^u}{\partial x_i}\right) + \bar{\rho}\tilde{\dot{S}}_{Fu}^u + \bar{\dot{\omega}}_{Fu}^u - \bar{\dot{\omega}}_{Fu}^{u\to b} \tag{3.2}$$

$$\frac{\partial(\bar{\rho}\tilde{Y}_{Fu}^b)}{\partial t} + \frac{\partial(\bar{\rho}\,\tilde{u}_i\,\tilde{Y}_{Fu}^b)}{\partial x_i} = \frac{\partial}{\partial x_i}\left(\left(\frac{\mu}{S_c} + \frac{\mu_t}{S_{ct}}\right)\frac{\partial \tilde{Y}_{Fu}^b}{\partial x_i}\right) + \bar{\rho}\tilde{S}_{Fu}^b + \bar{\omega}_{Fu}^b + \bar{\omega}_{Fu}^{u\rightarrow b} \tag{3.3}$$

The equations for these unmixed species are:

$$\frac{\partial(\bar{\rho}\tilde{Y}_{Fu}^F)}{\partial t} + \frac{\partial(\bar{\rho}\,\tilde{u}_i\,\tilde{Y}_{Fu}^F)}{\partial x_i} - \frac{\partial}{\partial x_i}\left(\left(\frac{\mu}{S_c} + \frac{\mu_t}{S_{ct}}\right)\frac{\partial \tilde{Y}_{Fu}^F}{\partial x_i}\right) = \bar{\rho}\tilde{S}_{Fu}^F + \bar{\rho}\tilde{E}_{Fu}^{F\rightarrow M} \tag{3.4}$$

$$\frac{\partial(\bar{\rho}\tilde{Y}_{O_2}^A)}{\partial t} + \frac{\partial(\bar{\rho}\,\tilde{u}_i\,\tilde{Y}_{O_2}^A)}{\partial x_i} - \frac{\partial}{\partial x_i}\left(\left(\frac{\mu}{S_c} + \frac{\mu_t}{S_{ct}}\right)\frac{\partial \tilde{Y}_{O_2}^A}{\partial x_i}\right) = \bar{\rho}\tilde{E}_{O_2}^{A\rightarrow M} \tag{3.5}$$

The amount of mixing is computed with a characteristic time scale based on the k-ε model.

$$\bar{\tilde{E}}_{Fu}^{F\rightarrow M} = -\frac{1}{\tau_m}\tilde{Y}_{Fu}^F\left(1 - \tilde{Y}_{Fu}^F\,\frac{\bar{\rho}M^M}{\bar{\rho}^u|_u M_{Fu}}\right) \tag{3.6}$$

$$\bar{\tilde{E}}_{O_2}^{A\rightarrow M} = -\frac{1}{\tau_m}\tilde{Y}_{O_2}^A\left(1 - \frac{\tilde{Y}_{O_2}^A}{\tilde{Y}_{O_2}^\infty}\,\frac{\bar{\rho}M^M}{\bar{\rho}^u|_u M_{air+EGR}}\right) \tag{3.7}$$

Where, τ_m is the mixing time defined as,

$$\tau_m^{-1} = \frac{\varepsilon}{k} \tag{3.8}$$

The oxygen mass fraction in unmixed air is computed as follows:

$$\tilde{Y}_{O_2}^\infty = \frac{\tilde{Y}_{TO_2}}{1 - \tilde{Y}_{TFu}} \tag{3.9}$$

Turbulent flow and heat transfer:

Since most of the IC engine related fluid flow problems are turbulent in nature, it is of utmost importance to model precisely the phenomenon of turbulence for accurate simulation of real flows. This is essential as turbulence not only determines the particulars of fluid flow but also strongly influences the chemical and physical methods that take

place during mixture formation and combustion. In IC engines the turbulent kinetic energy is a critical factor which predicts the propagation and evaporation of the fuel droplets and also the subsequent combustion of the air/fuel mixture (Tatschl 2012). In addition to the well-known standard turbulence models such as k-ε, Spalart-Allmaras, Reynolds Stress, etc., AVL FIRE offers the recently developed k-ξ-f turbulence model which is validated for IC-engine related flow, heat transfer and combustion processes (Basara 2006).

The k-ζ-f Model:

The k-ζ-f model is employed to treat turbulent flow inside the cylinder. To improve numerical stability, $\overline{v^2} - f$ model needs to be solved for the velocity scale ratio $\zeta = \overline{v^2}/k$ instead of velocity scale $\overline{v^2}$.

The eddy-viscosity is defined as

$$\nu_t = C_\mu \zeta \frac{k^2}{\varepsilon} \tag{3.10}$$

Where $k,\ \varepsilon,\ and\ \xi$ are obtained by solving the following set of model equations,

$$\rho \frac{Dk}{Dt} = \rho(\mathrm{P}_k - \varepsilon) + \frac{\partial}{\partial x_j}\left[\left(\mu + \frac{\mu_t}{\sigma_k}\right)\frac{\partial k}{\partial x_j}\right] \tag{3.11}$$

$$\rho \frac{D\varepsilon}{Dt} = \rho \frac{C_{\varepsilon 1}^* P_k - C_{\varepsilon_2}\varepsilon}{T} + \frac{\partial}{\partial x_j}\left[\left(\mu + \frac{\mu_\varepsilon}{\sigma_k}\right)\frac{\partial \varepsilon}{\partial x_j}\right] \tag{3.12}$$

$$\rho \frac{D\zeta}{Dt} = \rho f - \rho \frac{\zeta}{k} P_k + \frac{\partial}{\partial x_j}\left[\left(\mu + \frac{\mu_t}{\sigma_\zeta}\right)\frac{\partial \zeta}{\partial x_j}\right] \tag{3.13}$$

To obtain f following equation is adopted

$$f - L^2 \frac{\partial^2 f}{\partial x_j \partial x_j} = \left(C_1 + C_2 \frac{P_k}{\zeta}\right)\frac{(2/3 - \zeta)}{T} \tag{3.14}$$

Turbulent time scale T and length scale L are given by

$$T = \max\left(\min\left(\frac{k}{\varepsilon}, \frac{a}{\sqrt{6}C_\mu^v |S|\zeta}\right), C_T\left(\frac{v^3}{\varepsilon}\right)^{1/2}\right)$$

$$L = C_L \max\left(\min\left(\frac{k^{3/2}}{\varepsilon}\right), C_\eta \frac{v^{3/4}}{\varepsilon^{1/4}}\right)$$

Additional modifications to the ε equation is that the constant $C_{\varepsilon 1}$ is dampened close to the wall, thus $C_{\varepsilon 1}^* = C_{\varepsilon 1}\left(1 + 0.045\sqrt{1/\zeta}\right)$.

For flows in IC-engine, the k-ξ-f model not only leads to more accurate result in comparison to the much simpler two-equation eddy viscosity models of the k-ξ-f type, but also exhibits a high degree of numerical robustness. In combination with a hybrid wall treatment as proposed by Popovac and Hanjalic (2005), with standard wall functions, the k-ξ-f turbulence model is universally applicable to computational meshes and flow situations. In this study, the default model for turbulence and turbulent wall heat transfer modelling is the k-ξ-f model. One of the major advantages of using this model is its robustness while performing computations involving grids with moving boundaries and highly compressed flows as it is the case in IC-engines (Tatschl 2012).

Fuel Spray and wall film:

The spray model universally adopted in AVL FIRE for simulations of IC-engine spray and mixture formation is based on the Lagrangian discrete droplet method (DDM). While the standard Eulerian conservation equations describe the continuous gaseous phase, the dispersed phase transportation is calculated by tracking the trajectories of droplet parcels. A parcel consists of a number of droplets which are assumed to have the same physical properties and behave similarly when they move, break up, hit a wall or evaporate.

The standard wave model (Reitz 1987; Naber 1988; Corcione 2001) is used for the atomization modelling. In this model the wave length and other physical and dynamic parameters of the injected fuel and the domain fluid determine the growth of an initial perturbation on a liquid surface. The use of standard wave model with blob injection

(initial droplets have the diameter of the nozzle orifice) for simulation results in lower vaporisation of fuel near the nozzle as the droplets are still large in the beginning and therefore hardly get evaporated. This can be overcome by injecting a bimodal spectrum with about 90 % of the mass as blobs and 10 % as very small droplets that should be coming from the stripping process. This is done automatically by the wave child option. When a user defined mass is shed from the parent droplet, a new child droplet of stable diameter gets created. The differences between these two methods are illustrated in Fig 3.4.

WAVE Standard   WAVE Standard + Child
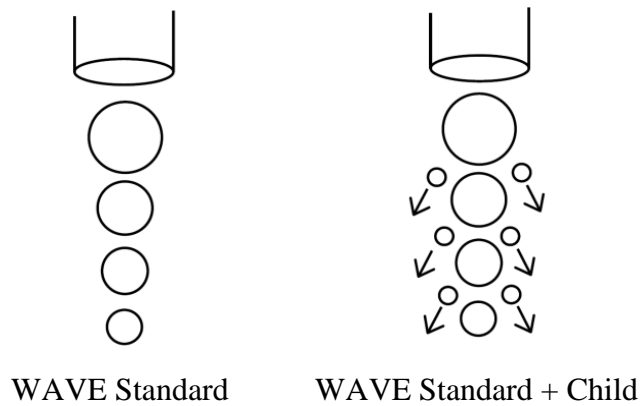
Fig. 3.4 Different ways of WAVE break-up

Wall interaction of liquid droplets plays a major role for diesel engines, especially for small bore diesel engines where the distance between the injector and the bowl is very small. If the large quantity of the fuel is not evaporated or atomized then it will hit the wall which influences the combustion and emissions characteristics, as incomplete combustion in the vicinity of the wall will result in high HC emission emissions and soot particles. The behavior of a droplet at wall interaction depends on several parameters like droplet velocity, diameter, droplet properties, wall surface roughness and wall temperature. At very low inlet velocities the droplet sticks to the wall or to the wall film, whereas for higher inlet velocity a vapor or gas boundary layer is trapped underneath the droplet which causes the liquid to rebound. During rebound, parts of the kinetic energy are dissipated and the outgoing normal velocity is usually lower than the incoming normal velocity and any further increase of the velocity leads either to the

spread or the splash regime. In the spread regime the complete liquid has hardly any normal velocity and is spread along the wall. In the splash regime a part of the liquid remains near the surface and the rest of it is reflected and broken up into secondary droplets (Tatschl 2012).

Evaporation model:

The Dukowicz model which assumes a uniform droplet temperature profile is applied for treating the heat-up and evaporation of the droplets. In addition, the rate of change of droplet temperature is determined by heat balance, it states that the heat convection from the gas to the droplet either heats up the droplet or supplies heat for vaporization. The heat and mass transfer processes are described by a model originally derived by Dukowicz (1979). Essentially it is based on the following assumptions:

- Spherical symmetry

- Quasi steady gas-film around the droplet

- Uniform droplet temperature along the drop diameter

- Uniform physical properties of the surrounding fluid

- Liquid -vapor thermal equilibrium on the droplet surface

In the evaporation model of Dukowicz (1979), it is considered that the droplet is evaporating in a non-condensable gas. Therefore, it uses a two-component system in the gas-phase composed of the vapor and the non-condensable gas, even though each component may consist of a mixture of different species.

Combustion model:

ECFM-3Z model is modified version of ECFM, which is based on flame surface density approach. ECFM features take cares of premixed flame, knock and pollution formation. With ECFM features, ECFM-3Z takes care of diffusion flame and mixing process. In this model, each computational cell is divided into three mixing zones. The three zones are pure fuel zone, air plus EGR zone and mixed zone. Various multi component capacity exist in

three zone extended coherent flame model (Colin and Benkenida, 2004). The schematic representation is shown in the Fig 3.5.

Flame propagation
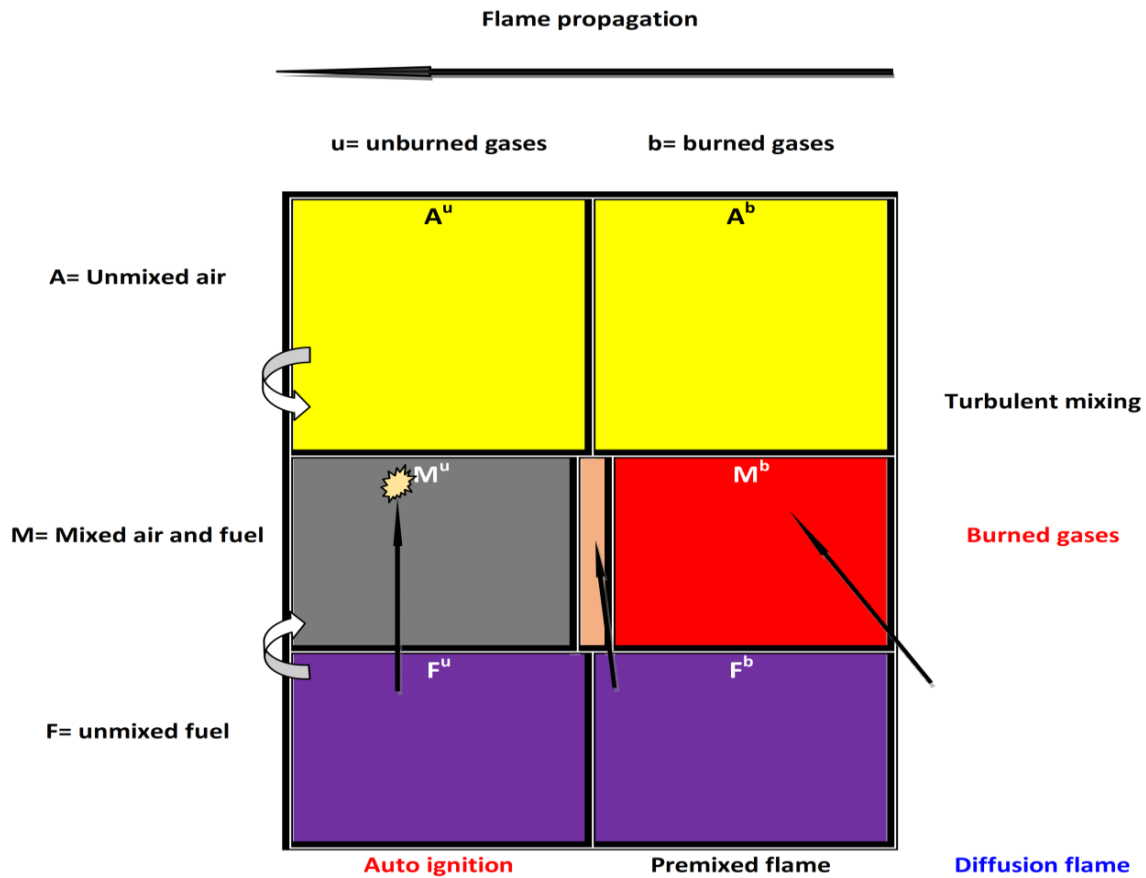
Fig. 3.5 Extended coherent flame model

Boundary conditions and models:

Boundary conditions and models employed in the simulation are listed in Table 3.4 and 3.5 respectively.

Table 3.4 Calculation domain and boundary conditions

Boundary type	Boundary condition	Values
Piston	Moving mesh	Temperature 550 K
Axis	Periodic inlet/outlet	Periodic
Cylinder head	Wall	Temperature 550 K
Compensation volume	Wall	Thermal/Adiabatic boundary
Liner	Wall	Temperature 425 K

Table 3.5 Models employed in CFD simulation

Model	Options
Turbulence model	*k-ζ-f model*
Breakup model	Wave
Turbulent dispersion model	Enable
Wall treatment	Hybrid wall treatment
Wall impingement model	Walljet 1
Heat transfer wall model	Standard wall function
Evaporation model	Dukowicz and Multi component model
Combustion model	CFM
Ignition Model	ECFM-3Z
Soot formation and oxidation	Kinetic model
NO_x mechanism	Extended Zeldovich
Chemistry solver	Fire internal chemistry interpreter (CHEMKIN-II)

3.7. Pollutant model

NO_x contains nitrogen oxide as a major component in IC engine emissions. Formation of NO_x during combustion is due to three main sources (Kuo 1986; Heywood 1998): (a) Thermal NO_X, (b) Prompt NO_X and (c) Fuel NO_X.

The transport equation model for NO_X is given by

$$\frac{\partial(\bar{\rho}\tilde{Y}_{NO})}{\partial t} + \frac{\partial(\bar{u}_i \bar{\rho}\tilde{Y}_{NO})}{\partial x_i} = \frac{\partial}{\partial x_i}\left(\bar{\rho}D_t \frac{\partial \tilde{Y}_{NO}}{\partial x_i}\right) + \bar{S}_{NO} \tag{3.15}$$

The term $\bar{S}_{NO}$ represents source term for NO_X formation in the equation.

$$\bar{S}_{NO} = M_{NO}\left(\frac{dc_{NO\,thermal}}{dt} + \frac{dc_{NO\,prompt}}{dt}\right) \tag{3.16}$$

Where, $\bar{\rho}$, $\tilde{Y}_{NO}$, $\tilde{u}_i$, x_i, and D_t are Reynolds averaged fuel density, the mean mass fraction of NO_x, density-weighted average velocity, cartesian coordinates and diffusion coefficient respectively.

The terms M_{NO}, $\dfrac{dc_{NO\,thermal}}{dt}$ and $\dfrac{dc_{NO\,prompt}}{dt}$ in the equation (3.16) are molar mass NO_X, rate of formation of thermal NO_X and rate of formation of prompt NO_X respectively.

3.7.1. Zeldovich Mechanism (Thermal NO$_X$ mechanism)

In the combustion of clean fuels with air, NO_X is formed mainly by the Zeldovich Mechanism. This mechanism consists of three principal reactions as follows:

Table 3.6 Reaction rates for NO formation mechanism in $m^3/k\,mol.s$, and T in K.

Reaction	Forward	Reverse
$N_2 + O \underset{k_{1b}}{\overset{k_{1f}}{\longleftrightarrow}} NO + N$	$k_{1f} = 1.8\times10^{11}\exp(-38370/T)$	$k_{1b} = 3.8\times10^{10}\exp(-425/T)$
$O_2 + N \underset{k_{2b}}{\overset{k_{2f}}{\longleftrightarrow}} NO + O$	$k_{2f} = 1.8\times10^{10}\exp(-4680/R_u T)$	$k_{2b} = 3.8\times10^{9}\exp(-20820/T)$
$N + OH \underset{k_{3b}}{\overset{k_{3f}}{\longleftrightarrow}} H + NO$	$k_{3f} = 7.1\times10^{10}\exp(-450/T)$	$k_{3b} = 1.7\times10^{11}\exp(-24560/T)$

The first equation in Table 3.6 is known as thermal mechanism as it requires very high activation energy (319 kJ/mol) due to the strong triple bond, and so the dissociation is sufficiently fast at high temperatures. NO_X is generally considered to be formed in the post – flame region. In general, this mechanism is coupled with the fuel combustion chemistry through the O_2, O, and OH species. Table 3.6 describes the NO_X formation reactions (Kuo 1986). The nitrogen reacts with the atomized oxygen O created due to the high combustion temperature. Unstable nitrogen of the initial reaction further oxidizes and forms NO_X.

The rate of NO_X formation for the reactions mentioned in the Table 3.4 is as follows (Pundir 1986).

$$\frac{d}{dt}[NO] = k_{1f}[O][N_2] - k_{1b}[NO][N] + k_{2f}[N][O_2] - k_{2b}[NO][O] + k_{3f}[N][OH] - k_{3b}[NO][H] \quad (3.17)$$

Where [ ] denotes the concentration of species moles/m^3. By using the Arrhenius law (equation 3.18), reaction rate coefficients k_{1f}, k_{1b}, k_{2f}, k_{2b}, k_{3f} and k_{3b} are modelled (Petranovic et al. 2014). Where, subscripts f and b represent the forward and backward reaction respectively. Arrhenius equation is given by,

$$k = AT^\beta \exp\left(-\frac{E_a}{RT}\right) \quad (3.18)$$

Where, the coefficients *A, b* and E_a (activation energy) are determined from the experimental data (Vujanovi 2009). *T* is the absolute temperature and *R* is the universal gas constant. Using the quasi-steady assumption, the overall rate of the thermal NO_X formation is modelled as shown in Equation (3.19).

$$\frac{dc_{NO\,thermal}}{dt} = 2k_{1f}c_O c_{N_2} \frac{\left(1 - \frac{k_{1b}k_{2b}c_{NO}^2}{k_{1f}c_{N_2}k_{2f}c_{O_2}}\right)}{\left(1 + \frac{k_{1b}c_{NO}}{k_{2f}c_{O_2} + k_{3f}c_{OH}}\right)} \quad (3.19)$$

Where, the term c_i denotes the concentration of a species i.

3.7.2 Prompt NOx Mechanism (Fenimore Mechanism)

Prompt NOx formation occurs at early stage of fuel rich regions of the flames. The prompt NOx is formed in the flame by reaction of intermediate chemical species of cyanide *(CN)* group with O and OH radicals. The hydrocarbon radicals *CH, CH₂, C, C₂* etc. formed in the flame front react with molecular nitrogen to give intermediate species such as hydrogen cyanide *(HCN)* and *CN*. The reactions are initiated by the hydrocarbon radicals due to fuel fragmentation in the presence of nitrogen. As the result, *HCN* is produced with the dissociation of nitrogen. *CH* and *CH₂* hydrocarbon radicals are the major contributors for prompt NOx formation process. Modelling approach for prompt NOx is as follows (Pundir 1986).

$$Fuel \rightarrow CH, CH_2 \tag{3.20}$$

$$CH + N_2 \leftrightarrow HCN + N \tag{3.21}$$

$$CH_2 + N_2 \leftrightarrow HCN + NH \tag{3.22}$$

$$N + O_2 \leftrightarrow NO + O \tag{3.23}$$

$$HCN + OH \leftrightarrow CN + H_2O \tag{3.24}$$

$$CN + O_2 \leftrightarrow NO + CO \tag{3.25}$$

Various hydrocarbon species are formed as the result of fuel fragmentation as shown in Equation (3.20). *HCN* is produced as the result of combining *CH* and *CH₂* radicals with the nitrogen. The expression for the rate of prompt NOx formation (Vujanovi 2009) is given by,

$$\frac{dc_{NO \text{ prompt}}}{dt} = FA_p \left(c_{O_2}\right)^b c_{N_2} c_{\text{fuel}} \exp\left(-\frac{E_a}{RT}\right) \tag{3.26}$$

Where, *F* is the correction factor, A_p is pre-exponential factor and *b* is the order of reaction for the molecular oxygen.

Mechanism for soot formation:

The transport equation model for soot mass fraction ϕ_s is given by

$$\frac{\partial}{\partial t}\left(\bar{\rho}\tilde{\phi}_s\right) + \frac{\partial}{\partial x_j}\left(\bar{\rho}\bar{u}_j\bar{\phi}_s\right) = \frac{\partial}{\partial x_j}\left(\frac{\mu_{eff}}{\sigma_s}\frac{\partial\bar{\phi}_s}{\partial x_j}\right) + S_{\varphi_s} \tag{3.27}$$

Soot formation rate is defined as

$$S_{\varphi_s} = S_n + S_g + S_{o_2} \tag{3.28}$$

Where, S_n = Soot nucleation, S_g = Soot growth, and S_{o_2} = Soot oxidation

Exhaust gas recirculation:

The EGR rate in steady state operation can be defined as the ratio of EGR mass flow rate $\left(\dot{m}_{egr}\right)$ and the total intake mass flow rate $\left(\dot{m}_{intake}\right)$.

$$\dot{m}_{intake} = \dot{m}_{air} + \dot{m}_{egr} \tag{3.19}$$

$$EGR = \dot{m}_{egr} / \dot{m}_{intake} \tag{3.20}$$

CHAPTER 4

INFLUENCE OF DME-DIESEL BLENDS WITH EGR IN CRDI ENGINE: A CFD STUDY

4.1 Introduction

The present study emphasizes the effect of dimethyl ether (DME)- diesel blends (0-20%) at various exhaust gas recirculation (EGR) rates (0-20%) on the performance, combustion characteristics and exhaust emissions of CRDI engine using three dimensional computational fluid dynamics (CFD) simulation. The CFD simulation is carried out for a four stroke CRDI engine to better comprehend the in-cylinder combustion.

4.2 Engine details

CRDI engine used by Mobasheri et al. (2012) and Han et al. (1996) is considered for CFD simulation in the present work. The details of the engine and injection system are listed in Table 4.1 & Table 4.2 respectively.

Table 4.1: Engine specifications

Engine Parameters	Values
Bore $\times$ Stroke	0.13719 m $\times$ 0.1651 m
Compression ratio	15.1:1
Connecting rod length	0.26162 m
Displacement	2441 cm^3
IVO/IVC	32° BTDC / 147° BTDC
EVO/EVC	134° ATDC / 29° ATDC
Engine speed	1600 RPM
IMAP	184 kPa
IMAT	310 K

Table 4.2: Injection system specifications

Injector Parameters	Values
Injector type	Common Rail
Injection Pressure	90 MPa
Number of nozzle holes	6
Nozzle hole diameter	0.00026 m
Injection duration	21.5° CA
Start of injection	9° BTDC
Fuel injected	0.0001622 kg/cycle

4.3 Fuel properties

The key properties of diesel and DME fuels are listed in the Table 1.3 in chapter 1.

4.4 CFD code and meshing of geometry

AVL ESE CFD tool is used for engine geometric modelling and meshing as portrayed in Fig. 4.1. Complete 3-dimensional CFD simulation is carried out using the AVL platform (FIRE v 2011). The injector with 6 holes is situated centrally on the top of piston, hence 60° sector is selected as computational domain. In order to reduce the computational time high pressure cycle is considered in the present work. Simulation is started and ended at inlet valve close and exhaust valve open position respectively. Grid independence test has been carried out to obtain optimum grid size as shown in Figures 4.2 (a) and (b). Simulation is carried out on 64 GB RAM 32 core work station with parallel processing. Results have been checked for peak pressure, peak temperature and computational time for various grid sizes. It is found that the considered output parameters are invariant with change in total number of grids at/after 4×10^5. Boundary conditions and models employed in the simulation are listed in Table 3.4 and 3.5 respectively.
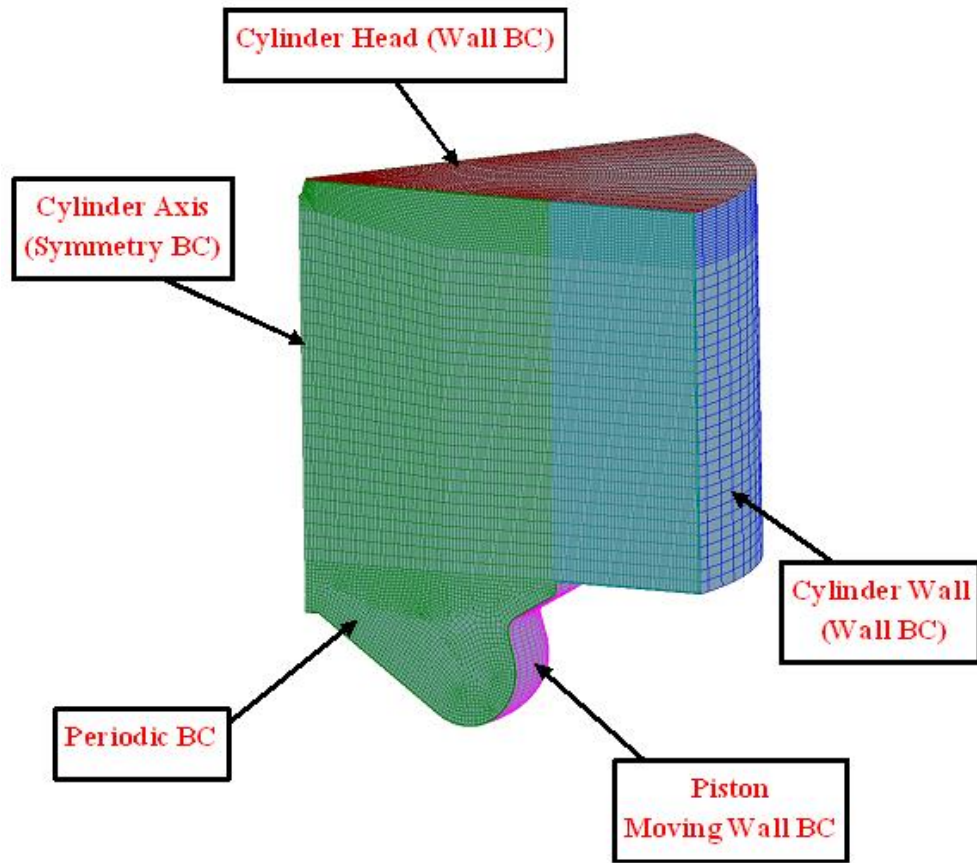
Fig. 4.1 Three dimensional computational domain at TDC position
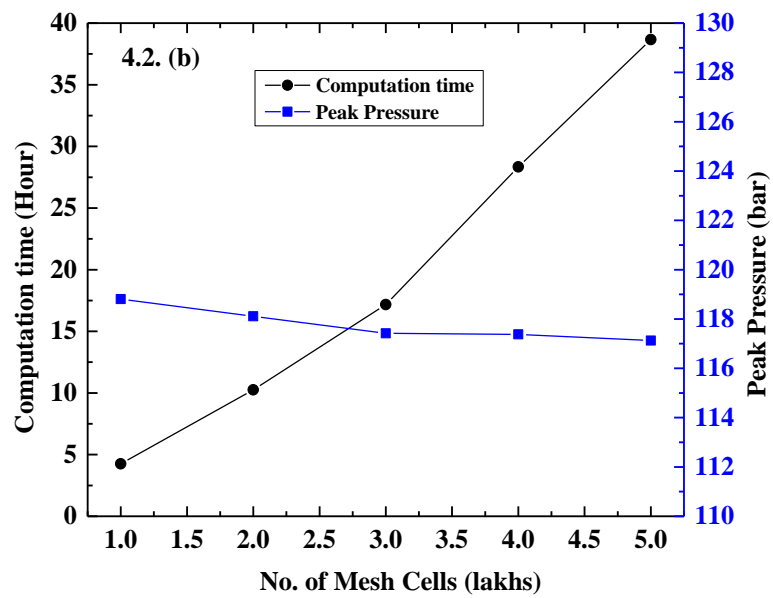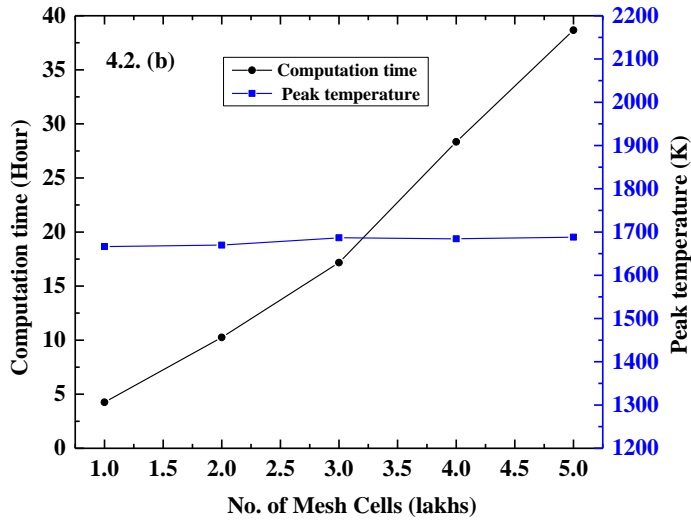
Fig. 4.2 Grid independence study carried out for (b) peak pressure (c) peak temperature

4.5 Validation

In the present study, engine simulation software AVL-FIRE is coupled with CHEMKIN-II with detailed reaction mechanisms. The simulation is validated from the literature Mobasheri et al. (2012) and Han et al. (1996) for conditions listed in Table 4.1 & Table 4.2.
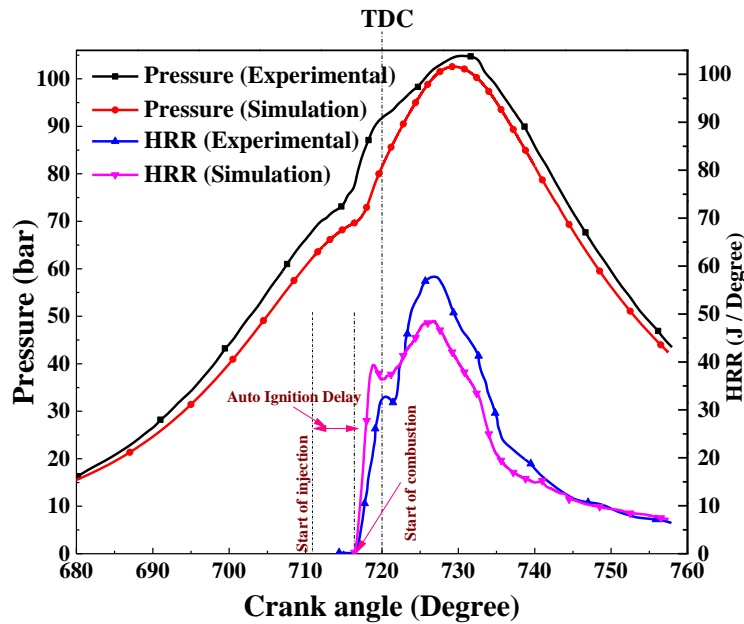
Fig. 4.3 In-cylinder pressure versus crank angle for validation with experimental results
Results are obtained for in-cylinder pressure and heat release rate versus crank angle portrayed in Fig 4.3. Simulation results show a good agreement with published experimental data.

4.6 Results and discussion

Results are obtained for various DME-diesel blends ratio (0, 5, 10, 15, 20%) at various EGR rates (0, 5, 10, 15, 20%) using three dimensional CFD simulation. Amount of the fuel injected is kept constant (0.0001622 kg/cycle) in all the cases.

4.6.1 Effect on engine performance

The effect of low temperature combustion and DME-diesel blend ratio on performance of CRDI engine is demonstrated in Fig 4.4. The higher cetane number, more oxygen content, active evaporation and low viscosity improve combustion characteristics for DME-diesel operations compared to the neat diesel (DME0). Results show the increase of ITE with DME-diesel blends and found to be highest in the case of DME20 EGR (5-10%). The adverse effect of EGR rate on ITE is insignificant in the case of DME-diesel blends and becomes significant in neat diesel operations.
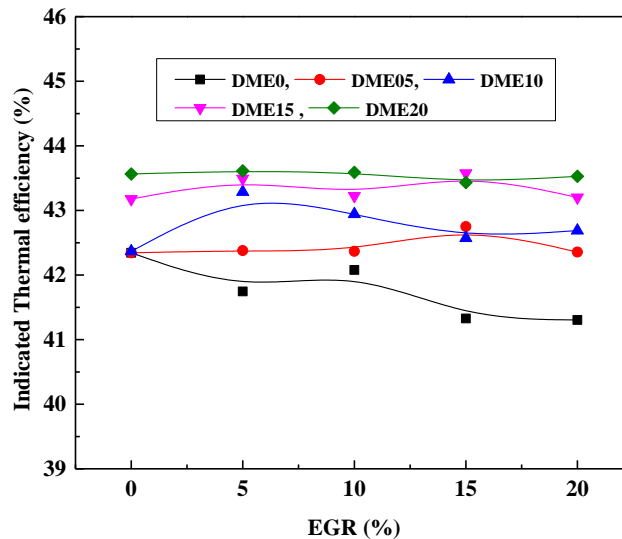
Fig. 4.4 Effects of DME-diesel blends ratio and EGR rate on ITE

4.6.2 Effect on in-cylinder pressure

Figure 4.5 (a) and (b) show the effect of the DME-diesel blends and EGR rates on in-cylinder pressure respectively. As DME-diesel blends ratio increases, the in cylinder peak pressure also increases as shown in the Fig 4.5 (a).
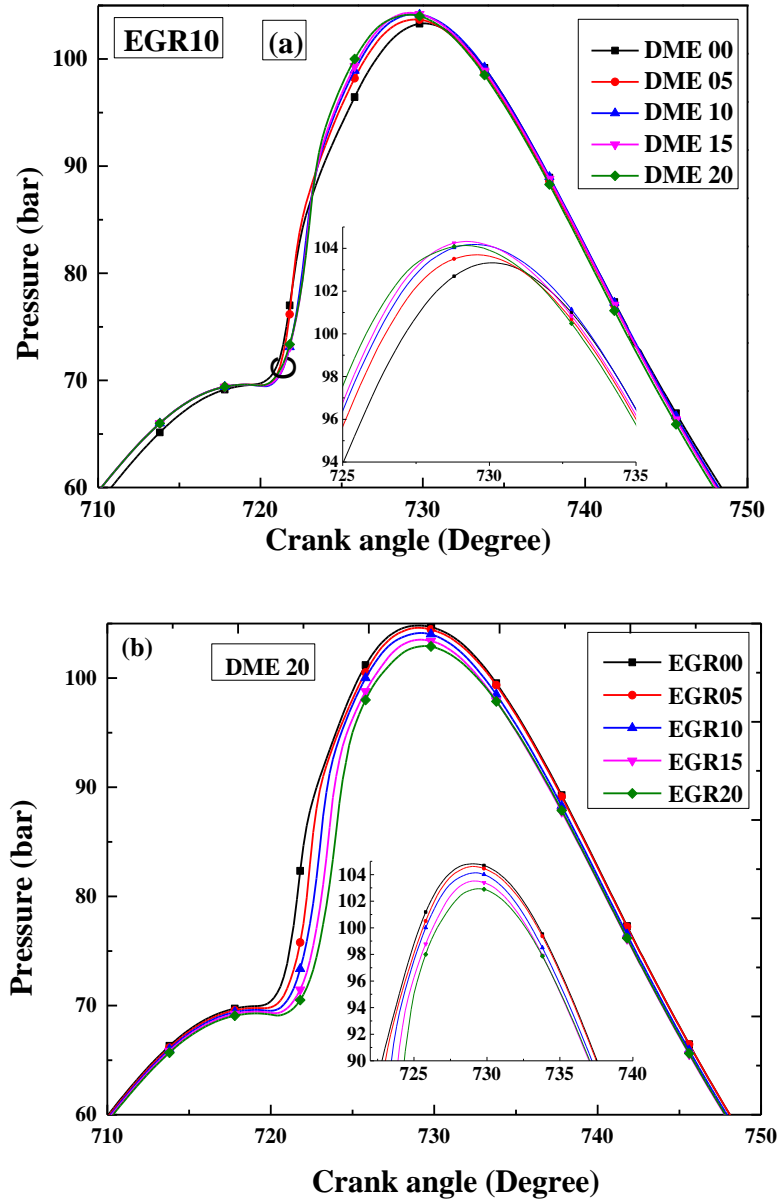
Fig. 4.5 In-cylinder pressure vs crank angle (a) Effects of various DME-diesel blends (b) Effect of various EGR rate

It occurs due to decrease in ignition delay with addition of DME. For all the cases, ignition delay increases with increase in EGR rates due to reduction in oxygen availability and increase in specific heat capacity of mixture as exhaust gas contains species of higher specific heat capacity. Hence, cylinder pressure decreases as EGR rate increases due to combustion delay.

4.6.3 Effect on in-cylinder temperature

Figure 4.6 (a) and (b) show the effect of EGR and various DME blends on in-cylinder temperature respectively. The cylinder temperature is one of the core features for controlling the auto-ignition process. EGR decreases the oxygen concentration in combustion chamber, and circulates the gases like H_2O and CO_2 of very high specific heat capacity. This composition acts like a thermal sink and reduces the adiabatic flame temperature of the cylinder. As EGR rate varies from 0-20%, the peak value of in-cylinder mean temperature decreases. In-cylinder temperature is found more for higher DME-diesel blend ratio due to better combustion as explained above in Fig 4.4.
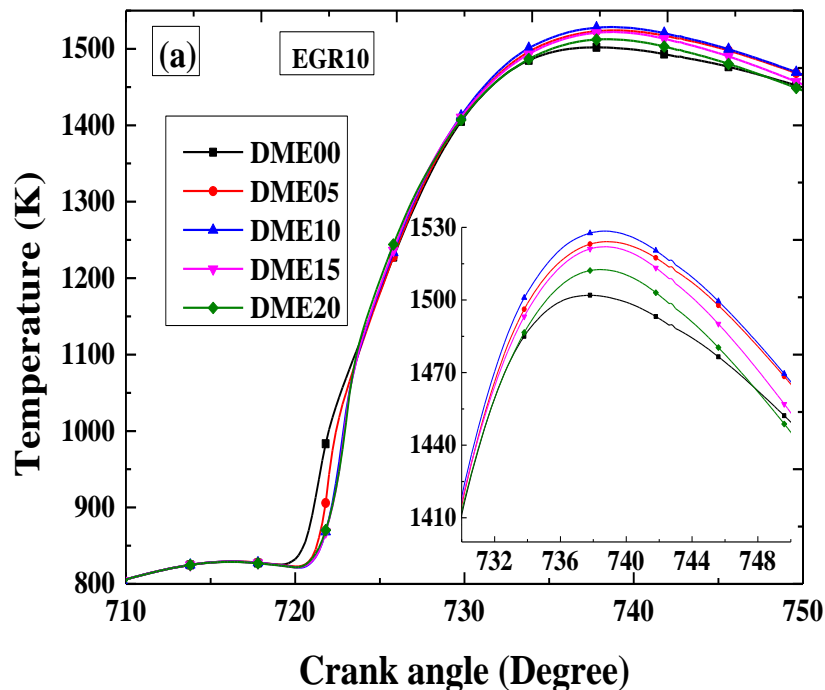
Fig. 4.6 (a) Effects of DME- diesel blends ratio on in-cylinder temperature
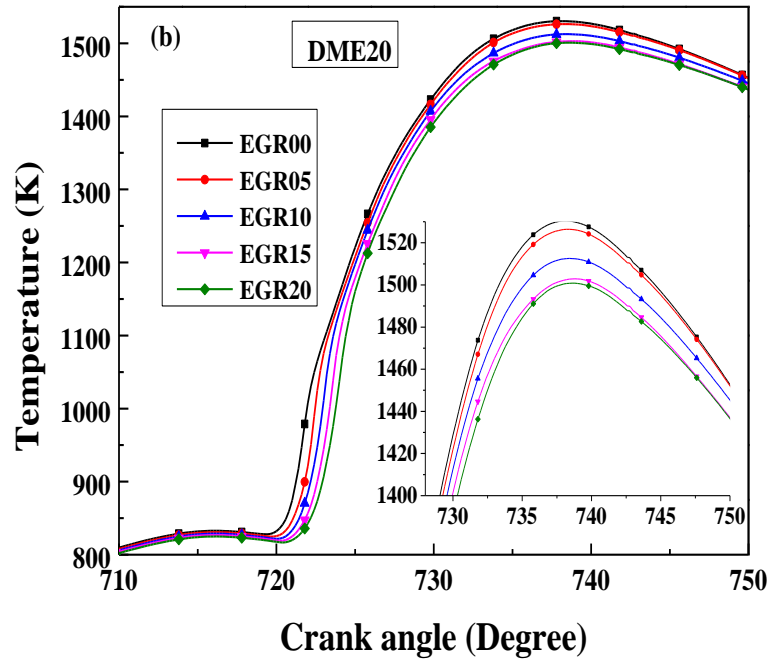
Fig. 4.6 (b) Effects of EGR rate on in-cylinder temperature

4.6.4 Effect on in-cylinder CO formation

Figure 4.7 shows the illustration of the CO formation for various DME-diesel blends at different EGR rates.
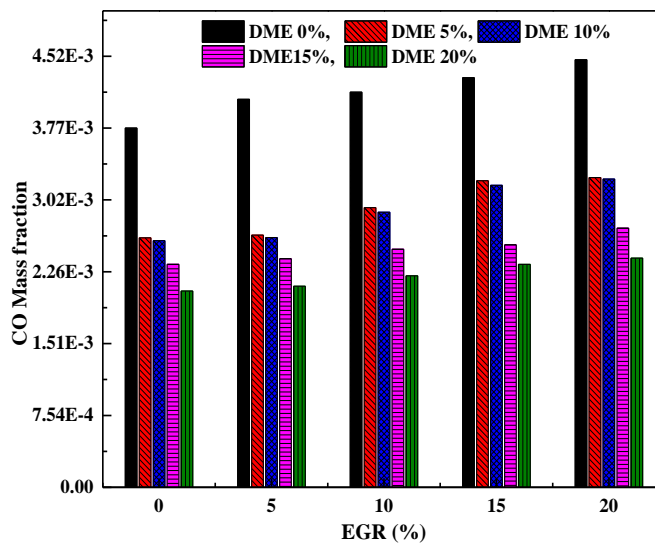
Fig. 4.7 Effects of DME-diesel blends ratio and EGR rate on CO mass fraction

CO formation trend is similar for all cases; it decreases with increase in DME-diesel blends and increases with EGR rates. Less CO formation is observed for DME20 blend with 5% EGR rate and found to be reduced by 48% compared to neat diesel without EGR. It occurs due to extra oxygen present in DME which causes oxidation of CO.

4.6.5 Effect on NOx formation

The key parameters to nitrogen oxide formation are local temperature, residence time and concentration of oxygen in higher flame temperature zone. Figure 4.8 shows the well-established advantage of EGR in decreasing NOx emissions from diesel engine. For all DME-diesel blends (0-20%) and EGR rates (0-20%), NO_X formation is marginally higher than neat diesel due to higher in-cylinder temperature as explained in Fig 4.6 (b). Similar trend is also observed by Kim et al. (2008). More cetane number and fuel bounded oxygen of DME compared to diesel result in higher NO_X formation. Less NO_X formation is observed for EGR20 for all DME-diesel blends compared to EGR0 case. It has been noticed that there is a significant drop in NO_X formation approximately by 60% (overall) due to EGR.
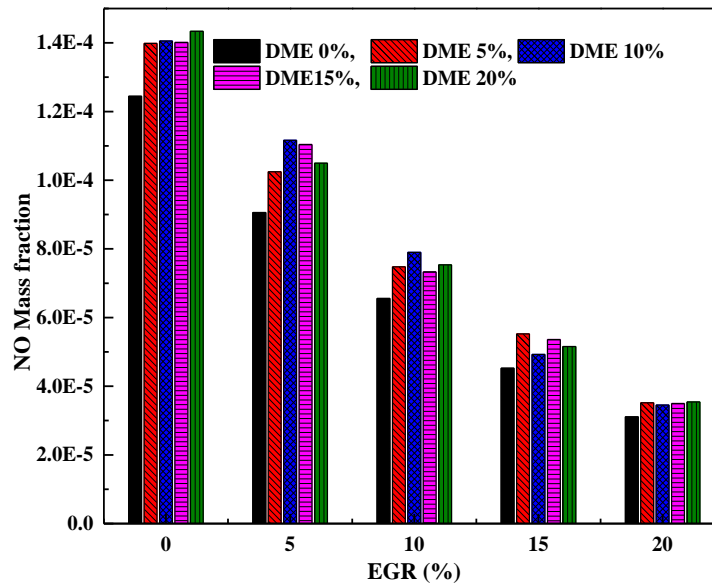
Fig. 4.8 Effects of DME-diesel blends ratio and EGR rate on NO_X mass fraction

4.6.6 Effect on soot formation

Figure 4.9 shows the effect of DME-diesel blend and EGR rate on soot formation. The DME-fuelled engine exhausts very less soot emissions due to its chemical compositions. Formation of soot occurs in rich fuel and medium temperature zone. The precursors of soot i.e., acetylene and polycyclic aromatic hydrocarbons (PAH) play a key role in soot formation (Jeon et al. 2014). The formation of the precursors depends largely on radicals with carbon-carbon bonds in the fuel chemical structure (Ying et al. 2008).
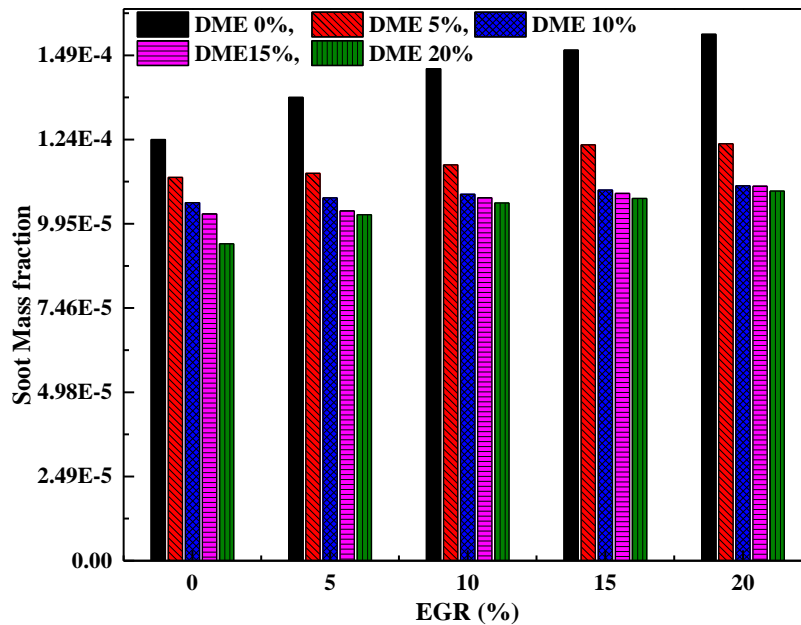
Fig. 4.9 Effects of DME-diesel blends ratio and EGR rate on Soot mass fraction

The chemical structure for DME (CH_3-O-CH_3) contains no C-C bonds and has more oxygen content which causes high particulate oxidation and suppresses soot formation. EGR decreases the oxygen concentration inside the combustion chamber which leads to a partial combustion and the high soot formation. It is observed that in-cylinder soot formation increases with increase in EGR rate. Obtained results are compared with neat diesel without EGR case. Less soot formation (25%) is observed for DME20 blend compared to DME0 for without EGR case. As EGR increases the effect of blends on soot formation is not significant. In the present range of study, it is noticed that the effect of

blends (10, 15 and 20%) on reduction in soot formation at 20% EGR is almost constant. Soot formation takes place due to the combined effect of in-cylinder temperature as well as oxygen content in the charge. Increase in oxygen content enhances the soot oxidation whereas reduction in temperature increases the soot formation. In-cylinder temperature decreases due to EGR rates as shown in figures 4.6 (a) and (b), whereas oxygen contents increase with blends and decreases with EGR. Finally, the overall effect of these parameters on soot formation is marginal at EGR rates.

4.6.7 Improved Exhaust emissions trade off

Figure 4.10 (a) and (b) illustrate the normalized emissions (NO_X, Soot and CO) versus EGR rates and DME-diesel blends respectively. Normalized emission values for all the cases are obtained with respect to the diesel fuel. By comparing the considered parameters, a trade-off can be established to optimize the operating conditions near to 10% EGR.
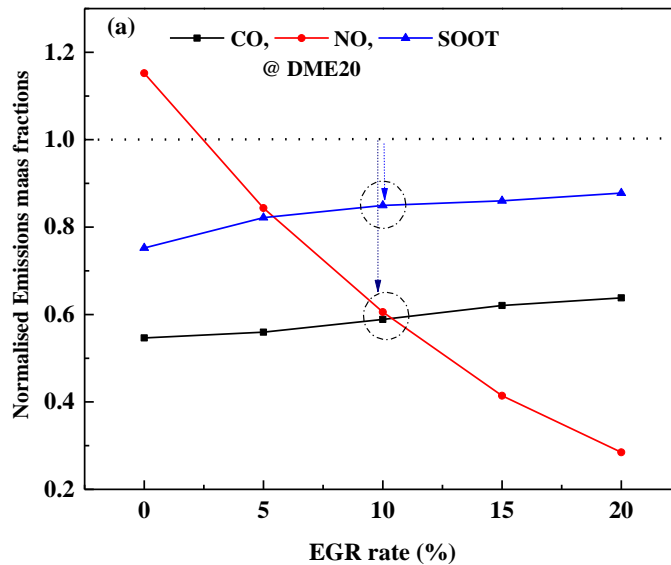
Fig. 4.10 (a) Trade-off among exhaust emissions (NO_X, CO, Soot) for DME20 at various EGR rate

Based on emission norms, higher EGR (20%) can be considered with minor loss of efficiency to get lower value of NOx. As discussed above, maximum efficiency is obtained

73

at DME20 in present range of study. Figure 4.10 (b) shows that the CO and soot emissions are minimum with marginal increases in NO_X for DME20. From the present study, it can be concluded that DME20 with EGR20 yields optimum performance with less emissions.
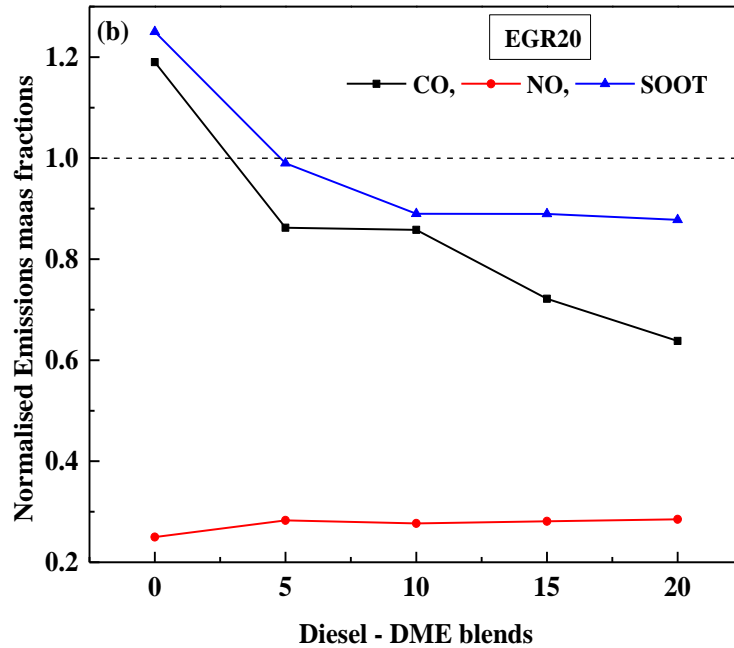
Fig. 4.10 (b) Trade-off among exhaust emissions (NO_X, CO, Soot) for EGR 20 rate at various DME-diesel blends

4.7 Conclusions

In the present study, CFD simulation is carried out to determine the effects of DME-diesel blend ratio and EGR rates on the performance, combustion and exhaust emission characteristics of CRDI engine. The results are summarized as follows:

i.   The cylinder pressure increases as the DME-diesel blend ratio increases.

ii. As EGR rate varies from 0 to 20%, the tail pipe NO_X emission decreases due to decrease in peak in-cylinder temperature.

iii. In post flame combustion, soot concentration increases marginally with an increase in EGR rate.

iv. Compared to neat diesel, CO and soot formations are less for all the cases of DME- diesel blends.

v. Effect of EGR on CO and soot formations are less for all the cases of DME-diesel blends compared to neat diesel.

vi. Least soot formation is observed for higher blend (DME20) without EGR rate and found to be decreased by 22% compared to neat diesel.

vii. In the present range of study, maximum efficiency is obtained at higher DME-diesel blend ratio (DME20) compared to other blends including neat diesel.

viii. Trade-off among exhaust emissions (CO, NO_X, soot) and efficiency establishes the optimum operating condition i.e., DME20 and EGR10.

CHAPTER 5

PART I: EFFECT OF BIOETHANOL-DIESEL BLENDS WITH EGR IN CRDI ENGINE: A CFD STUDY

5.1. Introduction

This investigation is focused on the effect of bioethanol-diesel blends with exhaust gas recirculation (EGR) on the combustion and exhaust emission characteristics of CRDI engine using CFD simulation. Simulation is carried out for various EGR rates (10%, 20%, and 30%) and two different bioethanol-diesel blends (10% and 20%) at two different injection timings (9° and 14° BTDC). Results show a significant effect of injection timing on in-cylinder pressure; hence it is essential to study the effect of injection timing on combustion characteristics of CRDI engine in detail. In view of this, Part-II is added in this chapter which focuses mainly the effect of injection timings with bioethanol-diesel blends on CRDI engine.

The governing equations, transport equations for chemical species, details of engine specification, computational geometry and meshing, grid independence study (GIS) and validation with experimental results are discussed in sections 3.6, 3.7, 4.2, 4.4 and 4.5 of chapter 3 and 4.

5.2 Fuel properties and simulation parameters

Bioethanol-diesel blend is considered in the present study with 0 to 20% by mass basis of bioethanol. The neat diesel and ethanol fuel properties are listed in the Table 1.3 in chapter 1. Range of simulation parameters considered for the study is given in Table 5.1.

Table 5.1 Range of simulation parameters

Parameters	Range
Blend (% of Bioethanol)	0, 10, 20
EGR (%)	0, 10, 20, 30
Injection timings	9° and 14° BTDC
Equivalence ratio	0.47

5.3 Results and discussion

5.3.1 Effect of EGR rates on in-cylinder pressure

Figure 5.1 (a) and (b) show the in-cylinder pressure development during combustion of 10% bioethanol-diesel blend with EGR rates for injection timing 9° and 14° BTDC respectively. Due to exhaust gas recirculation various effects on fuel charge such as dilution effect, ignition delay effect, chemical effect and thermal effects lead to marginal (1%) decrease in peak pressure in both the cases (9° and 14° BTDC).

On the other hand, it is observed that advancing injection timing (14° BTDC) yields higher in-cylinder pressure (~15%) for neat diesel as well as bioethanol-diesel blends. It occurs due to higher ignition delay which leads to better mixing and forms proper combustible mixture. As combustion starts, more fuel (accumulated fuel) burns instantly.

Fig. 5.1. Effect of various EGR rate with 10% bioethanol-diesel blend on in-cylinder pressure for injection timings (a) 9° BTDC and (b) 14° BTDC

5.3.2 Effect of blends on in-cylinder pressure

The diesel engine combustion is partially premixed and partially diffusive. Figure 5.2 (a) and (b) show the in-cylinder pressure development during combustion of various fuel blends with 20% EGR rate for injection timing 9° and 14° BTDC respectively. The in-cylinder peak pressures for the blends and neat diesel are almost same in each case of the

78

injection timings. Due to lower calorific value of bioethanol it was expected to get lower peak pressure compared to neat diesel, but due to additional oxygen contents and low viscosity which results in better combustion and spray characteristics of bioethanol, almost same pressure is obtained.
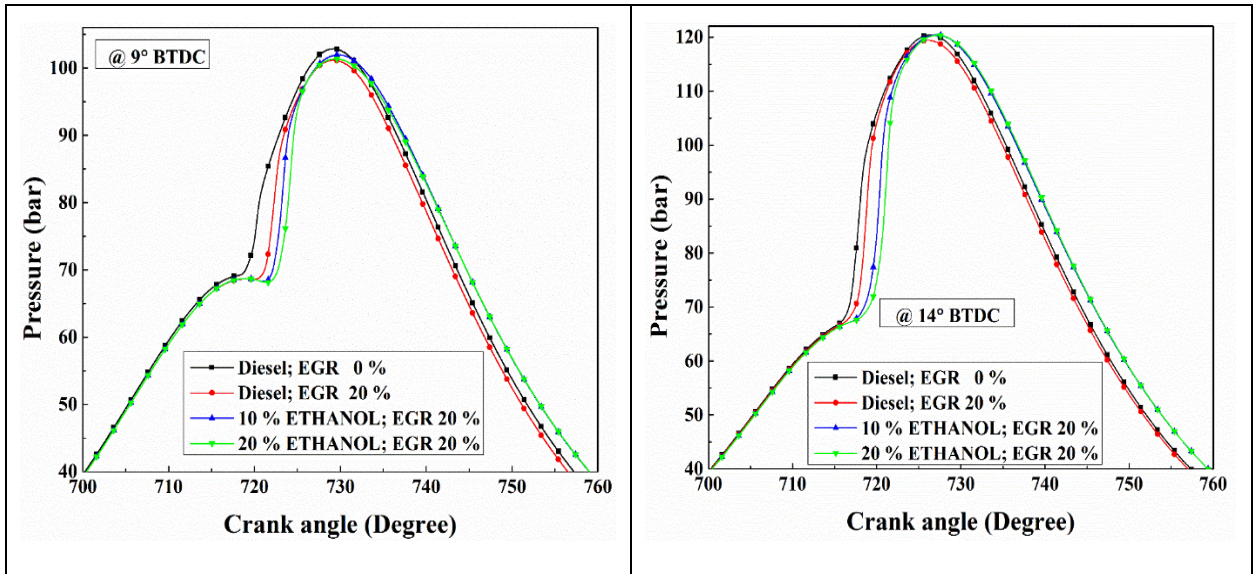
Fig. 5.2. Effect of various bioethanol-diesel blends with 20% EGR rate on in-cylinder pressure at (a) 9° BTDC (c) 14° BTDC injection timing

5.3.3 Effect of EGR rates on in-cylinder temperature

Figure 5.3 (a) show the in-cylinder temperature during combustion of 10% bioethanol-diesel blend with different EGR for injection timing 9° and 14° BTDC respectively. EGR reduces the oxygen percentage in combustion chamber results in decrease in temperature due to a dilution effect, thermal, and chemical effects. Specific heat capacity of the fuel mixture increases due to more CO_2 percentage, which reduces the adiabatic flame temperature. Higher in-cylinder peak temperature difference (90K) is observed in the case of 14° BTDC compared to 9° BTDC injection timing. Fig 5.3 (b) shows the contour plot of in-cylinder temperature at various crank angles (706°, 720° (TDC), 730°, 740°). 3-D temperature contours for 10% bioethanol-diesel blend with different EGR rates at injection timing of 14° BTDC are presented. These contour plots exhibit the clear picture of combustion process occurring inside the cylinder. The in-cylinder temperature contours

79

offer an opportunity to achieve a deeper insight into in-cylinder temperature distribution for bioethanol-diesel blend. At TDC (720°), combustion is witnessed up to 10% EGR rate, whereas for 20% and 30% EGR no combustion is viewed due to more diluition effect. After 730°, flame is propagating on the top of the piston surface and results in diffusion combustion in all the cases. In the case of higher EGR (20% and 30%), peak temperature is found less compared to low EGR.
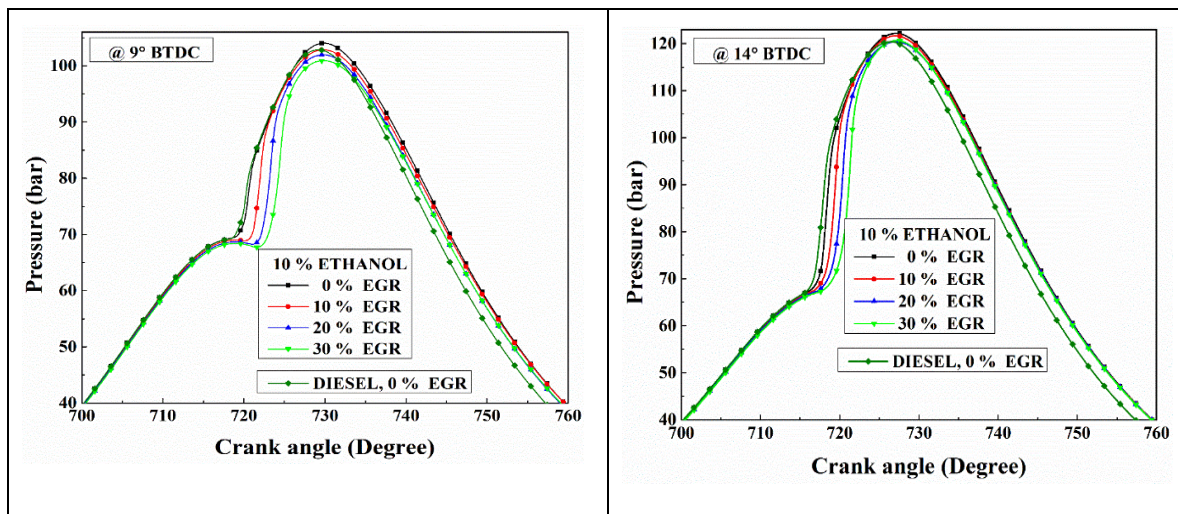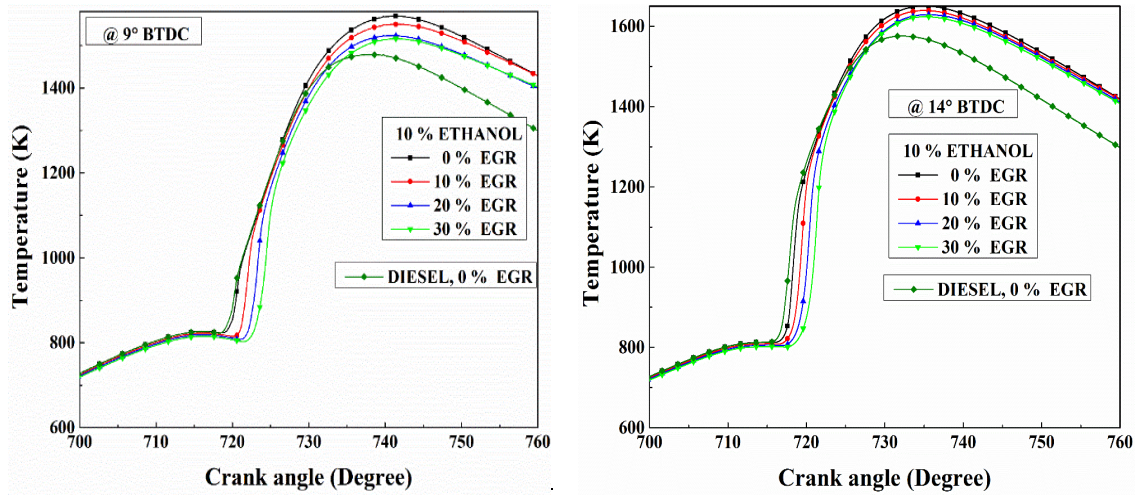

Fig. 5.3 (a) Effect of various EGR rate with 10% bioethanol-diesel blend on in-cylinder temperature for injection timings (9° BTDC and 14° BTDC)

Fig. 5.3 (b) Temperature contours of 10% bioethanol-diesel blend at 14° BTDC injection timing and various EGR rates i) 0%, ii) 10%, iii) 20%, and iv) 30%

5.3.4 Effect of blends on in-cylinder temperature

Figure 5.4 (a) and (b) show the in-cylinder temperature during combustion of various fuel blends with 20% EGR rate for injection timing 9° and 14° BTDC respectively. It has been observed that in-cylinder temperatures for bioethanol-diesel blends (10% bioethanol and 20% bioethanol) are less than that of neat diesel in pre flame combustion and more in post flame combustion.

Fig. 5.4 Effect of various bioethanol-diesel blends with 20% EGR rate on in-cylinder temperature for injection timings (a) 9° BTDC and (b) 14° BTDC

5.3.5 Effect of EGR on auto-ignition delay

Auto ignition delay is calculated as the difference of fuel injection timing to time at which in-cylinder heat release rate curve appears. Fig 5.5 shows the influence of EGR on ignition delay for various fuel blends. Cetane number plays a decisive role in start of combustion. Since bioethanol has lower cetane number, it increases the ignition delay as percentage of bioethanol in the fuel increases. Higher latent heat of vaporization of fuel (bioethanol) causes lower in-cylinder temperature and hence escalates the ignition delay. Results show that higher EGR rate increases the ignition delay due to low oxygen concentration. For all the cases of advanced injection timing, ignition delay is more as expected.
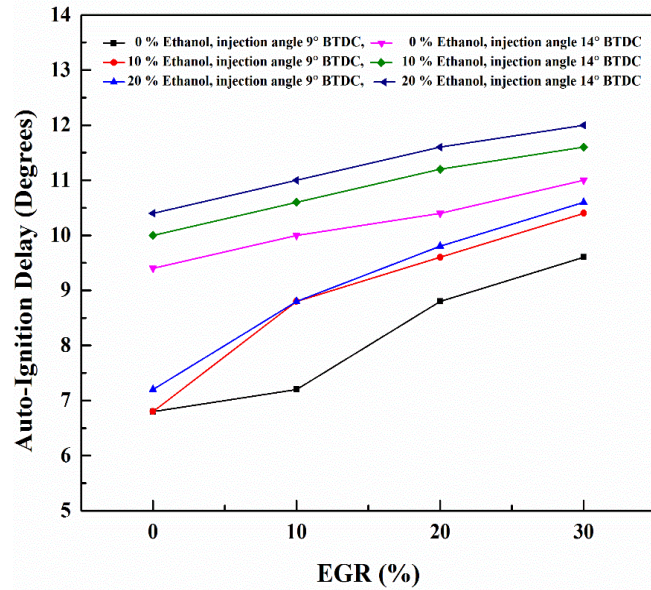
Fig. 5.5 Autoignition delay vs EGR ratefor different fuel blends and injection timings

5.3.6 Effect of EGR rate on in-cylinder NO formation

Figure 5.6 (a) and (b) show the formation of in-cylinder NO_X during combustion of 10% bioethanol-diesel blend with different EGR rate for injection timing 9°and 14° BTDC respectively.

Fig. 5.6 Effect of various EGR rate with 10% bioethanol-diesel blend on NO_X formation for injection timings (a) 9° BTDC and (b) 14° BTDC

As the overall in-cylinder temperature reduces with increase in EGR rate, the mean NO_X formation gets reduced. For injection timing 9° BTDC and 10% bioethanol-diesel blend, NO_X formation is decreased by 46%, 76%, and 90% for 10%, 20% and 30% EGR rates respectively compared to 0% EGR rate. The similar trend has been observed for 14° BTDC.

5.3.7 Effect of blends on NO formation

Figure 5.7(a) and (b) show the formation of in-cylinder NO_X during combustion of various fuel blends with 20% EGR rate for injection timing 9° and 14° BTDC respectively. For injection timing 9° BTDC and 20% EGR rate, NO_X formation for 10% and 20% bioethanol-diesel blends are increased by 33% and 16% compared to neat diesel (20% EGR) respectively. Results for neat diesel without EGR are also provided for comparison. For injection timing 14° BTDC and 20% EGR rate, NO_X formation for 10% and 20% bioethanol-diesel blends are decreased by 27% and 31% compared to neat diesel (20% EGR) respectively. For all the cases of advance injection timing, NO_X formation increases due to increase in in-cylinder temperature.

Fig. 5.7 Effect of various bioethanol-diesel blends with 20% EGR rate on NO_X formation for injection timings (a) 9° BTDC and (b) 14° BTDC

5.3.8 Effect of EGR on in-cylinder mean CO mass fraction

Figure 5.8 (a) and (b) show the formation of in-cylinder CO mass fraction during combustion of 10% bioethanol-diesel blend with different EGR for injection timing 9°and 14° BTDC respectively. It is interesting to know that for both injection timings (9°and 14° BTDC), CO formation is lesser for bio-ethanol diesel blend with EGR (10%, 20% and 30 %) compared to without EGR neat diesel operations. During fossil fuel combustion, CO formation is intermediate step. In further phase with help of OH radicals, in presence of oxygen inside the cylinder, oxidation occurs and CO_2 gets formed at temperature above 1200 K. If less oxygen available locally the oxidation of CO stops due to improper mixing of fuel and air. With more EGR rate, charge gets diluted and more CO formation occurs.
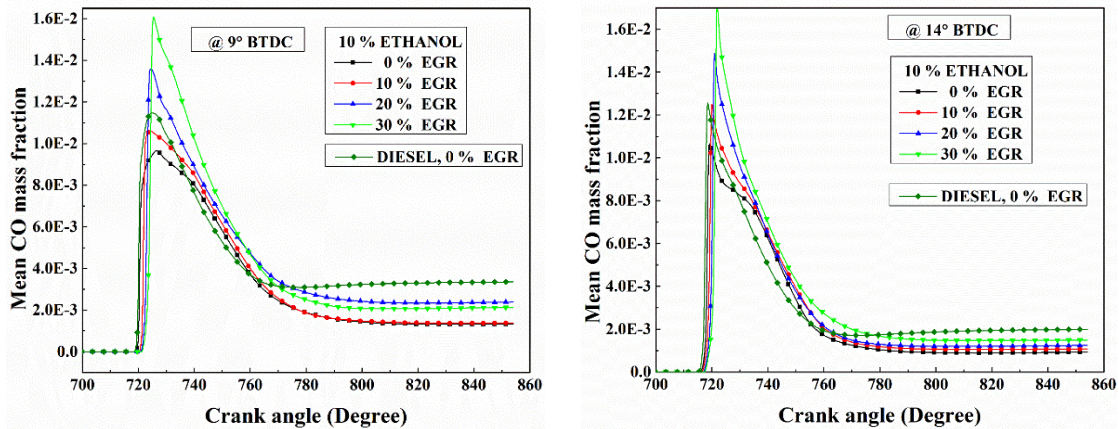
Fig. 5.8 Effect of various EGR rate with 10% bioethanol-diesel blend on CO formation for injection timings (a) 9° BTDC and (b) 14° BTDC
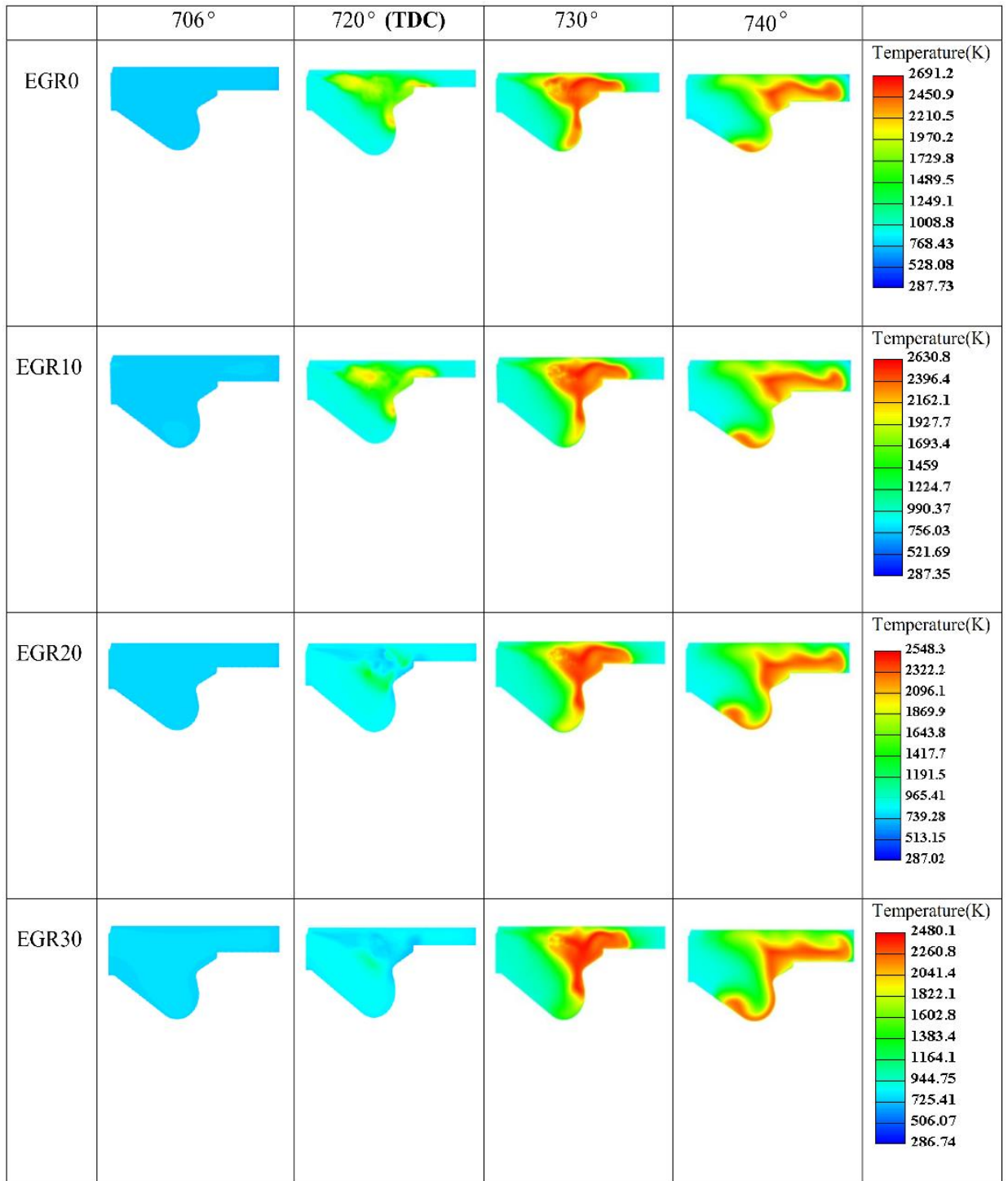
5.3.9 Effect of blends on in-cylinder CO formation

Figure 5.9 (a) and (b) show the formation of in-cylinder CO during combustion of various fuel blends with 20% EGR rate for injection timing 9°and 14° BTDC respectively. It has been found that at constant EGR rate, the CO formation is more in the case of neat diesel compared to that of blends. For injection timing 9° BTDC and 20% EGR rate, CO formation for 10% and 20% bioethanol-diesel blends are decreased by 34% and 70% compared to the neat diesel respectively. The similar trend is followed in the case of 14°

85

BTDC. Results for neat diesel without EGR are also provided for comparison. The oxygen content of bioethanol is higher than diesel which causes conversion of CO in rich fuel region into CO_2. The same trend was also observed by Petranovic (2014).
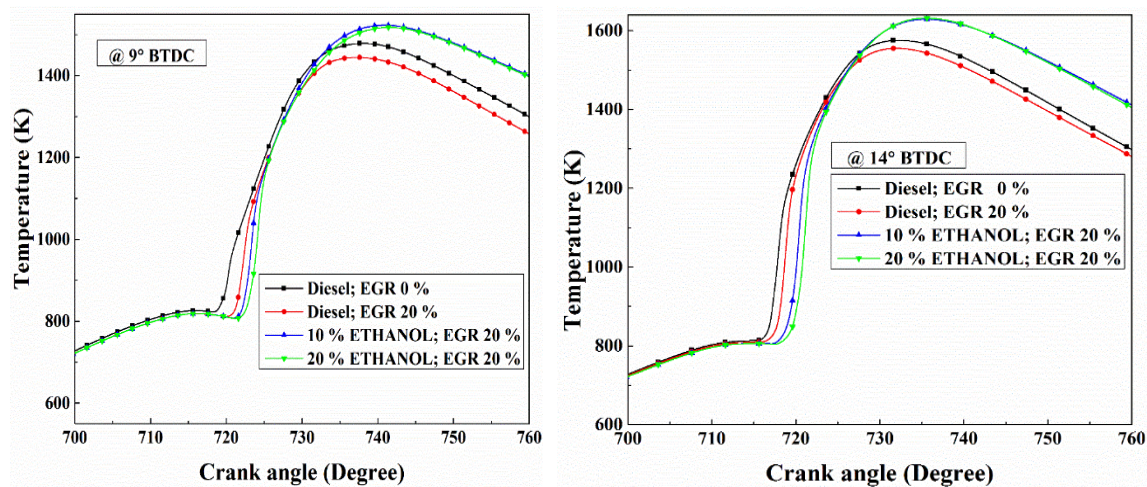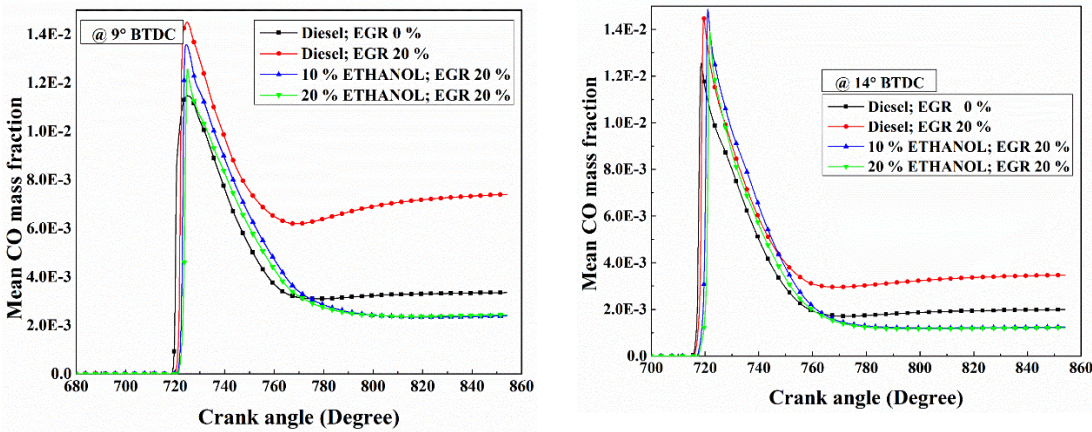

Fig. 5.9 Effect of various bioethanol-diesel blends with 20% EGR rate on CO formation for injection timings (a) 9° BTDC and (b) 14° BTDC

5.3.10 Effect of EGR rate on in-cylinder soot formation

Figure 4.10 (a) and (b) show the effect of EGR rates on in-cylinder soot formation during combustion for 10% ethanol-diesel blend at injection timings 9° and 14° BTDC respectively. It is well established fact that as EGR rate increases, more soot formation occurs due to dilution effect. Also, it is interesting to see the lower soot formation for 10% bioethanol-diesel blend with 0% and 10% EGR rates compared to neat diesel without EGR.

For injection timing 9° BTDC and 10% ethanol-diesel blend, soot formation for EGR rates 0% and 10% is decreased by approximately same percentage (21%) compared to neat diesel without EGR, whereas soot formations are increased by approximately 40% for 20% and 30% EGR rates respectively. For 14° BTDC and 10% bioethanol-diesel blend, soot formation for EGR0 and EGR10 are decreased by 25% and 20 % and increased by 15% and 16 % for EGR20 and EGR30 respectively.
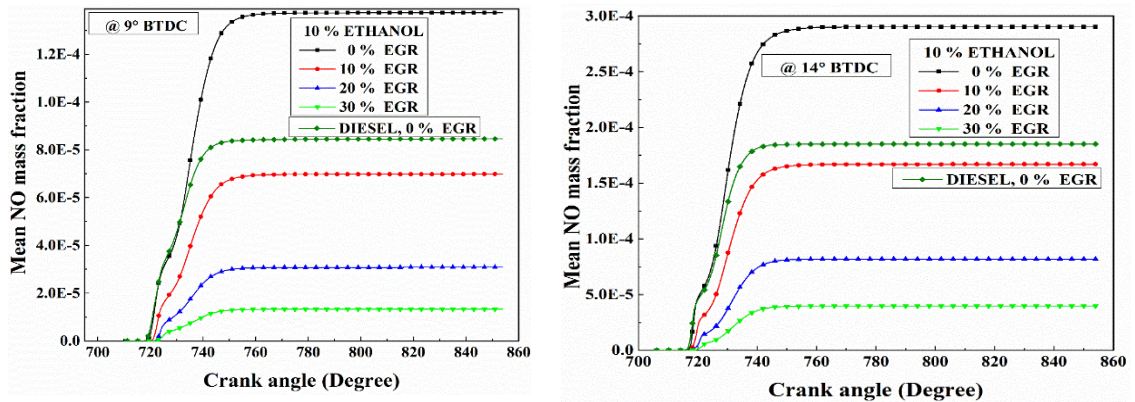
86
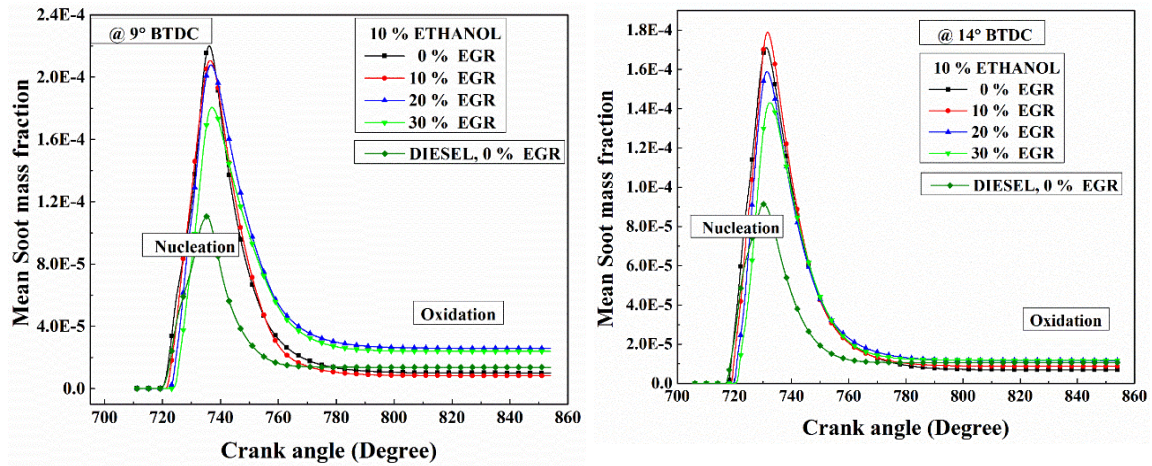
Fig. 5.10 Effect of various EGR rate with 10% bioethanol-diesel blend on Soot formation for injection timings (a) 9° BTDC and (b) 14° BTDC

5.3.11 Effect of blends on in-cylinder soot formation

Figure 5.11 (a) and (b) show the in-cylinder soot formation during combustion of various fuel blends with 20% EGR rate for injection timing 9° and 14° BTDC respectively. Soot emission can be remarkably reduced by adding bioethanol (an oxygenated fuel) to diesel. Results show that, for injection timing 9° BTDC and 20% EGR, reduction in soot formation for 10% bioethanol-diesel blend is 15%, and marginal increase (4%) in soot was observed for 20% blend as compared to neat diesel.

For injection timing 14° BTDC, reduction in soot formations are 40% and 25% for bioethanol-diesel blends of 10% and 20% compared to the neat diesel respectively.
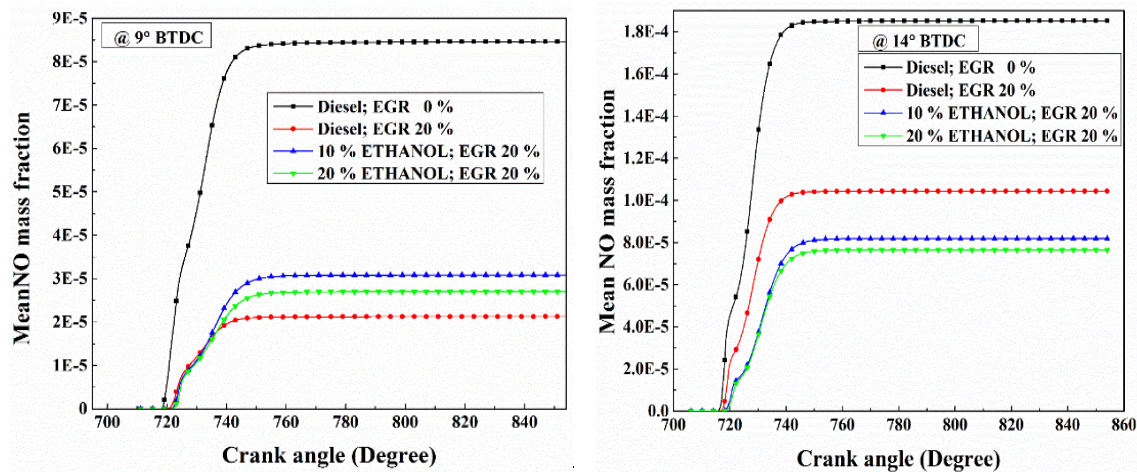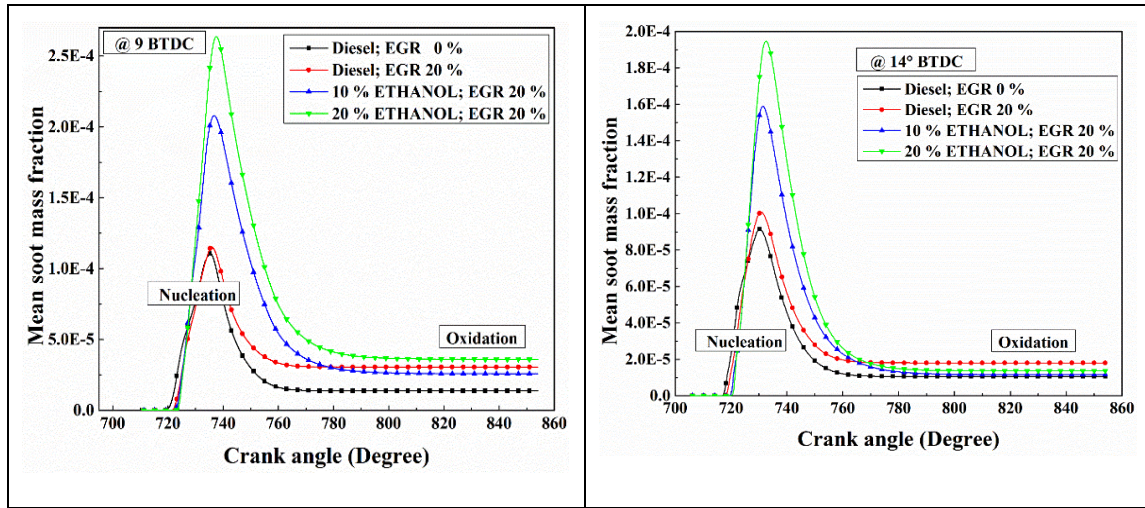
Fig. 5.11 Effect of various bioethanol-diesel blends with 20% EGR rate on soot formation for injection timings (a) 9° BTDC and (b) 14° BTDC

The improvement of soot emission can be explained by the enrichment of oxygen owing to bioethanol resulting in high local air-fuel ratio which promotes the oxidation of soot nuclei in fuel combustion. Bioethanol reduces the initial radicals for the formation of aromatic rings, which are considered as the soot precursors, mainly through reducing the amount of carbon that is available to form precursor species. Wu et al. (2006) perceived that bioethanol blended fuel decreases the soot due to formation of OH radicals as shown in equation (4.1).

$$C_2H_5OH \rightarrow C_2H_4 + H_2O$$
$$H_2O + H \rightarrow OH + H_2 \tag{4.1}$$

5.4 Conclusions

CFD analysis of 4-stroke CRDI engine with bioethanol-diesel blends for various EGR rates at injection timings of 9° BTDC and 14° BTDC is carried out. Following conclusions are made based on the obtained simulation results.

- For advanced injection timing of 14° BTDC, higher in-cylinder pressure (15%) is observed compared to 9° BTDC.

- For injection timing 9° BTDC and 20% EGR rate, NO_X formation for 10% and 20% bioethanol-diesel blends are increased by 33% and 16% compared to neat diesel respectively.

- For injection timing 9° BTDC and 10% bioethanol-diesel blend, NO formation is decreased by 46%, 76%, and 90% for 10%, 20% and 30% EGR rates compared to 0% EGR respectively

- Mean CO formation during combustion is less in the case of bioethanol blends compared to neat diesel.

- For injection timing 14° BTDC and 20% EGR, reduction in soot formation for bioethanol-diesel blends of 10% and 20% are 40% and 25% compared to neat diesel respectively.

- Higher latent heat of vaporization and lower cetane number of bioethanol escalate the ignition delay.

CHAPTER 5

PART II: EFFECT OF INJECTION TIMINGS WITH BIOETHANOL-DIESEL BLENDS IN CRDI ENGINE: A CFD STUDY

5.5. Introduction

In this study, we explore the effect of injection timings and various bioethanol-diesel blends on the engine performance, tailpipe emissions and combustion characteristics at constant equivalence ratio. In most of the available literature, mass of injected fuel per cycle is kept constant in the case of blending to find performance of engines, which is not justified because equivalence ratio may change due to different chemical composition of fuel. It is well known that the performance of an engine directly depends on equivalence ratio (rich or lean mixture). In the case of ethanol (C_2H_5OH), an extra oxygen atom is already present in the fuel which can change the stoichiometric air-fuel ratio and hence equivalence ratio gets changed. Since injection timing plays a key role on the engine performance and emissions, optimum injection timings (at which indicated thermal efficiency is maximum) for various blends are required to be obtained. The CFD simulation is carried out for a four stroke single cylinder CRDI engine to better comprehend the in-cylinder combustion.

5.6. Results and discussion

Results are obtained at various injection timings (21°, 24°, 27°, 30° and 33° BTDC) for different bioethanol-diesel blends ratio (10, 20 and 30%) in the three dimensional CFD simulation. To choose the range of injection timings, initially optimum condition for neat diesel (E0) is found by varying injection timing from 0° BTDC to 33° BTDC, and it was obtained at 27° BTDC. Results for injection timings between 21° to 33° BTDC are presented in this section. Since ethanol has extra oxygen, we need to supply more ethanol compared to diesel to maintain same equivalence ratio.

5.6.1. Effect of injection timing and blends on in-cylinder pressure

Figure 5.12 (a) to (d) shows the effect of injection timing for different bioethanol-diesel blends on in-cylinder pressure. As injection timing advances, the in-cylinder peak pressure increases for all blends. The charge gets sufficient time to diffuse throughout the combustion chamber thereby reduces the heterogeneity of the mixture.
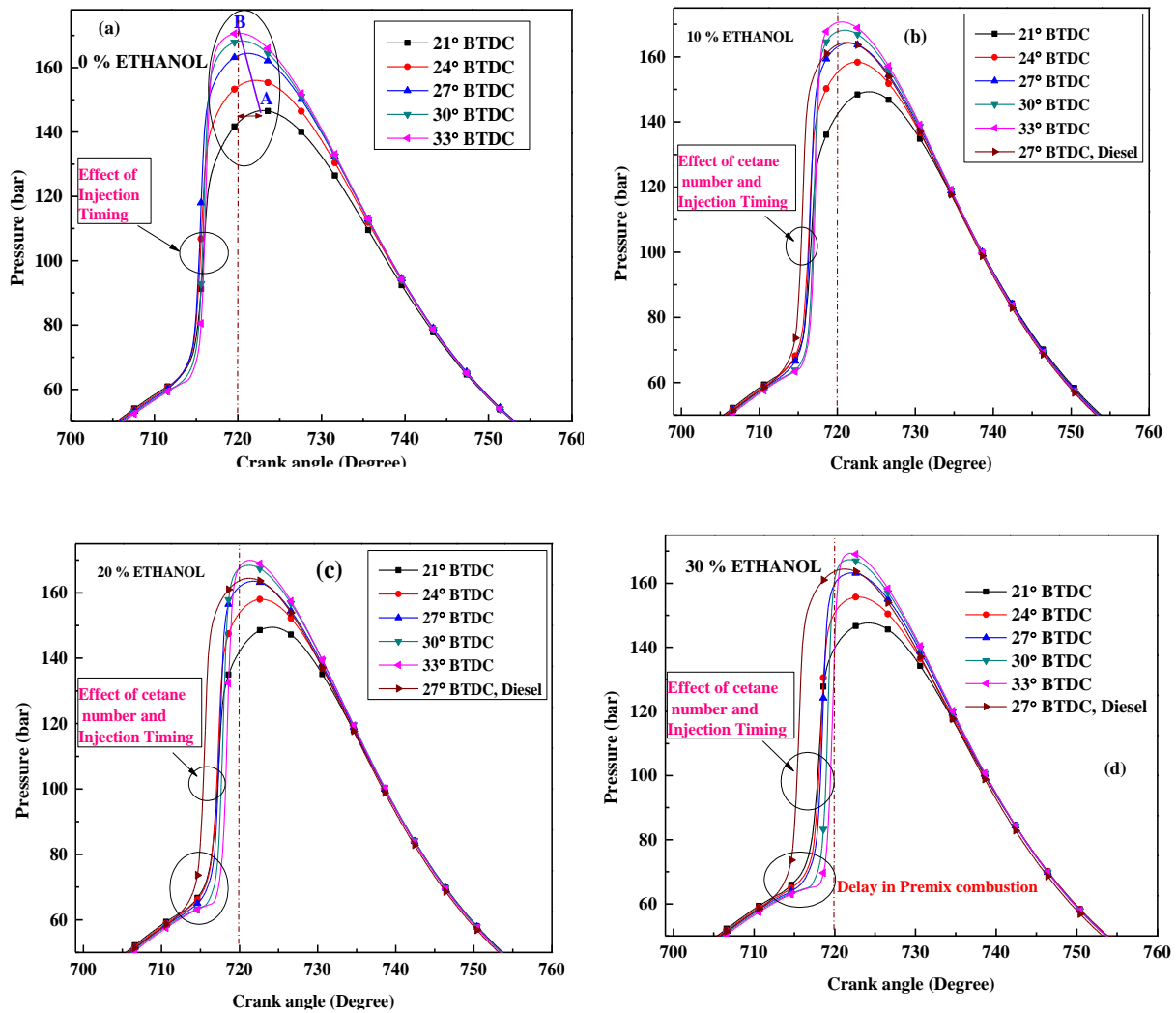
Fig. 5.12 Effects of injection timing on in-cylinder pressure for bioethanol-diesel blends (a) 0%, (b) 10%, (c) 20%, and (d) 30%

Therefore, major part of the fuel mass gets burned near TDC in the case of 33° BTDC, whereas burning persists even after TDC for all other injection timings (21°- 30° BTDC). Line AB represents a locus of the peaks of pressure curves. The horizontal distance from point on the peak of the curve to the vertical drawn at TDC signifies the further shifting of combustion in expansion stroke due to retard injection timing. Furthermore, high bioethanol-diesel blend ratio results in decrease of area under pressure versus crank angle curve as shown in Fig 5.12 (b) - (d). This occurs due to lower cetane number of ethanol causing higher ignition delay compared to diesel as shown in Fig 5.14.

5.6.2. Effect of injection timings and blends on in-cylinder temperature

Figures 5.13 (a)-(d) show the effect of injection timing and various bioethanol - diesel blends on in-cylinder temperature respectively. For given fuel, the peak of in-cylinder temperature increases upon advancing injection timing. Duration of higher temperature band decreases with increase in bioethanol-diesel blends. Fig 5.14 shows the effect of injection timing on ignition delay for different fuel blends. Cetane number plays a decisive role in start of combustion.
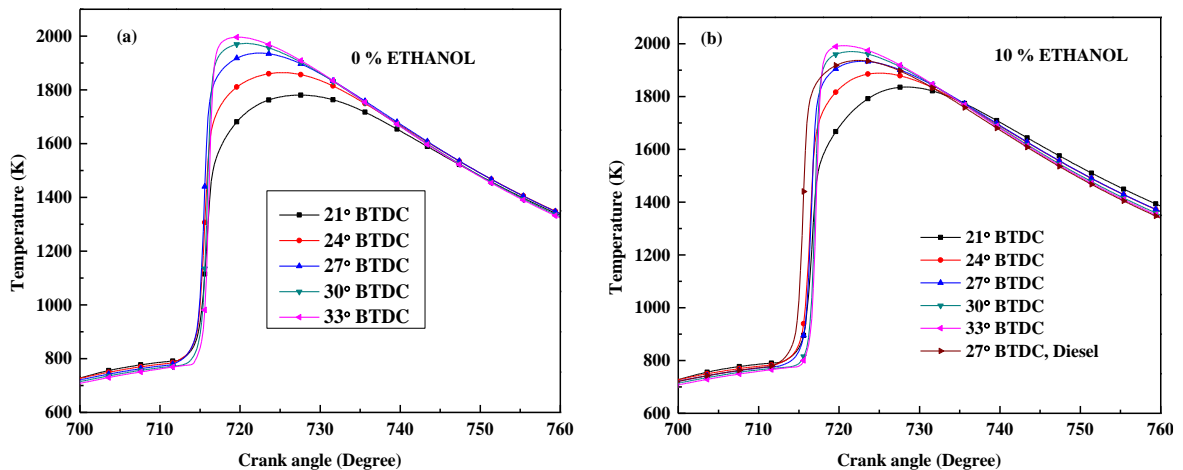
Fig. 5.13 Effects of injection timing on in-cylinder temperature for bioethanol-diesel blends (a) 0%, (b) 10%, (c) 20%, and (d) 30%
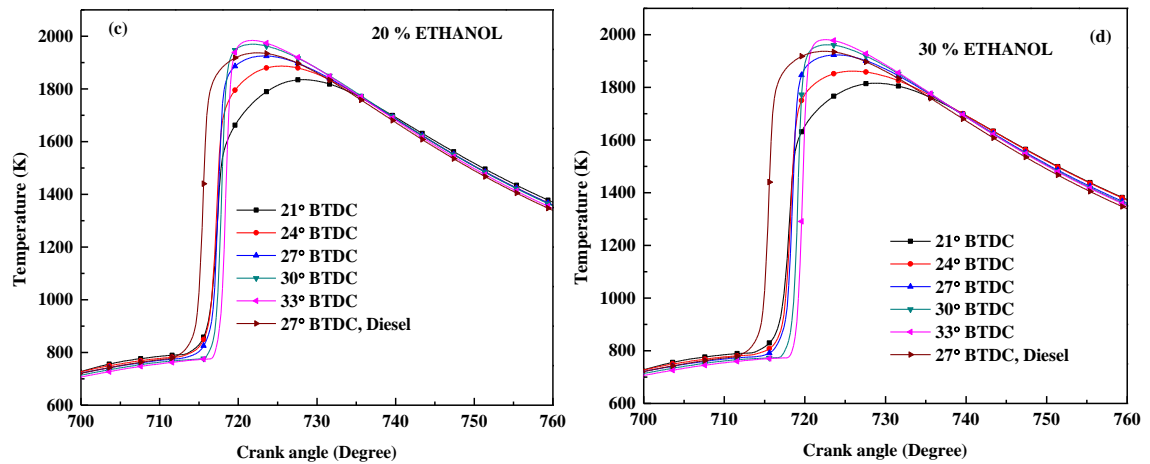
5.6.3 Effect of injection timing and blends on auto-ignition delay

Since bioethanol has lower cetane number, it increases the ignition delay as percentage of bioethanol in the blend increases. Higher latent heat of vaporization of fuel (bioethanol) causes lower in-cylinder temperature and hence escalates the ignition delay.
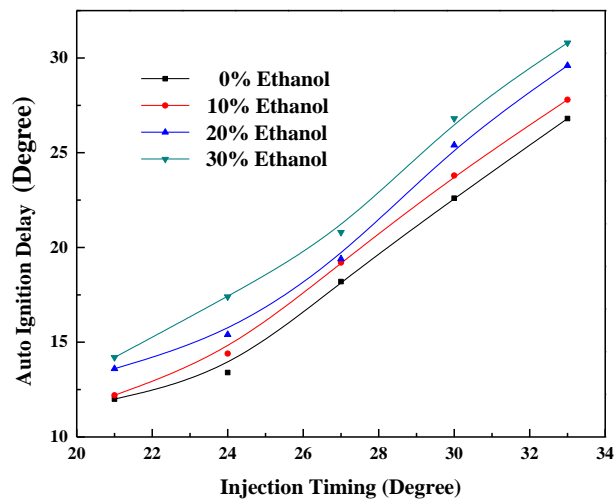
Fig. 5.14 Effects of injection timings and bioethanol-diesel blends on auto-ignition delay

In addition, consumption reaction of the hydroxyl radical (OH⁻) is an endothermic reaction, which confines the heat release and escalates ignition delay (Li et al. 2005). For all the cases of advanced injection timing, ignition delay is more as expected.

94

5.6.4. Effect of injection timing and blends on engine performance

The effect of injection timing and bioethanol-diesel blends ratio on performance of CRDI engine is demonstrated in Fig 5.15. The lower density, more oxygen content, active evaporation and low viscosity improve combustion characteristics for bioethanol-diesel operations compared to the neat diesel (E0). Further, the evaporation of ethanol droplets due to its lower surface tension leads to better combustion. Results show the increase of indicated thermal efficiency (ITE) with bioethanol-diesel blends and found to be highest in the case of bioethanol 30%. As bioethanol-diesel blend ratio increases the auto ignition delay also increases, which causes combustion to be initiated near TDC, and hence minimizes negative work (compression work) as explained above in the Fig. 5.12. Optimum injection timing in terms of maximum ITE is obtained for various blends.
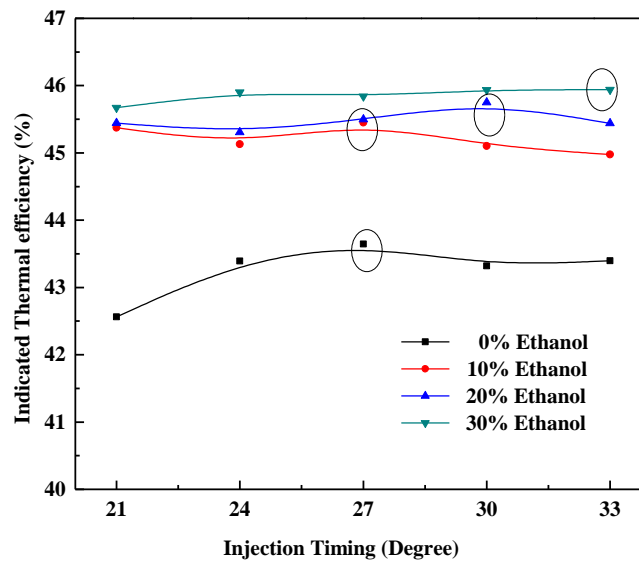
Fig. 5.15 Effects of injection timings and bio-ethanol-diesel blends on ITE

5.6.5. Effect of injection timing and blends on in-cylinder CO formation

Figure 5.16 illustrates the CO formation for different injection timings and various bioethanol-diesel blends. Advance injection timing results in less CO emission for the blends including neat diesel. As discussed earlier burning persist longer after TDC for retard injection timings, hence there is simultaneous CO formation along with oxidation, this restricts the CO oxidation which is observed in Fig 5.12.
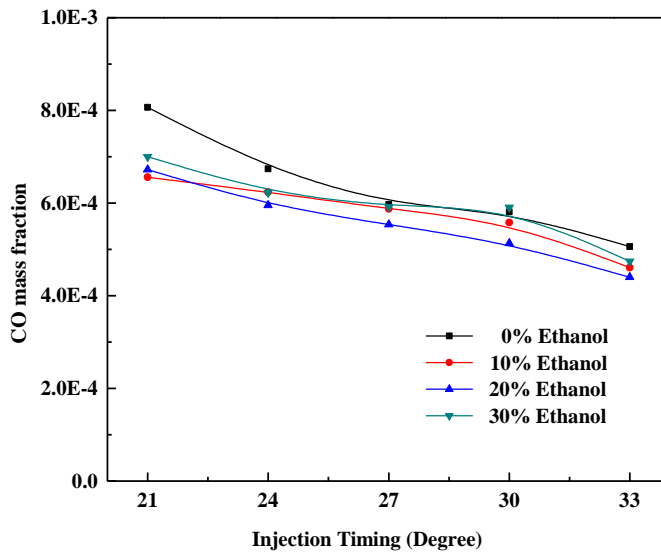
Fig. 5.16 Effects of injection timings and bioethanol-diesel blends on CO formation

5.6.6. Effect of injection timing and blends on NO$_X$ formation

Figure 5.17 shows the illustration of the NO$_X$ formation for different injection timings and various bioethanol-diesel blends. The in-cylinder NO$_X$ formation is explained by majorly Zeldovich mechanism, prompt and fuel bound nitrogen. The key parameters to nitrogen oxide formation are local temperature, residence time and concentration of oxygen in higher flame temperature zone. The peak temperature is higher in the case of advanced injection timing, but its duration reduces as we advance further and further. The formation of NO$_X$ as per Zeldowich mechanism is proportional to temperature i.e., $\frac{d[NO]}{dt} \alpha$ T.
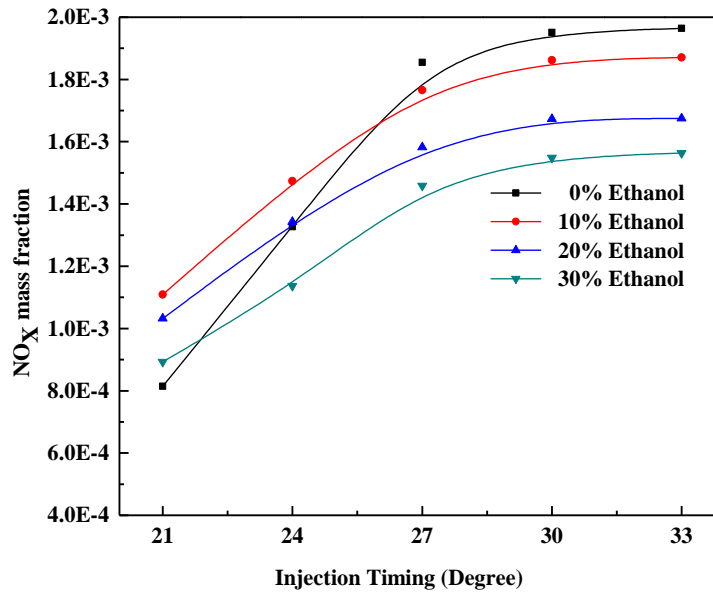
Fig. 5.17 Effects of injection timings and bioethanol-diesel blends on NO_X formation

5.6.7. Effect of injection timing and blends on soot formation

Figure 5.18 shows the effect of different injection timing and bioethanol-diesel blend on soot formation. Formation of soot occurs in rich fuel and medium temperature zone. For a given fuel, advancing the injection timing decreases the formation of soot due to more homogeneous mixture. The temperature promotes oxidation of the nucleated soot. Results show the least soot formation for injection timing 33° BTDC for all blends as well as for neat diesel. It is also seen that the soot formation for 21° BTDC is highest among all injection timings and drastically reduced for advanced injection timings due to existence of higher temperature. As the blend decreases, the cetane number of the fuel increases which makes combustion faster. The existence of high temperature during the start of combustion hampers the formation of soot. Hence for a given injection timing, least soot formation is found in the case of E0 and highest is for E30. Due to constant equivalence ratio employed in this investigation, presence of fuel bound oxygen in bioethanol plays insignificant role in reduction of soot formation.
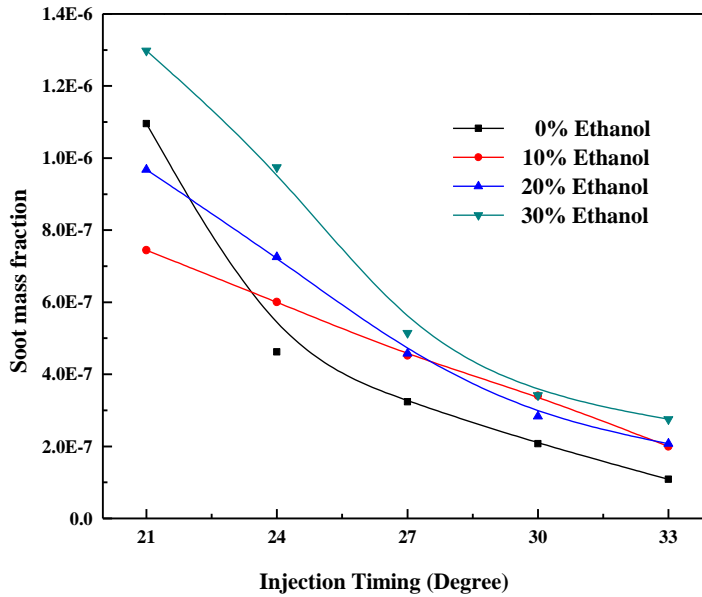
Fig. 5.18 Effect of injection timings and bioethanol-diesel blends on soot formation

5.7. Conclusions

CFD analysis of four-stroke CRDI engine with bioethanol-diesel blends for various injection timings is carried out. Following observations are made based on the obtained results.

- The maximum indicated thermal efficiency for E0, E10, E20 and E30 is found at 27°, 27°, 30° and 33° BTDC injection timing respectively.

- Indicated thermal efficiency increases with bioethanol-diesel blends and found to be 5% (absolute) higher in the case of E30 compared to E0.

- As bioethanol-diesel blend ratio increases the auto ignition delay increases, which require advance injection compared to neat diesel to initiate combustion before TDC.

- Evaporation of ethanol droplets due to its lower surface tension leads to better combustion.

98

- The peak temperature is higher for advanced injection timing, but its duration reduces as injection advances further.

- For all blends including neat diesel, reduction of soot formation is observed with advancing injection timings.

CHAPTER 6

PART I: EFFECT OF INJECTION TIMING AND n-BUTANOL-DIESEL BLENDS IN CRDI ENGINE

6.1 Introduction

In this chapter, numerical and experimental studies on the effect of injection timings and various n-biobutanol-diesel blends on the engine performance, tailpipe emissions and combustion characteristics of CRDI engine are presented. Optimum injection timings are obtained for different n-butanol-diesel blends (0-30%) experimentally to get maximum brake thermal efficiency (BTE). Tailpipe emissions (NO_X, CO and soot) at various injection timings (9º, 12º, 15º and 18º) are also measured. Further, CFD simulation is carried out for all injection timings and n-butanol-diesel blends considered for experimental studies.

6.2. Fuel properties and combustion strategy

The n-butanol (0 to 30% by volume) is blended with the neat diesel to obtain n-butanol-diesel blends. Bu0, Bu10, Bu20 and Bu30 represents 0%, 10%, 20% and 30% n-butanol in neat diesel respectively. Furthermore, stability analysis of n-butanol blends is carried out by observing the blends phase for six months and found stable without phase separation as shown in Fig 6.1. Basic physical properties of the n-butanol and neat diesel employed in this investigation are provided in Table 1.3 of chapter 1, and ranges of experimental and CFD simulation parameters are listed in Table 6.1.

Table 6.1: Range of simulation parameters

Parameters	Range
Blend (% of Butanol)	0, 10, 20 and 30
Injection timings (BTDC)	9º, 12º, 15º and 18º
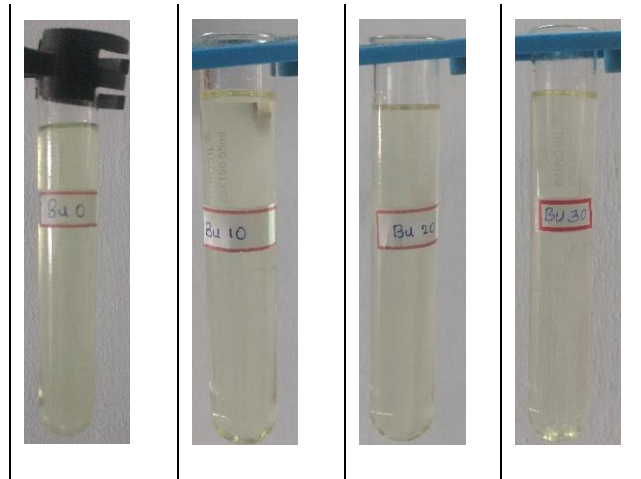
Fig. 6.1 Phase stability of n-butanol blends after six months

6.3. CFD code and meshing of geometry

AVL ESE CFD tool is used for engine geometric modelling and computational meshing as shown in Fig 6.2. The details of engine specifications, governing equations, transport equations for chemical species are discussed in sections 3.1 3.6 and 3.7 of chapter 3.
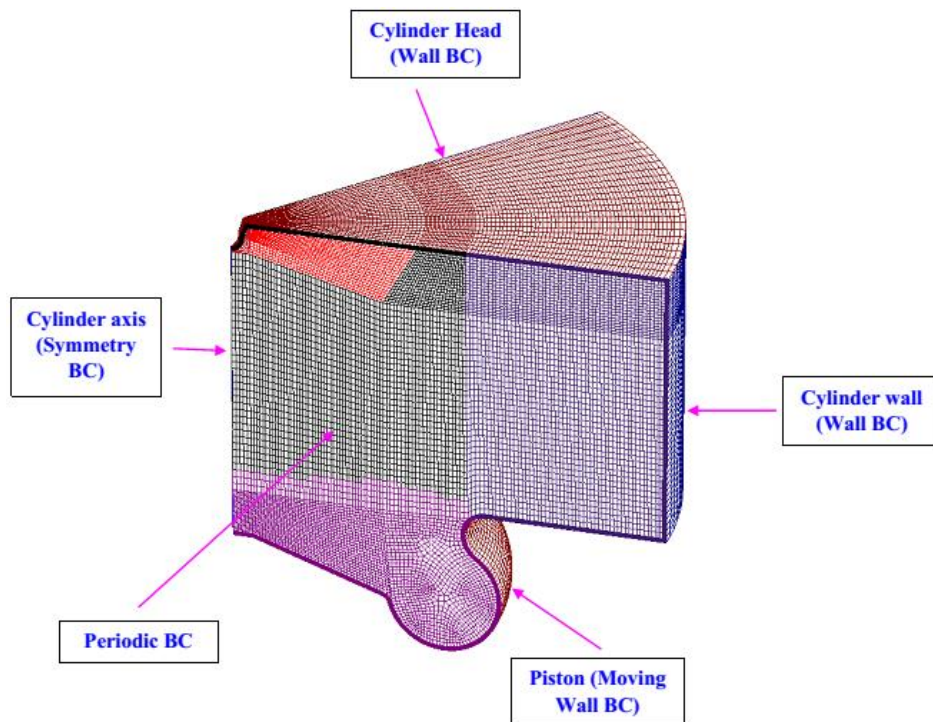
Fig. 6.2 Three dimensional computational domain
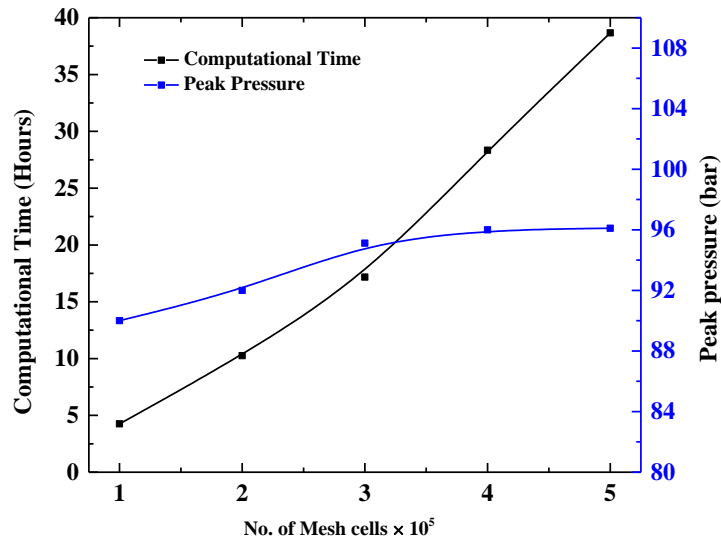
Fig. 6.3 Grid independence study of peak pressure

The injector with 7 holes is located centrally on the top of piston, hence ~52° sector is chosen for the simulation. In order to reduce the computational time high pressure cycle is considered. Simulation is started and ended at inlet valve close and exhaust valve open position respectively. Grid independence test has been carried out to obtain optimum grid size as shown in Fig 6.3. Simulation is carried out by 64 GB RAM 32 core work station with parallel processing. Results have been checked for peak pressure and computational time for various grid sizes. It has been observed that considered parameters are invariant with change in total number of grids at/after 3×10^5.

6.4. Results and discussion

In this section, results of experimental and numerical (CFD) studies on CRDI engine at constant rpm (2000) and 80% load are presented. In CFD simulation, amount of fuel injected/cycle for different blends are taken same as respective experimental case. Results are obtained for n-butanol-diesel blends (Bu10, Bu20 and Bu30) for various injection timings (9º, 12º, 15º and 18º).

6.4.1 Effect of blends and injection timing on brake thermal efficiency

The influence of injection timing and n-butanol-diesel blend ratio on BTE of CRDI engine is experimentally investigated and shown in Fig 6.4. Results show that there is a significant increase in BTE for all butanol-diesel blends at all injection timings compared to Bu0. This can be attributed to the prompt premixed combustion part possessed by butanol blends, enhanced mixing during ignition delay, oxygen enrichment leading to leaner combustion and less heat loss (Hansen et al. 1989; Hulwan et al. 2011).
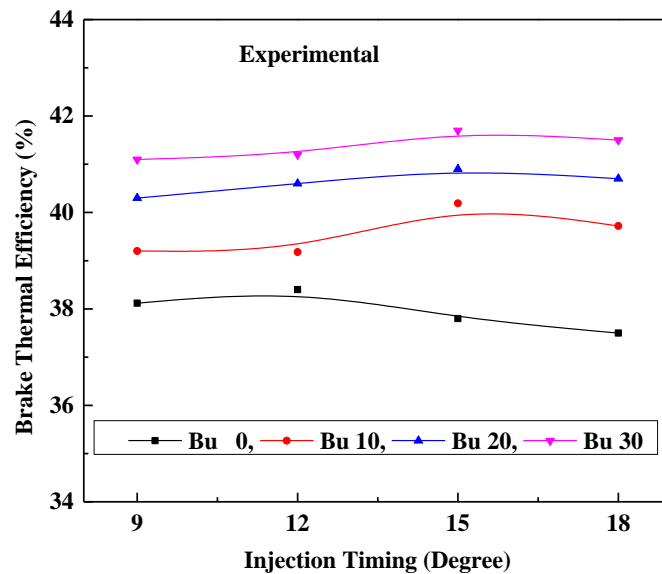
Fig. 6.4 Variation of brake thermal efficiency vs injection timing

The enhancement of diffusive combustion is obtained due to oxygen enriched blends, and hence the total combustion duration is shortened. The increase in BTE with butanol blends is also ascribed to its higher burning velocity of 45 cm/s (Sarathy et al. 2009) as compared to 33 cm/s for diesel (Sayin et al. 2010). The BTE is increased by ~4.5%, 6% and 8% for Bu10, Bu20 and Bu30 respectively compared to Bu0. Optimum BTE obtained for Bu0 is 38.4% at 12º BTDC injection timing, while for Bu10, Bu20 and Bu30 are 40.19%, 40.9% and 41.7% respectively at a common injection timing of 15° BTDC. Dogan (2011) and Rakopoulos et al. (2011) also observed a slight increase in BTE with increasing butanol blend ratio.

6.4.2. Validation of CFD results with experimental data

In the present study, the engine simulation software AVL-FIRE is coupled with CHEMKIN II for simulating the engine combustion and emission formation processes with detailed reaction mechanisms. The simulation results are validated with the experimental data obtained for conditions listed in Table 3.1.
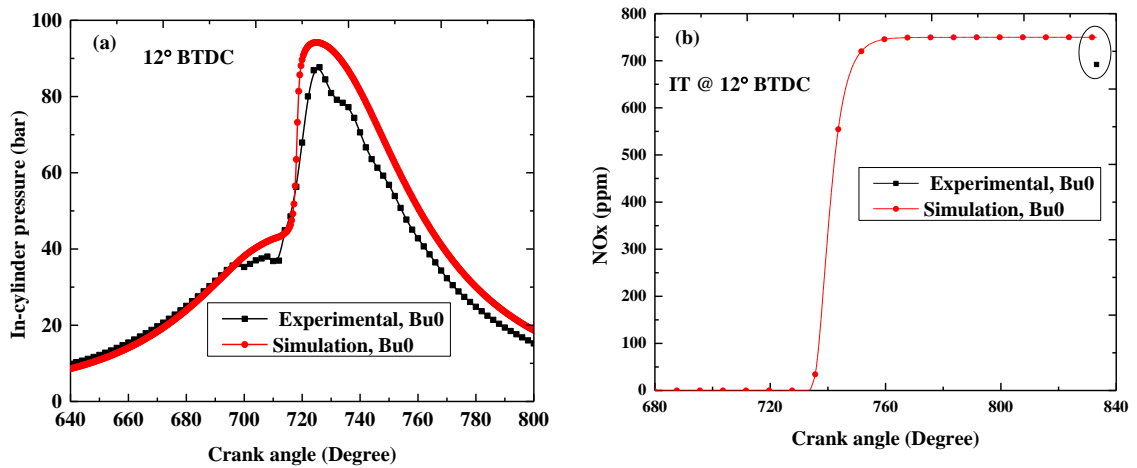
Fig. 6.5 Validation with experimental results, diesel a) In-cylinder pressure versus crank angle, (b) NOx versus crank angle
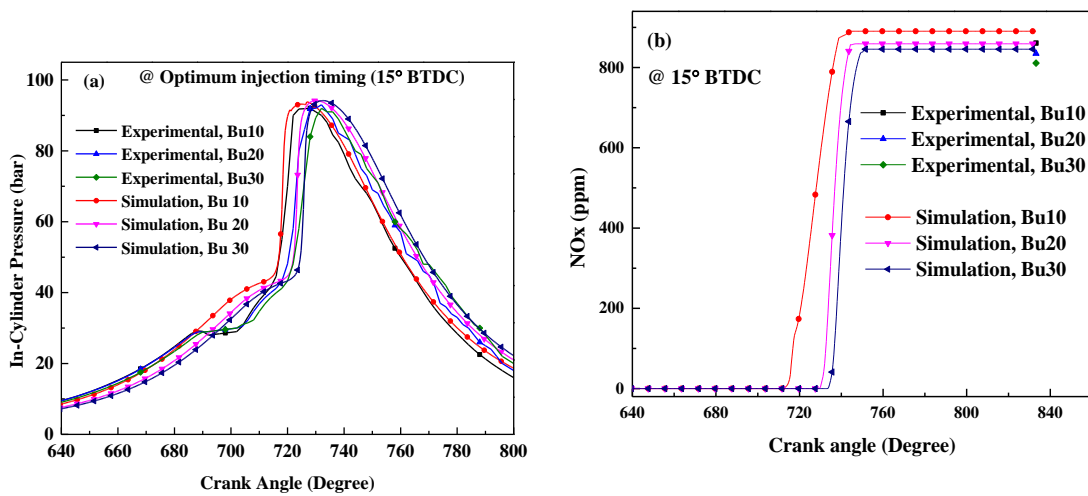
Fig. 6.6 Validation of simulation with experimental results for n-butanol-diesel blends (a) in-cylinder pressure, (b) NOx

Figures 6.5 and 6.6 show the comparison of experimental and numerical results of in-cylinder pressure and NOx emission versus crank angle for various blends respectively. For all validation cases, experimental and CFD results are showing good agreement. It can be seen from the results that peak cylinder pressure slightly increases for butanol blends. This may be because of enhanced pre mixed combustion phase due to extended ignition delay (Kumar et al. 2016). Results are presented for in-cylinder pressure and NO_X obtained at 12° BTDC (optimum IT) for Bu0, and 15° BTDC (optimum IT) for Bu10, Bu20 and Bu30 blend ratios.

6.4.3 Effect of blends and injection timings on temperature

The influence of injection timing and n-butanol-diesel blend ratio on in-cylinder temperature of CRDI engine is shown in Fig 6.7 (a-c). Temperature contours (Figure 6.7 (a) and (b)) are plotted for optimum injection timing i.e., 12° BTDC for neat diesel and 15° BTDC for n-butanol-diesel blends (Bu10, Bu20 and Bu30) at various crank angle (at Injection timing, at TDC and 10° ATDC). Contour plots for Bu0 at 15° BTDC IT is also provided to compare in-cylinder temperature with same IT cases for blends. These contour plots show the clear picture of combustion process occurring inside the cylinder for n-butanol-diesel blend. Figure 6.7 (c) represents in-cylinder temperature for neat diesel and n-butanol-diesel blends at optimum IT. Result shows that at same IT, in-cylinder temperature for Bu0 is higher than n-butanol-diesel blend cases, which occurs due to high latent heat of vaporisation of n-butanol fuel compared to diesel. At optimum IT, in-cylinder temperature for Bu0 is less than the blends. This occurs due advance IT for n-butanol-diesel blends compared to neat diesel.

IT	At IT	At TDC	At 10° ATDC	
12° BTDC (Bu0)				2798.3 2549.5 2300.6 2051.8 1803 1554.1 1305.3 1056.5 807.66 558.83 310
15° BTDC (Bu0)				2850 2596 2342 2088 1833.9 1579.9 1325.9 1071.9 817.89 563.88 309.87

Fig. 6.7 (a)

IT	At IT	At TDC	At 10° ATDC	
15° BTDC (Bu10)				2835.3 2582.8 2330.2 2077.7 1825.2 1572.6 1320.1 1067.6 815.06 562.53 310
15° BTDC (Bu20)				2817.7 2567 2316.2 2065.4 1814.6 1563.9 1313.1 1062.3 811.55 560.77 310
15° BTDC (Bu30)				2804.3 2555.3 2305.3 2056.4 1806.9 1557.4 1307.9 1058.4 808.96 559.48 310

Fig. 6.7 (b)

108

Fig. 6.7(c)

Fig. 6.7 (a) Temperature contours for diesel (b) Temperature contour for n-butanol-diesel blends (c) Temperature versus injection timings for diesel and blends

6.4.4 Effect of blends and injection timings on NO_X

The effect of injection timings and n-butanol-diesel blends on NO_X emission of CRDI engine is shown in Fig 6.8. It can be observed from experimental as well as simulation results that NO_X emission tends to decrease with increasing blend concentration. Low cetane number of n-butanol and high heat of evaporation result in a lower flame temperature leads to less NOx formation compared to neat diesel (Dogan 2011). Also the amount of NOx increases with advancement in injection timings as the fuel air mixture gets enough residence time for proper homogeneous mixing. The maximum NOx emission is 1090, 1001, 989 and 959 ppm for Bu0, Bu10, Bu20 and Bu30 respectively measured experimentally at 18° BTDC.

109
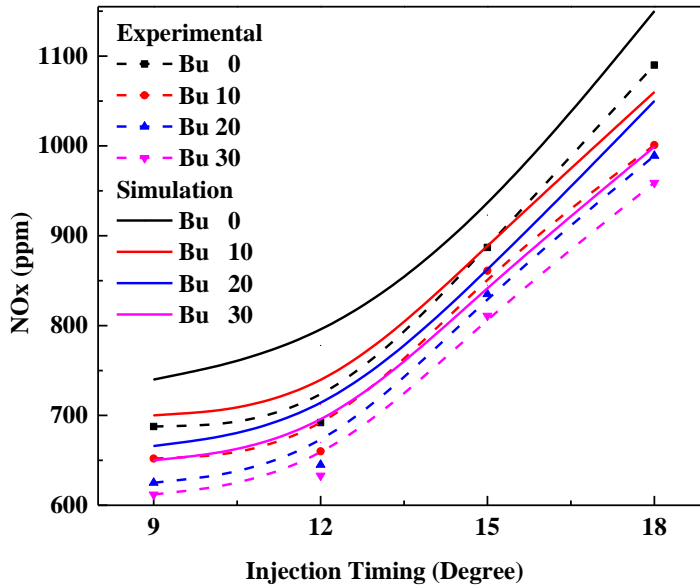
Fig. 6.8 Variation of NOx vs Injection timing

6.4.5 Effect of blends and injection timing on CO emissions

The effect of injection timing and n-butanol-diesel blend ratio on carbon monoxide (CO) emission of CRDI engine is shown in Fig 6.9. CO is formed because of incomplete combustion occurring due to lack of free oxygen during combustion. Since, butanol blends are oxygenated, they promote CO oxidation thereby enhancing the complete combustion process. As injection timing retards, CO emission increases because of incomplete oxidation taking place during the expansion stroke. CO emissions are found to be decreased with increasing blend ratio at all injection timings. Advance injection timing leads to early start of combustion causing higher cylinder temperature results in quick chemical reaction between carbon and oxygen in the combustion chamber which intensifies the oxidation process (Sayin et al. 2008). Obtained numerical results with proposed CFD model show marginal difference with experimental data.
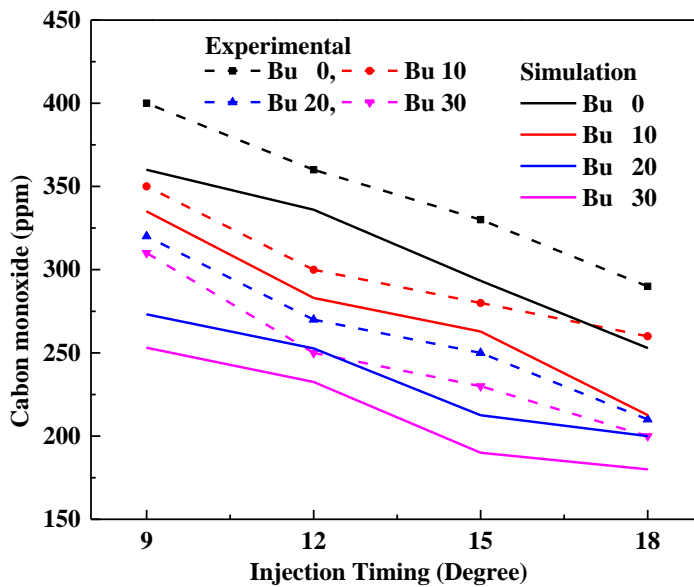
Fig. 6.9 Variation of CO vs Injection timing

6.4.6 Effect of blends with injection timing on soot opacity emissions

The particulate matter (PM) is basically composed of soot and is accountable for the smoke. Smoke opacity formation ensues at the air deficit conditions which locally exist in engine cylinder and increases as the air/fuel ratio declines.
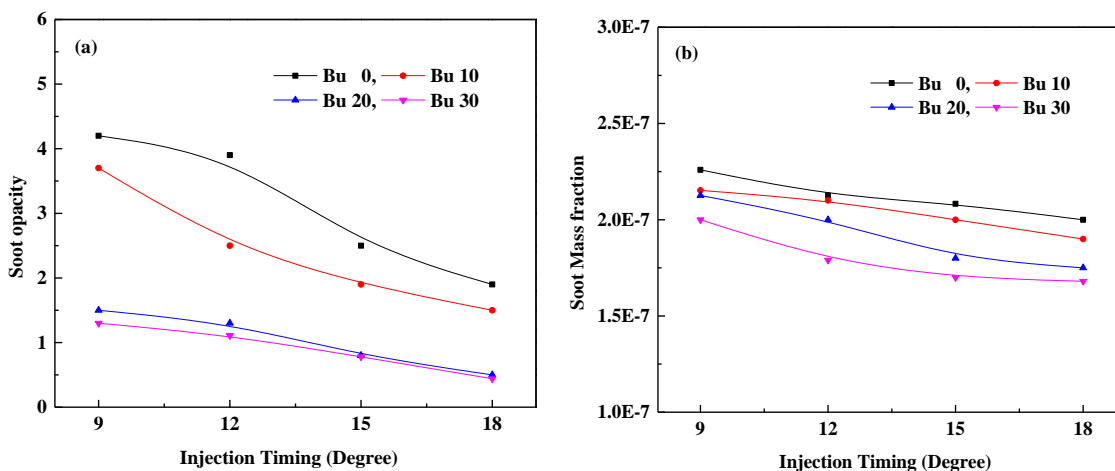
Fig. 6.10 Variation of soot opacity vs Injection timing (a) Experimental (b) Simulation

111

Soot is formed by poor oxygen thermal cracking of long-chain molecules (Schobert 2013). The effect of injection timing and n-butanol-diesel blend ratio on soot opacity emission of CRDI engine is studied experimentally as well as numerically and presented in Fig 6.10 (a) and (b) respectively. Increasing butanol content in the blend, results in the reduction of soot due to higher oxygen/carbon ratio. The existence of atomic oxygen bond in butanol fulfills progressive chemical control over soot formation. The ability to produce soot by the densed fuel region inside a blend diffusion flame sheath gets reduced due to improved mixing owing to better atomization and vaporization of blends. Higher soot formation with retardation in injection timing occurs due to low in-cylinder temperature which weakens soot oxidation. Maximum soot opacity for Bu0, Bu10, Bu20 and Bu30 are 0.042, 0.04, 0.035 and 0.032 measured at 9° BTDC respectively. Smoke meter used for present experimental studies measures soot opacity instead of soot mass fraction. CFD results are obtained for soot mass fraction and similar trends as compared to experimental results are observed.

6.5. Conclusion

In the present study, experimental and numerical investigations are carried out to determine the effects of n-butanol-diesel blend ratio and injection timing on the performance, combustion and exhaust emission characteristics of CRDI engine. Based on obtained results following conclusions are made:

- Peak in-cylinder pressure is marginally increased for n-butanol-diesel blends compared to neat diesel. The BTE are increased by ~4.5%, 6% and 8% respectively for Bu10, Bu20 and Bu30 respectively compared to neat diesel.

- Optimum injection timings for maximum BTE are obtained for various n-butanol-diesel blends including neat diesel. Injection timing of 12º BTDC is found optimum for neat diesel, whereas IT of 15º BTDC is found optimum for Bu10, Bu20 and Bu30.

- NO$_X$ emissions are reduced with increasing n-butanol-diesel blends. The maximum NO$_X$ emission is 1090, 1001, 989 and 959 ppm for Bu0, Bu10, Bu20 and Bu30 obtained experimentally IT at 18° BTDC respectively.

- Increasing butanol content in the blends results in enhanced oxidation leads to reduction of soot and CO due to higher oxygen/carbon ratio.

- Results obtained from CFD study are showing good agreement with experimental data.

CHAPTER 6

PART II: EFFECT OF EGR WITH BUTANOL-DIESEL BLENDS IN CRDI ENGINE

6.6. Introduction

This part of the study is focused on the effect of exhaust gas recirculation (EGR) on the performance, combustion and emission characteristics of CRDI engine fuelled with n-butanol blended diesel using experimental and CFD simulation. Experiments are conducted for two different EGR rates (10% and 20%) for various n-butanol-diesel blends (0%, 10%, 20% and 30%) and four different injection timings. Further, CFD simulation is carried out for three EGR rates (10%, 20%, and 30%), four different injection timings and different butanol-diesel blends (10%, 20% and 30%). EGR technique is employed in both experiments as well as CFD simulation. EGR is a promising technique to mitigate the NO_X emission significantly.

6.7. Experimental and simulation strategy

Parameters employed to perform experimental and simulation studies are presented in Table 6.2.

Table 6.2: Range of parameters

Parameters	Range
Blend (% of n-Butanol)	0, 10, 20, 30
EGR (%) Experimental	0, 10, 20
EGR (%) Simulation	0, 10, 20, 30
Injection timings	9º, 12º, 15º and 18º

The details of the experimental and simulation methodology employed are discussed in part 1.

6.8. Results and discussion

In this section, results of experimental and numerical (CFD) studies on CRDI engine are presented. Results are obtained for n-butanol-diesel blends for various EGR rates at different injection timings.

6.8.1 Effect of EGR on brake thermal efficiency

The effect of EGR rates and n-butanol-diesel blends on BTE of CRDI engine is investigated experimentally and depicted in Fig 6.11. The brake thermal efficiency is presented for optimum injection timings (i.e., IT @ 12° BTDC for neat diesel and IT @ 15° BTDC for blends) obtained from Fig 6.4.
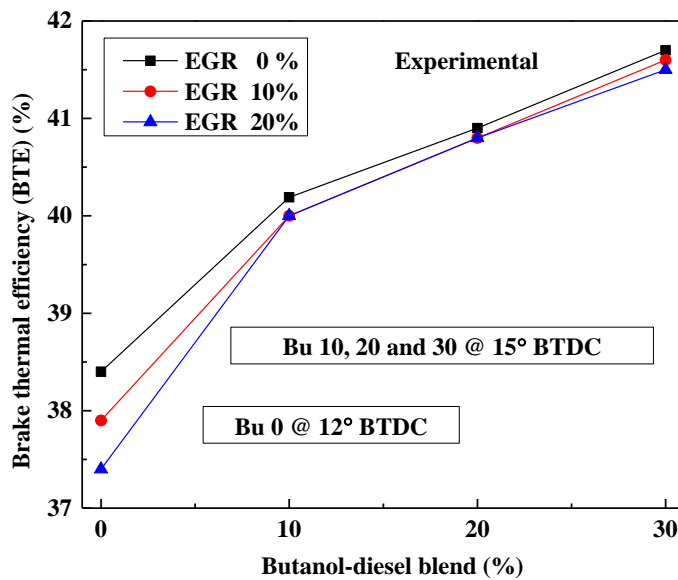
Fig. 6.11 Variation of brake thermal efficiency vs butanol-diesel blends

It is observed that with increase in the EGR rate, BTE is decreased approximately by 1 % for neat diesel (Bu0), whereas insignificant reduction in BTE is observed for butanol-diesel blends. The reduction in BTE is due to displacement of intake oxygen (dilution effect), endothermic dissociation of CO_2 and H_2O, and increase in heat capacity of intake charge (thermal effect), which also results in overall reduction of in-cylinder temperature.

6.8.2 Effect of EGR on in-cylinder pressure (Validation)

The simulation is validated for pressure versus crank angle with the experimental results obtained from author's laboratory for conditions listed in Table 3.1. Comparison between experimental and simulation results for Bu0 at 0% EGR, and Bu20 at 0, 10 and 20% EGR are portrayed in Fig 6.12. For all cases, CFD results are showing good agreement with experimental data. Hence, this CFD model can be used for further parametric study.
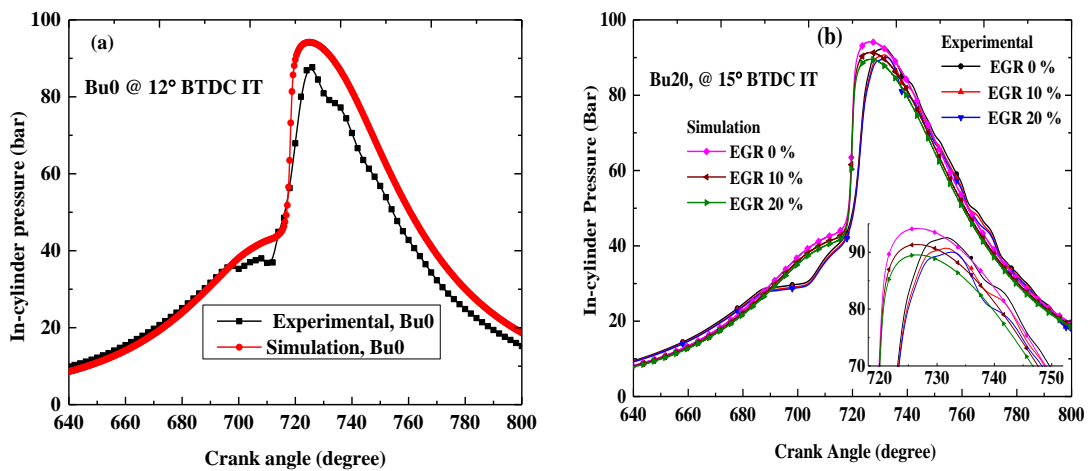
Fig. 6.12 Pressure versus crank angle for different EGR rates (a) Bu0 at 0% EGR and (b) Bu20 at 0, 10 and 20% EGR rates

6.8.3 Effect of EGR on NO_X emission

Figures 6.13 show experimental and simulation results of NO_X emission during combustion for various n-butanol-diesel blends at different EGR rates (experiment: 0, 10 and 20%; simulation: 0, 10, 20 and 30%). Due to some restrictions with experimental setup, higher EGR rates (30%) could not be used in experimental study unlike simulation. Results show that NO_X emission reduces with n-butanol-diesel blends, which occur due to high latent heat of vaporization of n-butanol results in lower in-cylinder temperature compared to diesel. Further, increase in EGR rates leads to decrease in overall in-cylinder temperature due to dilution, thermal and chemical effects. Hence, NO_X emission reduces

117

drastically. Results presented in figure 6.13 are showing similar trends compared to experimental results, which approves the selection of NOx model for simulation.
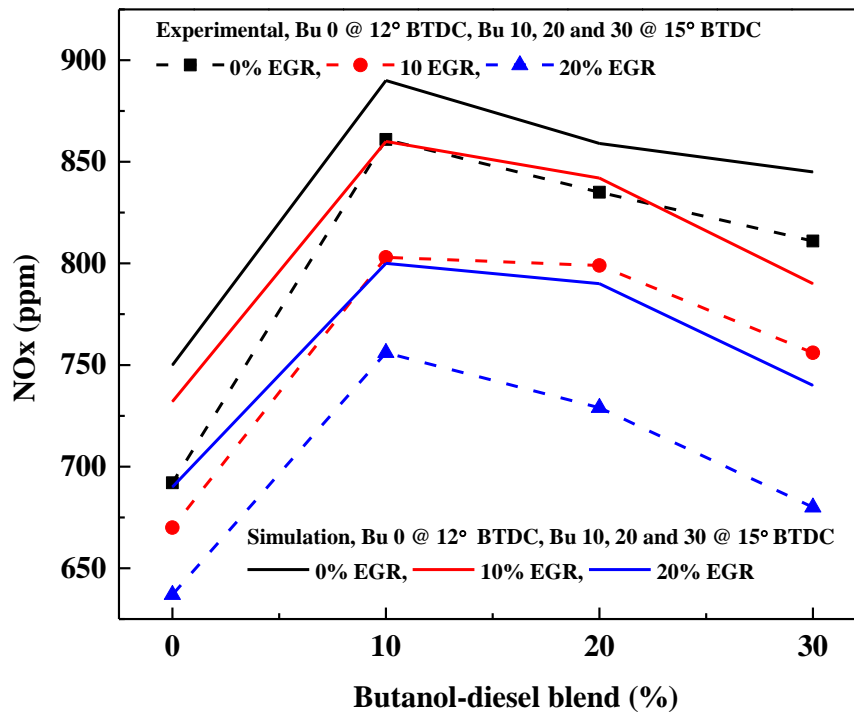
Fig. 6.13 Effect of various EGR rates on NO_X emissions for various n-butanol-diesel blends

6.8.4 Effect of EGR on CO emission

Figures 6.14 show CO emission during combustion of various n-butanol-diesel blends at different EGR rates experimentally (0, 10 and 20%) and by CFD simulation (0, 10, 20 and 30%) respectively. During combustion in engine, CO formation is an intermediate step. In further phase with help of OH radicals, in presence of oxygen inside the cylinder, oxidation takes place and CO_2 gets formed at temperature above 1200 K. In anoxygenated region, the oxidation of CO stops due to improper mixing of fuel and air. With more EGR rate, charge gets diluted and more CO formation occurs. It is interesting to know that CO formation is lesser for n-butanol-diesel blends with EGR rates compared to neat diesel. From experimental results it is observed that CO emission for Bu30 (IT @ 15° BTDC) is decreased by 36%, 31% and 38% for 0, 10 and 20 % EGR rates respectively compared to Bu0 (IT @ 12° BTDC). The oxygen content of n-butanol is higher than diesel which causes

118

conversion of CO in rich fuel region into CO_2. Similar trend is also observed in simulation studies.
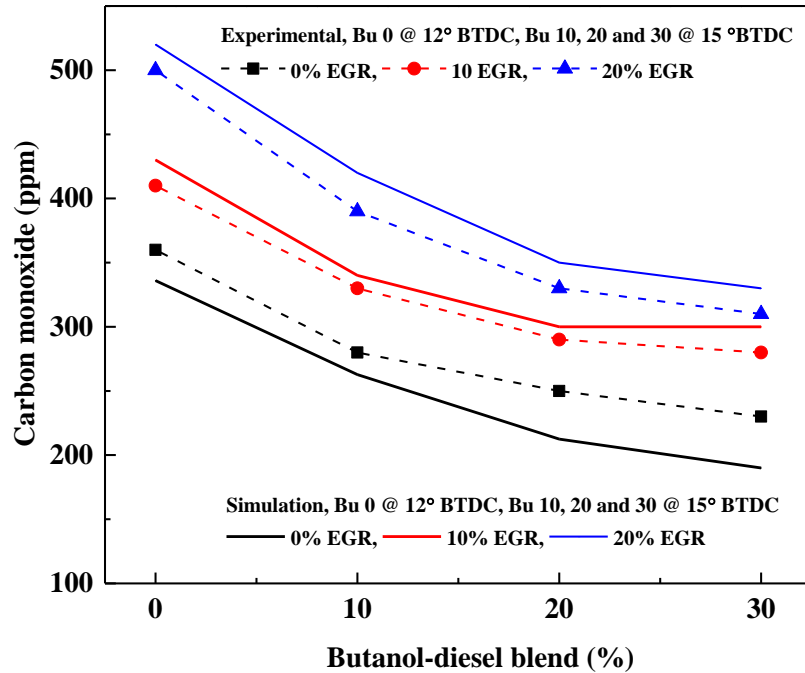
Fig. 6.14 Effect of various EGR rates on CO emissions for various n-butanol-diesel blends

6.8.5 Effect of EGR on soot emission

Figures 6.15 (a) and (b) show soot emission during combustion for various n-butanol-diesel blends at different EGR rates experimentally (0, 10 and 20%), and by simulation (0, 10, 20 and 30%) respectively. The particulate matter (PM) is basically composed of soot and is accountable for the smoke. Increasing butanol content in the blends, result in the reduction of soot due to higher oxygen/carbon ratio.
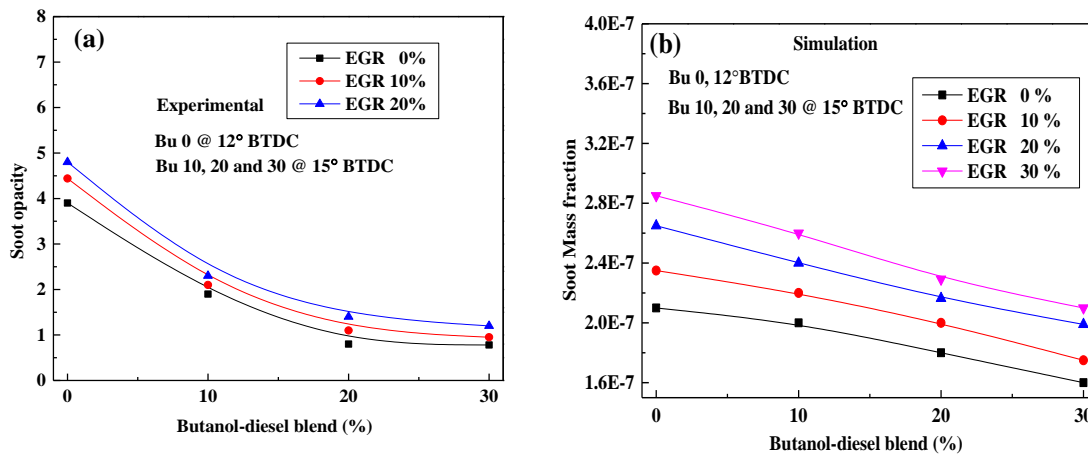
Fig. 6.15 Effect of various EGR rates on soot emissions for various butanol-diesel blends
(a) Experimental and (b) Simulation

From simulation results it is observed that soot emission for Bu30 (IT @15° BTDC) is decreased by 23%, 25%, 24% and 26% for 0, 10, 20 and 30 % EGR rates respectively compared to Bu0 (IT @12° BTDC). The existence of atomic oxygen bond in butanol fulfills progressive chemical control over soot formation. Smoke meter used for present experimental studies measures soot opacity instead of soot mass fraction. Local equivalence ratio is the key parameter for soot formation. Soot gets oxidized in contact with oxygen and water at elevated temperature. To incorporate soot formation in CFD simulation, kinetic soot model is employed. CFD results are obtained for soot mass fraction and similar trend compared to experimental results is observed.

6.9. Conclusion

Experimental and CFD analyses of four-stroke CRDI engine fuelled with n-butanol-diesel blends for various EGR rates are carried out. Following inferences are made based on the obtained results.

- With the help of experimental results, an appropriate CFD model to capture the effect of butanol-diesel blends and EGR in CRDI engine is established.

- BTE is decreased approximately 1 % with EGR rate for neat diesel and insignificant effects on bioethanol-diesel blends.

- NO_X emission reduces with n-butanol-diesel blends which occur due to high latent heat of vaporization of n-butanol results in lower in-cylinder temperature compared to diesel.

- Increase in EGR rates leads to decrease in overall in-cylinder temperature due to dilution, thermal and chemical effects. Hence, NO_X emission reduces drastically

- CO emission for Bu30 (IT @ 15° BTDC) is decreased by 36%, 31% and 38% for 0, 10 and 20 % EGR rates respectively compared to Bu0 (IT @ 12° BTDC).

- Soot emission for Bu30 (15° BTDC) is decreased by 23%, 25%, 24% and 26% for 0, 10, 20 and 30 % EGR rates respectively compared to Bu0 (12° BTDC).

CHAPTER 7

EXPERIMENTAL STUDY ON CRDI ENGINE FUELLED WITH WASTE PLASTIC OIL - DIESEL BLENDS

7.1. Introduction

The demand for plastic is eternally growing in urban areas and producing enormous quantity of plastic waste. The management and disposal of plastic waste have become a major concern worldwide. The awareness of waste to energy retrieval is one of the promising modes used for treatment of waste plastics. Present investigation evaluates the prospective use of waste plastic oil (WPO) as an alternative fuel for diesel engine. Different blends (WPO0, WPO30 and WPO50) with diesel are prepared on a volume basis and the engine is operated. Experiments are conducted on twin cylinder CRDI engine with open - ECU for various injection timings (9°, 12°, 15° and 18° BTDC) and for different exhaust gas recirculation rates (10%, 15% and 20%) at 100 MPa injection pressure. Effects on combustion characteristics, performance and tail pipe emissions of CRDI engine are studied.

Furthermore, to reduce excess NO_X emission caused by WPO, multiple injection technique is employed in experimental study. Results are obtained for various pilot injection timings (25º, 35º, and 45º BTDC) and different main injection timings (9º, 12º and 15º BTDC) at 100 MPa injection pressure. It also includes 5%, 10% and 15% fuel quantity injected in pilot and 95%, 90% and 85% fuel in main injection respectively.

7.2. Fuel Properties and operating range of parameters

The WPO is mixed with the neat diesel to obtain different WPO-diesel blends. WPO0, WPO30, and WPO50 represents 0%, 30% and 50% waste plastic oil in neat diesel by volume. Basic physical properties of the WPO and neat diesel employed in this investigation are provided in Table 7.1 (Damodharan et al. 2017) and range of experimental parameters considered for study are listed in Table 6.2.

Table 7.1: Properties of diesel and waste plastic oil

Properties	Test method	ULSD	WPO
LHV(MJ/kg)	ASTM D240	41.82	40.35
ν at 40 °C (mm^2/s)	ASTM D445	3.8	2.16
ρ (kg/m^3)	ASTM D4052	838	813
CCI	ASTM D4737	54	51
Flash point (°C)	ASTM D93	70	38

Abbreviations: ULSD- Ultra low sulphur diesel; LHV-low heating value;
ν -kinematic viscosity; ρ-density; CCI- calculated cetane index

Table 7.2: Range of engine operating parameters

Parameters	Range
Blend (% of WPO)	0, 30 and 50
Injection timings (CA BTDC)	9º, 12 º, 15 º and 18º
EGR (%)	0, 10, 15 and 20

Chemical structure of WPO using FTIR spectroscopy:

The chemical structure of WPO is studied using Fourier transform infrared spectroscopy (FTIR) as shown in Fig 7.1. This method categorizes the chemical bonds in a molecule by generating an infrared absorption spectrum for several functional groups present in the waste plastic oil. WPO has absorption bands in the region of 4000-400 cm^{-1} with several peaks. The chemical bond will stretch, contract and absorb infrared radiation in a precise wavelength range during the interaction of infrared light with the oil. Bruker series FTIR spectroscopy is used to record the spectra. Table 7.3 shows the functional groups present in the WPO which were obtained by matching the peak wave numbers with standard data given by Coates (2000).
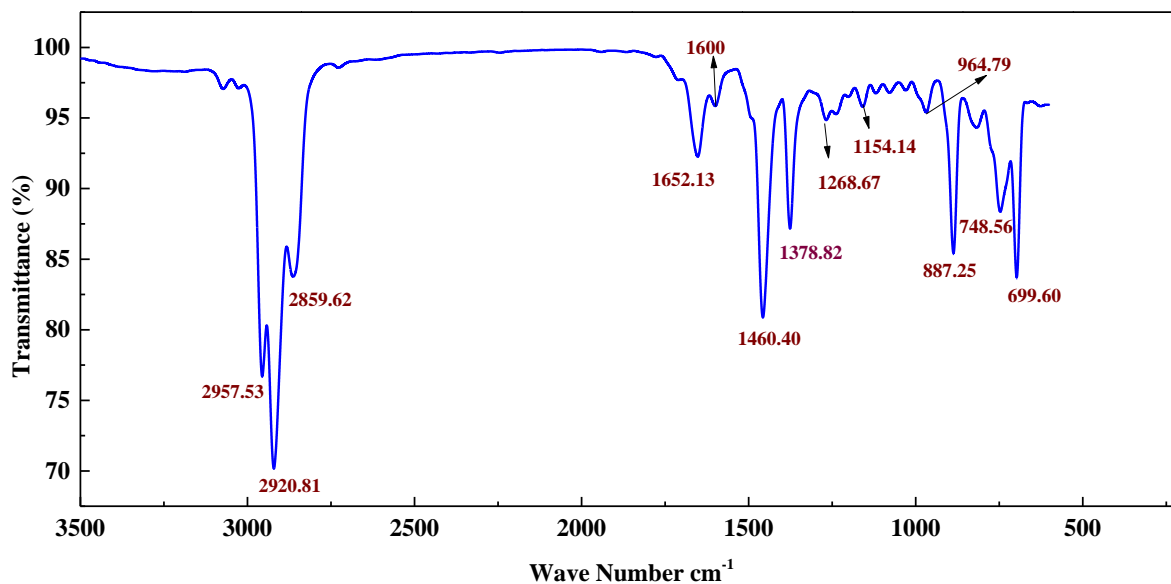
Fig. 7.1 FTIR spectrum of waste plastic oil

Table 7.3: FTIR analysis of waste plastic oil indicating functional groups

Functional group	Assignment	Wave number (cm^{-1})
$-CH_3$, branched alkane	Methyl C$-$H stretch	2957.5
CH_2, branched alkane	Methylene C$-$H stretch	2920.8 & 2859.6
C $=$ C, Alkene	Alkenyl C=C stretch	1652.1
C=C	Conjugated C=C	1600
CH_2, Alkane	Methylene C$-$H bend	1460.4
$-CH_3$, Alkane	Methyl C$-$H stretch	1378.8
C$-$C	Skeletal C$-$C vibrations	1268.6
C$-$O, Alcohol	Tertiary alcohol, C$-$O stretch	1154.1
=C$-$H, Alkene	Trans-C$-$H out-of-plane bend	964.7
C$-$H, Alkene	Vinylidene C$-$H out-of-plane bend	887.2
CH_2	Methylene -$(CH_2)_n$ - rocking	748.5
C-H	cis-C H out-of-plane bend	699.6

7.3 Experimental methodology: The details of the experimental methodology employed for the study is discussed in section 3.1-3.4 of chapter 3.

7.4 Results and discussion

In this section, results of experimental studies for WPO-diesel blends and EGR rates at different injection timings on CRDI engine are presented.

7.4.1 Variation of in-cylinder pressure versus crank angle

The variation of in-cylinder pressure versus crank angle for various injection timings (9º, 12º, 15º and 18º), different EGR rates (10%, 15% and 20%) and different WPO-diesel blends (WPO30 and WPO50) is shown in Fig 7.2 and 7.3.
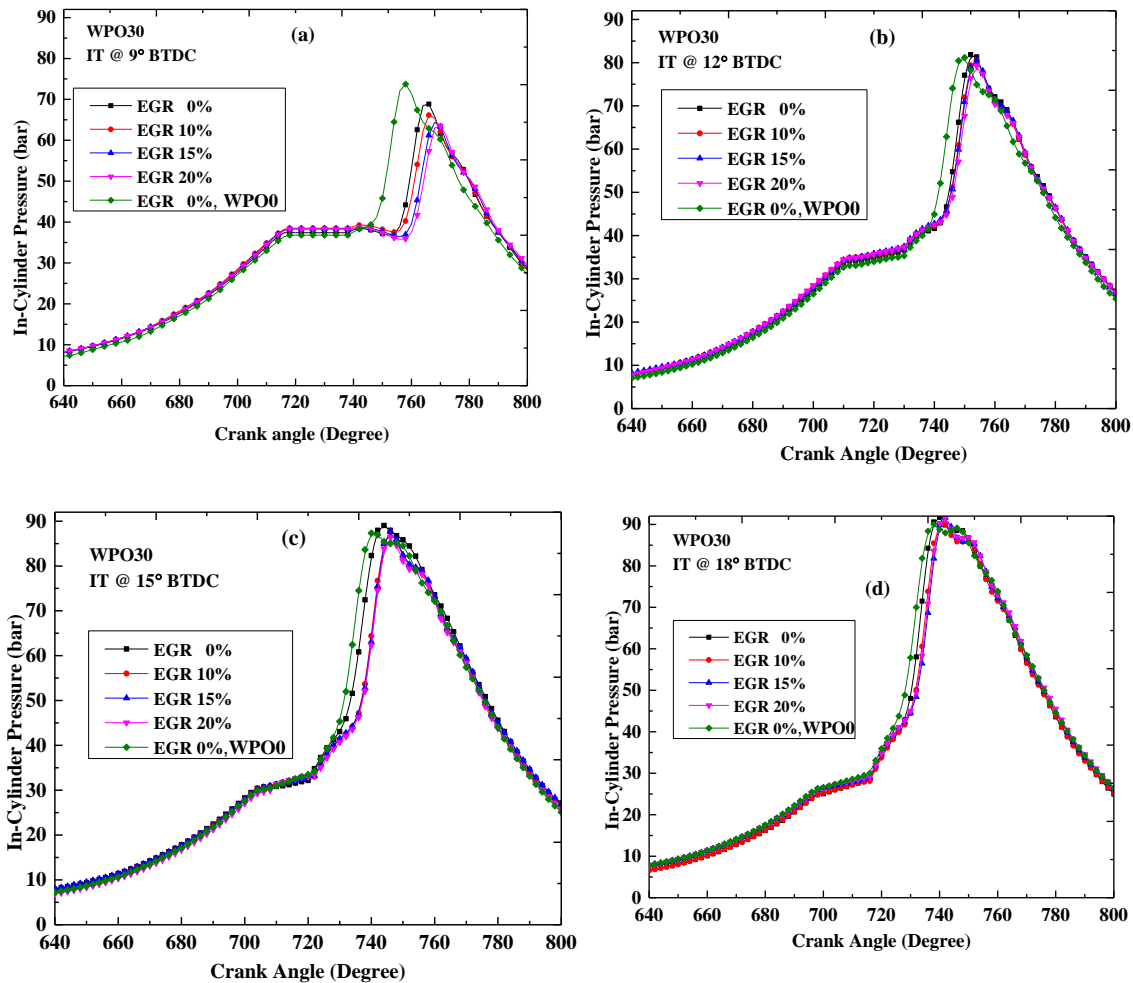
Fig. 7.2 (a-d): In-cylinder pressure versus crank angle for WPO30 blend for various EGR rates
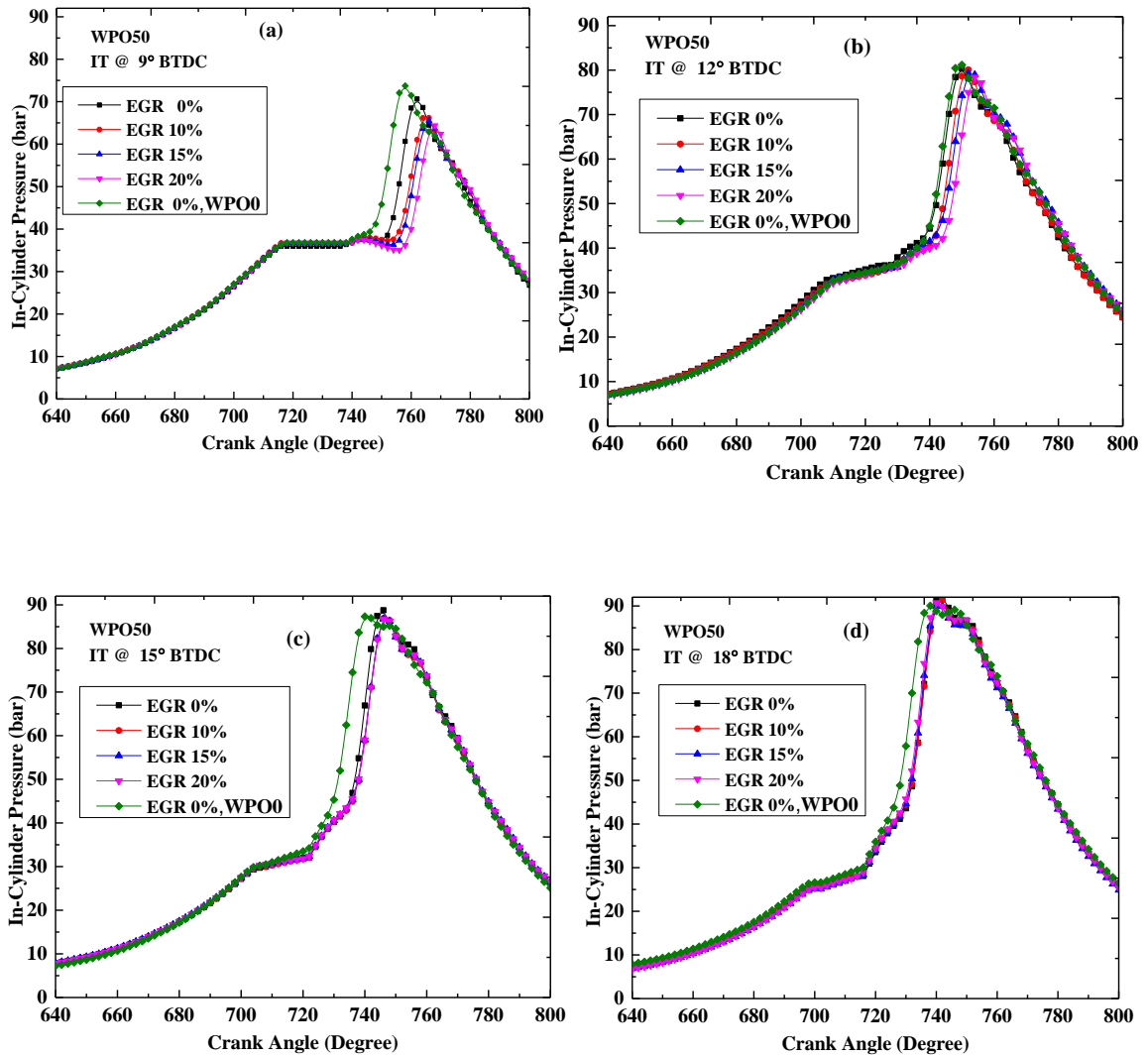
Fig. 7.3 (a-d): In-cylinder pressure versus crank angle for WPO50 for various EGR rates

Results show that as injection timing advances the in-cylinder peak pressure increases. It occurs due to the charge gets sufficient time to diffuse throughout the combustion chamber thereby reducing the heterogeneity of the mixture. The low temperature combustion (EGR) results in marginally drop in in-cylinder pressure and more ignition delay as expected, similar trend was observed for all the blends.

7.4.2 Effect of waste plastic oil-diesel blends and injection timings on NOx

Figure 7.4 shows the illustration of the NO_X emissions for various injection timings at various EGR rates and different WPO-diesel blends. NO_X at tail pipe decreases with increase in EGR rates, and increases with advance injection timing. Similar observation is found for all WPO-diesel blends (WPO30 and WPO50) considered in the study. NO_X is found to be less for diesel compared to the WPO-diesel blends and similar trends were observed by Mani et al. (2010).
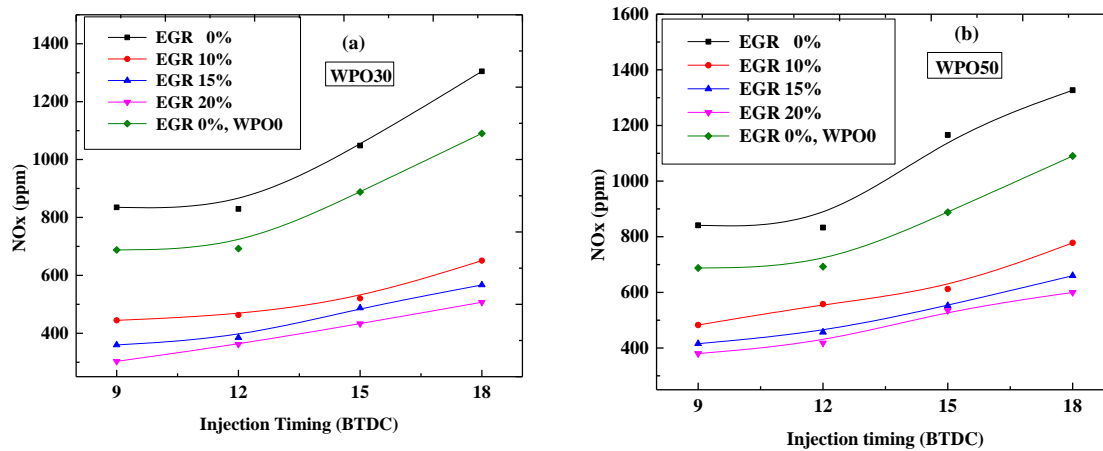
Fig. 7.4: NO_X versus injection timing for various EGR rates (a) WPO30 (b) WPO50

Compression ignition engines always run with lean fuel-air mixtures and emit higher amounts of NO_X. WPO comprises certain oxygenated hydrocarbons which stimulate combustion and thus the formation of NO_X in exhaust takes place (Kumar et al. 2013). NO_X emission gets increased with advanced injection timing due to increased ignition delay because of more air and fuel mixture burns in premixed combustion. At 12° BTDC injection timing, the NO_X emission gets reduced from 830 ppm to 362 ppm and 833 ppm to 418 ppm for 0 and 20% EGR rates for WPOP30 and WPOP50 respectively. Hence, EGR technique is recommended to control NO_X for higher WPO-diesel blends.

7.4.3 Effect of WPO-diesel blends and injection timings on CO

Figure 7.5 shows the illustration of the carbon monoxide emissions for various injection timings at different EGR rates and for different WPO-diesel blends. CO at tail pipe

128

increases with increase in EGR rate and declines with increase in injection timing for all the cases of blends (WPO30 and WPO50).
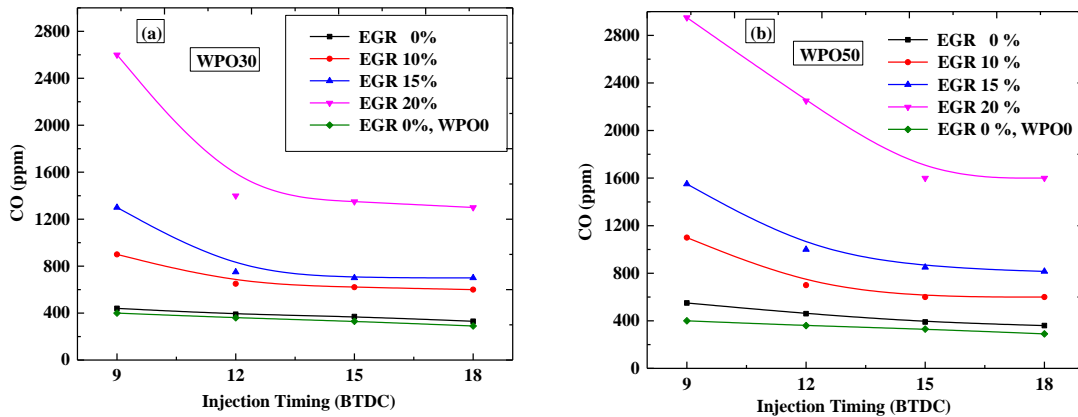
Fig. 7.5 CO versus injection timing for various EGR rates (a) WPO30 (b) WPO50

At 20% EGR rate, the CO emission gets reduced from 2600 to 1300 ppm and 2950 to 1600 ppm from 9º BTDC to 18º BTDC injection timing for WPOP30 and WPOP50 respectively. Figure 7.5 shows that CO emissions are lower for diesel compared to blends. Since calorific value of WPO is lesser than diesel, more quantity of WPO is required to meet same engine load condition which may result in higher CO formation. In advance injection timing the increase in cylinder temperature leads to early start of combustion due to increase in the chemical reaction and oxidation process between carbon and oxygen molecules in the combustion chamber (Hulwan et al. 2011).

7.4.4 Effect of WPO-diesel blends and injection timings on smoke (soot) emission

Figure 7.6 represents the smoke opacity emissions for various injection timings at different EGR rates and WPO-diesel blends. The exhaust smoke emission at tail pipe increases with increase in EGR rates and declines with advance injection timing for blends (WPO30 and WPO50). Smoke number represents solid unburned hydrocarbon particles in exhaust emission. Formation of smoke occurs in rich-fuel and moderate temperature zones. With advancing the injection timing, soot formation decreases due to more homogeneous mixture forms in the cylinder (Damodharan et al. 2017). Also, higher cylinder temperature which occurs due to advancing IT, promotes oxidation of the nucleated soot during

combustion. Further, retard injection results in inadequate time for soot oxidation (exhaust valve opens before the completion of soot oxidation) and augments smoke formation. At 20% EGR rate, the smoke opacity gets reduced from 13.7 to 9 and 15.5 to 8.8 % from 9º BTDC to 18º BTDC injection timing for WPOP30 and WPOP50 respectively. Also, smoke opacity increases significantly with increase in EGR because of increase in anoxygenated region in combustion chamber. As explained above, since more quantity of WPO is required (compared to diesel) to maintain same engine load which may cause higher soot formation.
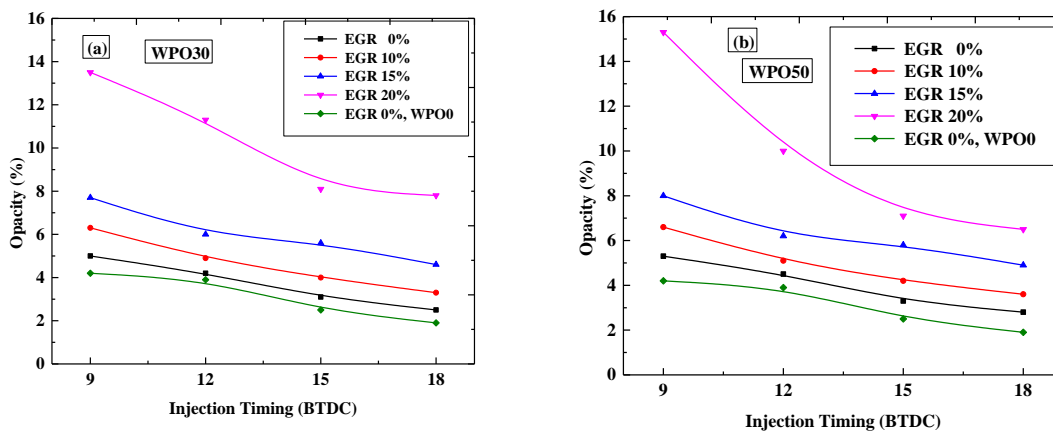
Fig. 7.6 Opacity versus injection timing for various EGR rates (a) WPO30 (b) WPO50

7.4.5 Effect of various WPO-diesel blends and injection timings on BTE

The effect of injection timing and EGR for various WPO-Diesel blends on performance of CRDI engine is demonstrated in Fig 7.7. Results show the increase of brake thermal efficiency (BTE) with WPO-diesel blends and found to be highest in the case of higher blend (WPO50). The optimum BTE is obsreved at 9º and 12º BTDC for WPO30 and WPO50 respectively. The maximum BTE observed (@ EGR0) for WPO0, WPO30 and WPO30 are 38.5, 42.3 and 42.5% respectively. With increase in EGR rate, BTE is reduced due to insufficient oxygen in combustion process and more replacement of air by the exhaust gases.
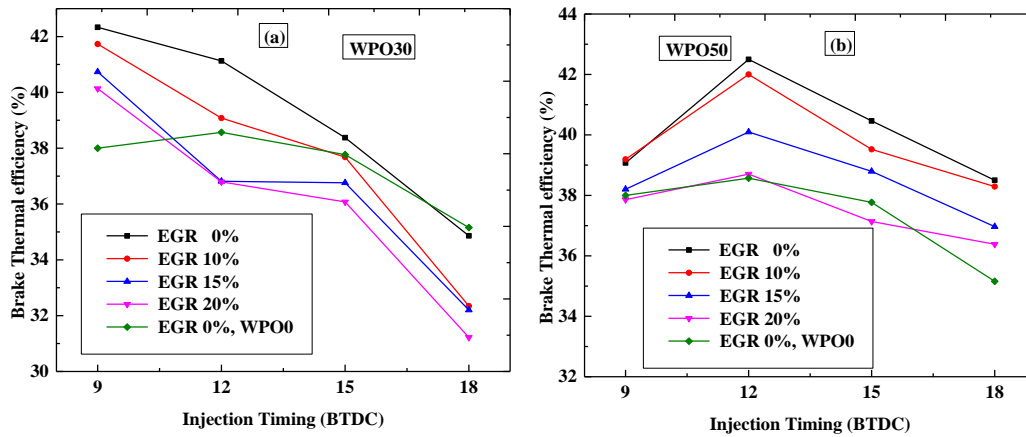
Fig. 7.7 BTE versus injection timing for various EGR rates (a) WPO30 (b) WPO50

7.4.6 Effect of WPO-diesel blends with multiple injection on in-cylinder pressure and temperature

Figure 7.8 show the in-cylinder pressure versus crank angle for WPO30. Higher peak in-cylinder pressure is observed for advanced main injection timing. For advanced main IT, start of combustion is before TDC, hence all the injected fuel is burned early in high pressure and high temperature region, resulted in higher peak pressure. It is also observed that main fuel injection timing prominently decides the start of combustion which results in different pressure zones as shown in Fig.
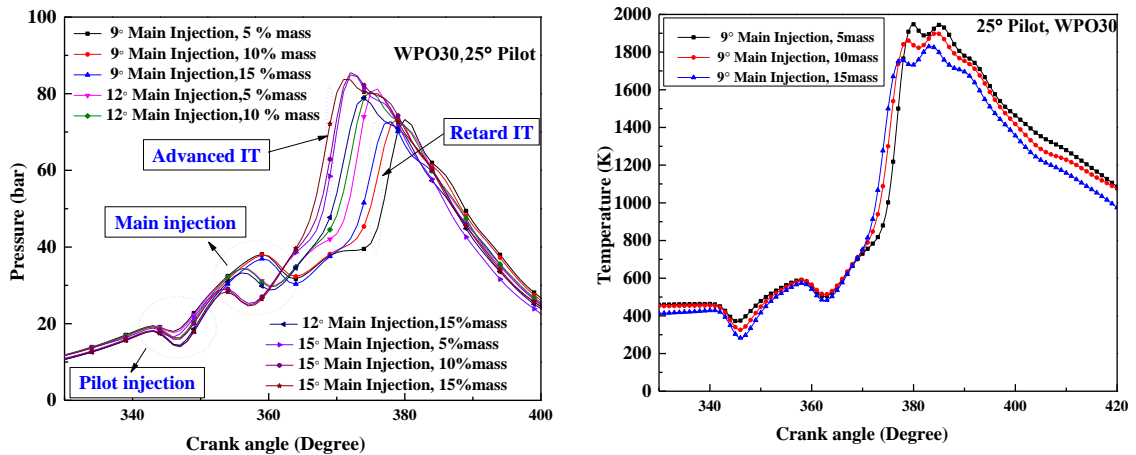
Fig. 7.8 Effect of multiple injection on In-cylinder pressure
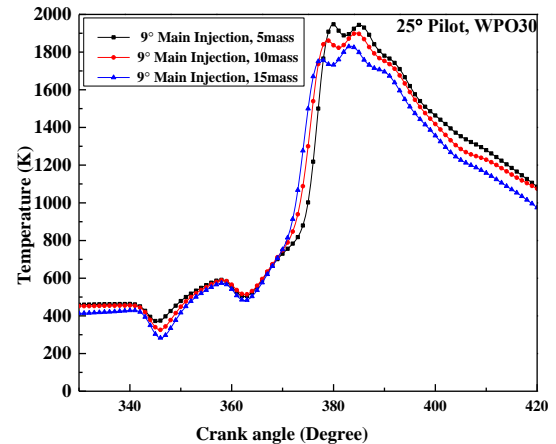
Fig. 7.9 Effect of multiple injection on Mean gas temperature

131

For retarded main injection timings, start of combustion is found after TDC. It is observed that a higher spike of in-cylinder pressure is found for lesser quantity of fuel injection in pilot. Similar results are witnessed for all injection timings. Figure 7.9 shows the mean gas temperature versus crank angle for 25º pilot at 9º main injection before TDC with different mass of fuel in pilot injection for WPO30-diesel blends. As mass of fuel in pilot injection increases, the in-cylinder peak temperature decreases due to decrease in peak pressure.

7.4.7 Effect of WPO-diesel blends with multiple injection on NO$_X$ emission

Figure 7.10 shows the exhaust NO$_X$ emission versus percentage of pilot fuel injection quantity of WPO30 for various pilot and main injections. It is interesting to note that NO$_X$ is reduced drastically with retarding main injection timings and increasing fuel quantity in pilot injection. For higher fuel quantity in pilot injection, reduction of NO$_X$ is observed due to decrease in peak in-cylinder temperature as shown in Fig 7.9. Further, reduction of NOx is observed for all multiple injection cases with higher fuel quantity in pilot injection. At 12º BTDC main injection timing, the NO$_X$ emission gets reduced from 835 to 580 ppm at 25º BTDC pilot injection (for 15% fuel mass) compared to single injection for WPOP30. A remarkable NOx reduction is observed for all multiple injection cases compared to single injection as shown in Fig 7.10.
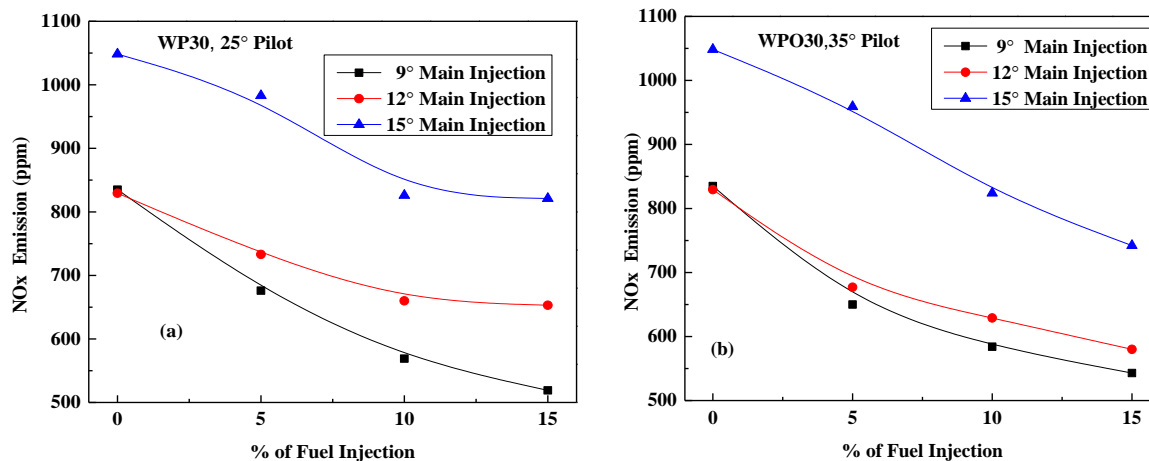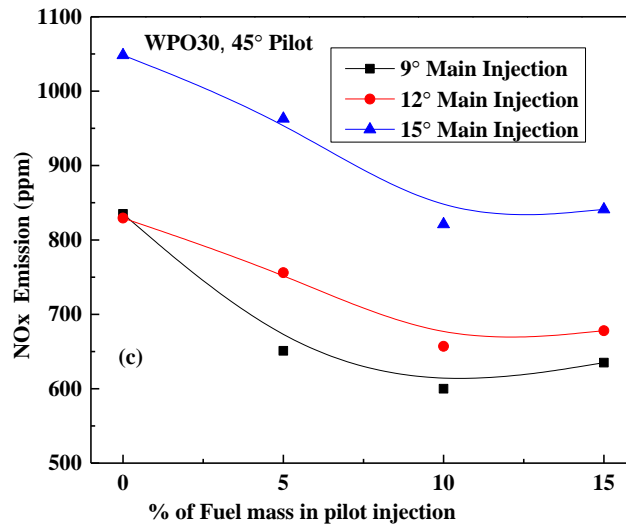
Fig. 7.10 Effect of multiple injection on NO_X, (a) 25° BTDC pilot (b) 35° BTDC pilot (c) 45° BTDC pilot

7.5 Conclusion

In the present study, experimental investigations are carried out to determine the effects of WPO-diesel blends, EGR rates, injection timing and multiple injection on the performance, combustion and exhaust emission characteristics of CRDI engine. Based on obtained results following conclusions are made:

- The optimum BTE is observed at 9° and 12° BTDC for WPO30 and WPO50 respectively. The maximum BTE observed at EGR0 for WPO0, WPO30 and WPO30 are 38.5, 42.3 and 42.5% respectively.

- At 12° BTDC injection timing, the NO_X emission gets reduced from 830 ppm to 362 ppm and 833 ppm to 418 ppm for 0 and 20% EGR rates for WPOP30 and WPOP50 respectively

- At 20% EGR rate, the CO emission gets reduced from 2600 to 1300 ppm and 2950 to 1600 ppm from 9° BTDC to 18° BTDC injection timing for WPOP30 and WPOP50 respectively.

- At 20% EGR rate, the soot emission gets reduced from 13.7 to 9 and 15.5 to 8.8 % smoke opacity from 9º BTDC to 18º BTDC injection timing for WPO0, WPOP30 and WPOP50 respectively.

- It is interesting to note that reduction of NOx is observed for all multiple injection cases with higher fuel quantity in pilot injection. At 12º BTDC main injection timing, the NO_X emission gets reduced from 835 to 580 ppm at 25º BTDC pilot injection (for 15% fuel mass) compared to single injection for WPOP30.

- Multiple injection technique is a promising technique to mitigate the NO_X emission significantly from diesel engine.

- Waste plastic oil is better alternative to diesel engine fuel as it gives solution to multiple problems in concern to environment. Along with EGR and suitable after treatment techniques, all the emissions can be controlled simultaneously.

CHAPTER 8

CONCLUSION

8.1 Conclusions

This dissertation presents an array of numerical and experimental studies on CRDI engine based on alternative fuel. Exercises covered include EGR, injection timing and injection strategies for various types of oxygenated fuels and experimental studies for waste plastic oil. To provide a comprehensive overview of the dissertation, all the investigations are briefly summarized and the salient observations are reiterated in the following sections.

8.1.1 DME-diesel blends with EGR

The present study emphasizes the effect of dimethyl ether (DME)- diesel blends (0-20%) at various exhaust gas recirculation (EGR) rates (0-20%) on the performance, combustion characteristics and exhaust emissions of CRDI engine using three dimensional computational fluid dynamics (CFD) simulation. Results show that in-cylinder pressure marginally decreases with employing EGR compared to without EGR case. As EGR rate increases, nitrogen oxide (NO) formation decreases, whereas soot increases marginally. Due to better combustion characteristics of DME, indicated thermal efficiency (ITE) increases with the increases in DME-diesel blend ratio. The trade-off among NO, soot, carbon monoxide (CO) formation and efficiency is studied by normalizing the parameters.

8.1.2 Bioethanol-diesel blends, EGR and injection timings

This investigation is focused on the effect of exhaust gas recirculation (EGR) and injection timing on the performance, combustion and exhaust emission characteristics of common rail direct injection (CRDI) engine fueled with bioethanol-blended diesel using computational fluid dynamics (CFD) simulation. The results indicate that the mean CO formation and ignition delay increase, whereas mean NO formation and in-cylinder temperature decrease, with increase in the EGR rate. Further, with an increase in percentage of the bioethanol blends, CO and soot formation decrease as compared to neat diesel. Optimum injection timing is obtained for maximum indicated thermal efficiency

(ITE) for bioethanol diesel blends operation. Significant increase in ITE is observed in the case of E30 compared to diesel (E0). Effect of injection timing on tail pipe emissions such as NO, soot and CO formation is also obtained. The results indicate that ignition delay increases and mean soot formation decreases with advancing the injection timings. For all advanced injection timing higher in-cylinder peak pressure and temperature are observed.

8.1.3 Butanol-diesel blends, EGR and injection timings

In this section, numerical and experimental studies on the effect of injection timings, EGR and various n-biobutanol-diesel blends on the engine performance, tailpipe emissions and combustion characteristics of CRDI engine are presented. Optimum injection timings are obtained for different n-butanol-diesel blends (0-30%) experimentally to get maximum brake thermal efficiency (BTE). Tailpipe emissions (NO_X, CO and soot) at various injection timings (9º, 12º, 15º and 18º) are also measured.

Experimental results reveals the increase in brake thermal efficiency for butanol-diesel blends compared to neat diesel (Bu0). Both experimental and simulation results witnessed in reduction of smoke opacity, NOx and carbon monoxide emissions with the increasing n-butanol percentage in diesel fuel. Further, for all EGR rates and blends, BTE is decreased approximately 1 % with EGR rate for neat diesel and insignificant effects on bioethanol-diesel blends. Nitrogen oxide (NO) emission gets reduced drastically whereas carbon monoxide (CO) and soot emissions get decreased moderately with increase in n-butanol-diesel blends. The CO and soot emissions increase with EGR rate due to oxygen deficiency as well.

8.1.4 WPO-diesel blends with EGR and various injection timings

In the present study, experimental investigations are carried out to determine the effects of WPO-diesel blends, EGR rates, injection timing and multiple injection on the performance, combustion and exhaust emission characteristics of CRDI engine. Results shows higher BTE for WPO diesel blends compared to diesel. For all WPO-diesel blends higher emissions is observed. It is also interesting to note that reduction of NOx is observed for

all multiple injection cases with higher fuel quantity in pilot injection. Multiple injection technique is a promising technique to mitigate the NO_X emission significantly from diesel engine. Waste plastic oil is better alternative to diesel engine fuel as it gives solution to multiple problems in concern to environment. Along with EGR and suitable after treatment techniques, all the emissions can be controlled simultaneously.

8.2 Scope for future study

The present dissertation analyses several aspects of CRDI engine based on alternative fuel. In course of the present study, a few areas have been earmarked which deserve further attention, as enumerated below:

- It is suggested to carryout performance testing with still higher fuel injection pressures, changing the shape of combustion chamber, different injectors.
- It is suggested perform the comparative study with additives
- The reduction of exhaust emissions can be done by using exhaust after treatment devices.

Acknowledgments

REFERENCES

Aradhey, A. (2017) "India-Biofuels Annual." USDA Foreign Agricultural Service, GAIN Report Number. https://gain.fas.usda.gov/Lists/Advanced%20Search/AllItems.aspx)

Arcoumanis, (2000). "The second European Auto-Oil programme (AOLII) European Commission." vol. 2, Alternative fuels for Transportation.

Arcoumanis, C., Bae, C., Crookes, R. and Kinoshita, E. (2008). "The potential of di-methyl ether (DME) as an alternative fuel for compression-ignition engines: a review." Fuel. 87(7): 1014-1030.

Arcoumanis, C., Nagwaney, A., Hentschel, W., and Ropke, S., (1995). "Effect of EGR on Spray Development, Combustion and Emissions in a 1.9L Direct-Injection Diesel Engine", SAE Technical Paper 952356.

Armas, O., Martinez-Martinez, S., and Mata, C. (2011). "Effect of an ethanol–biodiesel–diesel blend on a common rail injection system." Fuel Processing Technology, 92: 2145-2153.

Bang, S. H., and Lee, C. S. (2010). "Fuel injection characteristics and spray behavior of DME blended with methyl ester derived from soybean oil." Fuel, 89(3):797-800.

Bansal, G., and Bandivadekar, A. (2013). "Overview of India's vehicle emissions control program." ICCT, Beijing, Berlin, Brussels, San Francisco, Washington.

Basara, B., (2006). "An eddy viscosity transport model based on elliptic relaxation approach", AIAA J 44(7):1686–1690.

Beatrice. C., Napolitano. P. and Guido, C. (2014). "Injection parameter optimization by DoE of a light-duty diesel engine fed by Bio-ethanol/RME/diesel blend." Applied Energy, 113: 373-384.

Benajes, J., López, J. J., Novella, R. and Redón, P. (2014). "Comprehensive modeling study analyzing the insights of the NO–NO$_2$ conversion process in current diesel engines." Energy Conversion and Management, 84:691-700.

Bianchi, G.M., Pelloni, P.P., Corcione, F.E., Allocca, L.L., and Luppino, F.F. (2000). "Modeling Atomization of High-Pressure Diesel Sprays." ASME. J. Eng. Gas Turbines

Power, 123(2):419-427.

Buekens, A. G., and Huang, H. (1998). "Catalytic plastics cracking for recovery of gasoline-range hydrocarbons from municipal plastic wastes". Resources, Conservation and Recycling, 23(3), 163-181.

Chen, C., Fawcett, A., Posner, A., and Raviv, T. (2009). "Butanol by two stage fermentation." Senior Design Reports (CBE), 4.

Chen, Z., Liu, J., Wu, Z., and Lee, C. (2013). "Effects of port fuel injection (PFI) of n-butanol and EGR on combustion and emissions of a direct injection diesel engine." Energy Conversion and Management, 76: 725-731.

Cheng, X., Li, S., Yang, J., and Liu, B. (2016). "Investigation into partially premixed combustion fueled with N-butanol-diesel blends." Renewable Energy, 86: 723-732.

Cipolat, D. (2007). "Analysis of Energy Release and NO x Emissions of a CI Engine Fuelled on Diesel and DME." Applied Thermal Engineering, 27(11):2095-2103.

Cipolat, D., and Bhana, N. (2009). "Fuelling of a compression ignition engine on ethanol with DME as ignition promoter: Effect of injector configuration." Fuel Processing Technology, 90(9):1107-1113.

Coates J. (2000). "Interpretation of infrared spectra, a practical approach." Encyclopedia of analytical chemistry.

Colin, O. and Benkenida, A. (2004). "The 3-zones extended coherent flame model (ECFM3Z) for computing premixed/diffusion combustion." Oil & Gas Science and Technology, 59(6): 593-609.

Corcione, F. E., Allocca, L., Pelloni, P., Bianchi, G. M., and Luppino, F., Corporation, New York, 1989.

CPCB:(http://cpcb.nic.in/)

Da Silva Trindade, W. R., and dos Santos, R. G. (2017). "Review on the characteristics of butanol, its production and use as fuel in internal combustion engines." Renewable and Sustainable Energy Reviews, 69:642-651.

Damodharan, D., Sathiyagnanam, A. P., Rana, D., Kumar, B. R., and Saravanan, S. (2017). "Extraction and characterization of waste plastic oil (WPO) with the effect of n-butanol addition on the performance and emissions of a DI diesel engine fueled with WPO/diesel blends." Energy Conversion and Management, 131:117-126.

Dernotte, J., Mounaim-Rousselle, C., Halter, F., and Seers, P. (2010). "Evaluation of butanol–gasoline blends in a port fuel-injection, spark-ignition engine." Oil & Gas Science and Technology–Revue de l'Institut Français du Pétrole, 65(2):345-351.

Devaraj, J., Robinson, Y., and Ganapathi, P. (2015). "Experimental investigation of performance, emission and combustion characteristics of waste plastic pyrolysis oil blended with diethyl ether used as fuel for diesel engine." Energy, 85:304–9.

Dogan, O. (2011). "The influence of n-butanol/diesel fuel blends utilization on a small diesel engine performance and emissions." Fuel, 90(7): 2467-2472.

Dronniou, N., Lejeune, M., Balloul, I., and Higelin, P., (2005). "Combination of High EGR Rates and Multiple Injection Strategies to Reduce Pollutant Emissions," SAE Technical Paper, 2005-01-3726.

Dukowicz, J.K. (1979). "Quasi-steady droplet change in the presence of convection." Informal report Los Alamos Scientific Laboratory, LA7997-MS.

Edgar, B., Dibble, R.W., and Naegeli, D.W. (1997). "Autoignition of di-methyl ether and di-methoxy methane sprays at high pressures." SAE Paper 971677, SAE Trans J Fuel Lubr, 106(4):625–639.

EIA report: (http://www.eia.gov/countries/analysisbriefs/India/india.pdf)

Fang, Q., Fang, J., Zhuang, J., and Huang, Z. (2013). "Effects of ethanol–diesel–biodiesel blends on combustion and emissions in premixed low temperature combustion." Applied Thermal Engineering, 54:541-548.

FIRE v2011 Manuals, 2011, Graz, Austria, AVL LIST GmbH.

Furey, R. L. (1985). "Volatility characteristics of gasoline-alcohol and gasoline-ether fuel blends" (No. 852116). SAE Technical Paper.

Fraioli, V., Mancaruso, E., Migliaccio, M., and Vaglieco, B.M. (2014). "Ethanol effect as premixed fuel in dual-fuel CI engines: Experimental and numerical investigations." Appl Energy, 119: 394-404.

Ghazikhani, M., Feyz, M. E., and Joharchi, A. (2010). "Experimental investigation of the exhaust gas recirculation effects on irreversibility and brake specific fuel consumption of indirect injection diesel engines." Applied Thermal Engineering, 30(13): 1711-1718.

Han, X., Yang, Z., Wang, M., Tjong, J., and Zheng, M. (2016). "Clean combustion of n-butanol as a next generation biofuel for diesel engines." Applied Energy.

Han, Z., Uludogan, A., Hampson, G.J. and Reitz, R.D. (1966). "Mechanism of soot and NOx emission reduction using multiple-injection in a diesel engine" SAE Technical Paper (No. 960633).

Hansen, A.C., Taylor, A.B., Lyne, P.W.L., and Meiring, P. (1989). "Heat release in the compression-ignition combustion of ethanol." Transactions of the ASAE 32(5):1507-1511.

Heat Release in Diesel Combustion", SAE Technical Paper 980184, 1998.

Heywood, J. B. (1988) Internal combustion engine fundamentals (Vol. 930). New York.

Huang, H., Liu, Q., Yang, R., Zhu, T., Zhao, R., and Wang, Y. (2015). "Investigation on the effects of pilot injection on low temperature combustion in high-speed diesel engine fueled with n-butanol–diesel blends." Energy Conversion and Management, 106: 748-758.

Hulwan, D. B. and Joshi, S.V. (2011). "Performance, emission and combustion characteristic of a multicylinder DI diesel engine running on diesel–ethanol–biodiesel blends of high ethanol content." Applied Energy; 88: 5042-5055.

Imtenan, S., Varman, M., Masjuki, H. H., Kalam, M. A., Sajjad, H., Arbab, M. I. and Rizwanul Fattah, I. M. (2014). "Impact of low temperature combustion attaining strategies on diesel engine emissions for diesel and biodiesels: A review." Energy Conversion and Management, 80:329-356.

Isık M. Z., Bayındır, H., İscan, B., and Aydın, H. (2016). The effect of n-butanol additive on low load combustion, performance and emissions of biodiesel-diesel blend in a heavy duty diesel power generator. Journal of the Energy Institute.

Jeon, J., Kwon, S.I.I., Park, Y.H., Oh, Y., and Park, S. (2014). "Visualizations of combustion and fuel/air mixture formation processes in a single cylinder engine fueled with DME." Appl Energy, 113:294–301.

Jin, C., Yao, M., Liu, H., Chia-fon, F. L., and Ji, J. (2011). "Progress in the production and application of n-butanol as a biofuel." Renewable and Sustainable Energy Reviews, 15(8): 4080-4106.

Kaimal, V. K., and Vijayabalan, P. (2015). "A detailed study of combustion characteristics of a DI diesel engine using waste plastic oil and its blends." Energy conversion and Management, 105, 951-956.

Kapus, P., and Ofner, H. (1995). "Development of fuel injection equipment and combustion system for DI diesels operated on dimethyl ether (No. 950062).' SAE Technical Paper.

Kim, H. J., Park, S. H., Lee, K. S., and Lee, C. S. (2011). "A study of spray strategies on improvement of engine performance and emissions reduction characteristics in a DME fueled diesel engine." Energy, 36(3):1802-1813.

Kim, H., and Choi, B. (2008). "Effect of ethanol–diesel blend fuels on emission and particle size distribution in a common-rail direct injection diesel engine with warm-up catalytic converter." Renewable Energy, 33:2222–2228.

Kim, M.Y., Yoon, S.H., Ryu, B.W., and Lee, C.S. (2008). "Combustion and emission characteristics of DME as an alternative fuel for compression ignition engines with a high pressure injection system." Fuel 87(12): 2779–2786.

Kumar Agrawal, A., Singh, S. K., Sinha, S. and Shukla, M. K. (2004). "Effect of EGR on the exhaust gas temperature and exhaust opacity in compression ignition engines." Sadhana, 29(3):275-284.

Kumar, B. R., and Saravanan, S. (2016). "Use of higher alcohol biofuels in diesel engines: a review." Renewable and Sustainable Energy Reviews, 60:84-115.

Kumar, S., Prakash, R., Murugan, S. and Singh, R.K. (2013). "Performance and emission analysis of blends of waste plastic oil obtained by catalytic pyrolysis of waste HDPE with diesel in a CI engine." Energy Conversion and Management, 74:323-331.

Kuo KK. Principles of combustion, Wiley India1986.

Labeckas, G., Slavinskas, S. and Mazeika, M., (2014). "The effect of ethanol–diesel–biodiesel blends on combustion, performance and emissions of a direct injection diesel engine." Energy Conversion and Management, 79: 698-720.

Ladommatos, N., Abdelhalim, S., Zhao, H., and Hu, Z., (1997). "The Dilution, Chemical, and Thermal Effects of Exhaust Gas Recirculation on Disesel Engine Emissions - Part 4: Effects of Carbon Dioxide and Water Vapour", SAE Technical Paper 971660.

Ladommatos, N., Balian, R., Horrocks, R., and Cooper, L., (1996). "The Effect of Exhaust Gas Recirculation on Combustion and NOx Emissions in a High-Speed Direct-injection Diesel Engine." SAE Technical Paper 960840.

Lakshminarayanan, P. A. and Aghav, Y. V. (2010). "Modelling diesel combustion." Springer.

Lapuerta, M., Armas, O., and Herreros, J. M. (2008). Emissions from a diesel–bioethanol blend in an automotive diesel engine. Fuel, 87(1): 25-31.

Lettieri, P., and Al-Salem, S. (2011). "Thermochemical treatment of plastic solid waste. In: Letcher TM, Vallero D, editors. Waste: A handbook for management." p. 233–42.

Lee, S., Yoshida, K. and Yoshikawa, K. (2015). "Application of waste plastic pyrolysis oil in a direct injection diesel engine: for a small scale non-grid electrification." Energy and Environment Research, 5(1), 18.

Li, D.G., Zhen, H., Xingcai, L., Wu-gao, Z., and Jian-Guang, Y. (2005). "Physico-chemical properties of ethanol–diesel blend fuel and its effect on performance and emissions of diesel engines." Renewable energy, 30:967-976.

Liu, H., Wang, G., Zhang, J. (2013). The Promising Fuel: Biobutanol, INTECH, Ch. 6, p. 175–98.

Mani, M., and Nagarajan, G. (2009). "Influence of injection timing on performance, emission and combustion characteristics of a DI diesel engine running on waste plastic oil." Energy, 34(10):1617–23.

Mani, M., Nagarajan, G. and Sampath, S. (2010). "An experimental investigation on a DI diesel engine using waste plastic oil with exhaust gas recirculation." Fuel, 89 (8):1826-32.

Mattarelli, E., Bianchi, G., and Ivaldi, D. (2000). "Experimental and Numerical Investigation on the EGR System of a New Automotive Diesel Engine", SAE Technical Paper 2000-01-0224.

Mendez, S., and Thirouard, B. (2009). "Using Multiple Injection Strategies in Diesel Combustion: Potential to Improve Emissions, Noise and Fuel Economy Trade- Off in Low CR Engines", SAE Int. J. Fuels Lubr., 1(1):662-674.

Miandad, R., Barakat, M.A., Aburiazaiza, A.S., Rehan, M., Ismail, I.M., and Nizami, A.S. (2016). "Effect of plastic waste types on pyrolysis liquid oil." International Bio deterioration & Biodegradation. 2016 Oct 10.

Mills G. A. (1994). "Status and future opportunities for conversion of synthesis gas to liquid fuels" Fuel, 73:1243-1279.

Minami, T., Takeuchi, K., and Shimazaki, N., (1995). "Reduction of Diesel Engine NOx Using Pilot Injection", SAE Technical Paper 950611.

Mobasheri, R., Peng, Z. and Mirsalim, S.M. (2012). "Analysis the effect of advanced injection strategies on engine performance and pollutant emissions in a heavy duty DI-diesel engine by CFD modeling." International Journal of Heat and Fluid Flow, 33: 59-69.

Naber, J. and Reitz, R., (1988). "Modeling Engine Spray/Wall Impingement", SAE Technical Paper 880107.

Palash, S. M., Masjuki, H. H., Kalam, M. A., Masum, B. M., Sanjid, A. and Abedin, M. J. (2013). "State of the art of NOx mitigation technologies and their effect on the performance and emission characteristics of biodiesel-fueled Compression Ignition engines." Energy conversion and management, 76: 400-420.

Park, S. H., and Lee, C. S. (2013). "Combustion performance and emission reduction characteristics of automotive DME engine system." Progress in Energy and Combustion Science, 39(1):147-168.

Park, S. H., and Lee, C. S. (2014). "Applicability of dimethyl ether (DME) in a compression ignition engine as an alternative fuel." Energy Conversion and Management, 86:848-863.

Park, S. H., and Yoon, S. H. (2015). "Injection strategy for simultaneous reduction of NO x and soot emissions using two-stage injection in DME fueled engine." Applied Energy, 143:262-270.

Park, S. H., Kim, H. J., and Lee, C. S. (2010). "Effects of dimethyl-ether (DME) spray behavior in the cylinder on the combustion and exhaust emissions characteristics of a high speed diesel engine." Fuel Processing Technology, 91(5):504-513.

Petranovic, Z., Vujanovic, M., and Duic, N. (2014). "Towards a More Sustainable Transport Sector by Numerically Simulating Fuel Spray and Pollutant Formation in Diesel Engines." Journal of Cleaner Production, 88:272-279.

Popovac, M., and Hanjalic, K. (2005). "Compound wall treatment for RANS computation of complex turbulent flows", Proceedings of third MIT conference on computational fluid and solid mechanics, vol 1. Elsevier, Amsterdam, pp.802–806.

Pundir, B. P. (2007). "Engine Emissions–Pollutant formation and advancement in control technology."

Putrasari, Y., Jamsran, N., and Lim, O. (2017). "An investigation on the DME HCCI autoignition under EGR and boosted operation." Fuel, 200:447-457.

Qi, D., Leick, M., Liu, Y., and Chia-fon, F.L. (2011). "Effect of EGR and injection timing on combustion and emission characteristics of split injection strategy DI-diesel engine fuelled with biodiesel." Fuel, 90:1884-1891.

Rakopoulos, D.C., Rakopoulos, C.D., Giakoumis, E.G., Dimaratos, A.M., and Kyritsis, D.C. (2010). "Effects of butanol–diesel fuel blends on the performance and emissions of a high-speed DI diesel engine." Energy Conversion and Management, 51(10):1989-1997.

Rakopoulos, D.C., Rakopoulos, C.D., Hountalas, D.T., Kakaras, E.C., Giakoumis, E.G. and Papagiannakis, R. G. (2010). "Investigation of the performance and emissions of bus engine operating on butanol/diesel fuel blends." Fuel, 2010; 89(10): 2781-2790.

Rakopoulos, D.C., Rakopoulos, C.D., Kakaras, E.C., and Giakoumis, E.G. (2008). "Effects of ethanol–diesel fuel blends on the performance and exhaust emissions of heavy duty DI diesel engine." Energy Conversion and Management, 49:3155-3162.

Rakopoulos, D.C., Rakopoulos, C.D., Papagiannakis, R.G., and Kyritsis, D.C. (2011). "Combustion heat release analysis of ethanol or n-butanol diesel fuel blends in heavy-duty DI diesel engine." Fuel 90(5):1855-1867.

Ramos, J. I., Internal combustion Engine Modeling, Hemisphere Publishing

Reitz, R. D. (1987). "Modeling Atomization Processes in High-Pressure Vaporizing Sprays", Atomization and Spray Technology, Vol. 3: 309-337.

Ricaud, J.C., and Lavoisier, F. (2002). "Optimizing the Multiple Injection Settings on an HSDI Diesel Engine", THIESEL 2002 conference.

Sarathy, S.M., Thomson, M.J., Togbe, C., Dagaut, P., Halter, F. and Mounaim-Rousselle, C. (2009). "An experimental and kinetic modeling study of n-butanol combustion." Combustion and Flame, 156(4): 852-864.

Sarker, M., Rashid, M. M., and Molla, M. (2011). "Waste Plastic Conversion into Hydrocarbon Fuel Materials." Journal of Environmental Science and Engineering, 5(5) : 1-8.

Sayin, C., Uslu, K., Canakci, M. (2008) "Influence of injection timing on the exhaust emissions of a dual-fuel CI engine." Renewable Energy 33(6): 1314-1323.

Sayin, C. (2010) "Engine performance and exhaust gas emissions of methanol and ethanol–diesel blends." Fuel 89(11):3410-3415.

Schobert HH (2013) The chemistry of hydrocarbon fuels. Butterworth-Heinemann.

Scott, D.S., Czernik, S.R., Piskorz, J, Radlein, DSAG. (1990). "Fast pyrolysis of plastic wastes." Energy Fuels, 4(4):407-11.

Sorenson, S. C., Glensvig, M., and Abata, D. L. (1998). Dimethyl ether in diesel fuel injection systems (No. 981159). SAE Technical Paper.

Szwaja, S. and Naber, J.D. (2010). "Combustion of n-butanol in a spark-ignition IC engine." Fuel, 89:1573-82.

Tatschl, R., (2012). "3D-CFD Simulation of IC-Engine Flow, Mixture Formation and Combustion with AVL FIRE", Combustion Engines Development, Springer Berlin Heidelberg. p. 601-630.

Teng, H., McCandless, J.C., and Schneyer, J.B. (2001). "Thermo-chemical characteristics of di-methyl ether – an alternative fuel for compression-ignition engines." SAE Paper 2001-01-0154, SAE Trans J Fuel Lubr, 110(4):96–106.

Thompson, R.C., Swan, S.H., Moore, C.J., and Saal, F.S.V. (2009). "Our plastic age." Philos Trans R Soc B, 364(1526):1973–6.

Tier, I. (2015). "California Dimethyl Ether Multimedia Evaluation." (https://www.arb.ca.gov/fuels/multimedia/meetings/DMETierIReport_Feb2015.pdf).

Ucar, S., Karagoz, S., Yanik, J., Saglam, M. and Yuksel, M. (2005). "Co-pyrolysis of scrap tires with waste lubricant oil." Fuel Process Technol, 87(1):53-8.

Verbeek, R.P., Van, D.A. and Van, W.M. (1996). "Global assessment of di-methyl ether as an automotive fuel." Second ed.,96.OR.VM.029.1/RV, TNO Road-Vehicles Research Institute.

Vujanovi, M., Dui, N., and Tatschl, R. (2009). "Validation of reduced mechanisms for nitrogen chemistry in numerical simulation of a turbulent non-premixed flame." React. Kinetics Catal. Lett., 96:125-138. doi: 10.1007/s11144-009-5463-2

Wallner, T., Miers, S. A., and McConnell, S. (2009). "A comparison of ethanol and butanol as oxygenates using a direct-injection, spark-ignition engine." Journal of Engineering for Gas Tur

Wu, J,, Song Ki, H., Litzinger, T., Lee, S.Y., Santoro, R., Linevsky, M., Colket, M., and Liscinsky, D. (2006). "Reduction of PAH and soot in premixed ethylene–air flames by addition of ethanol." Combustion and flame, 144:675-687.

Yamamoto, T., Yasuhara, A., Shiraishi, H. and Nakasugi, O.,Bisphenol. (2001). "A, in hazardous waste landfill leachates" Chemosphere; 42(4):415-8.

Yilmaz, N., and Vigil, F.M. (2014). "Potential use of a blend of diesel, biodiesel, alcohols and vegetable oil in compression ignition engines." Fuel, 124:168-172.

Yilmaz, N., Vigil, F.M., Burl, Donaldson, A., and Darabseh, T. (2014). "Investigation of CI engine emissions in biodiesel–ethanol–diesel blends as a function of ethanol concentration." Fuel, 115:790-793.

Ying, W., and Longbao, Z. (2008). "Experimental study on exhaust emissions from a multi-cylinder DME engine operating with EGR and oxidation catalyst." Appl Therm Eng, 28:1589–1595.

Ying, W., Longbao, Z., and Wei, L. (2010). "Effects of DME Pilot Quantity on the Performance of a DME PCCI-DI Engine." Energy Conversion and Management, 51(4): 648-654.

Yoon, S. H., Cha, J. P., and Lee, C. S. (2010). "An investigation of the effects of spray angle and injection strategy on dimethyl ether (DME) combustion and exhaust emission characteristics in a common-rail diesel engine." Fuel Processing Technology, 91(11): 1364-1372.

Youn, I. M., Park, S. H., Roh, H. G., and Lee, C. S. (2011). "Investigation on the fuel spray and emission reduction characteristics for dimethyl ether (DME) fueled multi-cylinder diesel engine with common-rail injection system." Fuel processing technology, 92(7):1280-1287.

Yu, J., and Bae, C. (2003). "Dimethyl ether (DME) spray characteristics compared to diesel in a common-rail fuel injection system." J Autom Eng Proc IMechE Pt D, 217:1135–44.

Yun, H., Choi, K., and Lee, C. S. (2016). "Effects of biobutanol and biobutanol–diesel blends on combustion and emission characteristics in a passenger car diesel engine with pilot injection strategies." Energy Conversion and Management, 111: 79-88.

Zabed, H., Sahu, J. N., Suely, A., Boyce, A. N., and Faruq, G. (2017). "Bioethanol production from renewable sources: Current perspectives and technological progress." Renewable and Sustainable Energy Reviews.

Zhang, L., (1999). "A Study of Pilot Injection in a DI Diesel Engine", SAE Technical Paper 1999-01-3493.

Zhao, Y., Wang, Y., Li, D., Lei, X., and Liu, S. (2014). "Combustion and emission characteristics of a DME (dimethyl ether)-diesel dual fuel premixed charge compression ignition engine with EGR (exhaust gas recirculation)." Energy, 72:608-617.

Zheng, Z., Li, C., Liu, H., Zhang, Y., Zhong, X., and Yao, M. (2015). "Experimental study on diesel conventional and low temperature combustion by fueling four isomers of butanol." Fuel, 141: 109-119.

Zhou, C., Fang, W., Xu, W., Cao, A., and Wang, R. (2014). "Characteristics and the recovery potential of plastic wastes obtained from landfill mining", 80:80–6.

Zhu, L., Cheung, C.S., Zhang, W, G. and Zhen, H. (2011). "Combustion, performance and emission characteristics of a DI diesel engine fueled with ethanol-biodiesel blends." Fuel, 90:1743-1750.

Zhu, Y., Chen, Z., and Liu, J. (2014). Emission, efficiency, and influence in a diesel n-butanol dual-injection engine. Energy conversion and management, 87, 385-391.

LIST OF PUBLICATIONS BASED ON RESEARCH WORK

International Journals

1. **Venkatesh T. Lamani**, Ajay Kumar Yadav, Kumar G.N, Influence of low temperature combustion and dimethyl ether-diesel blends on performance, combustion and emission characteristics of common rail diesel engine, Environmental Science and Pollution Research (2017) Volume 24, Issue 18, pp 15500–15509. DOI: 10.1007/s11356-017-9113-3 - **Springer**.

2. **Venkatesh T. Lamani**, Ajay Kumar Yadav, Kumar G.N, Performance, emission and combustion characteristics of twin cylinder common rail diesel engine fuelled with butanol-diesel blends, Environmental Science and Pollution Research (2017) Volume 24, Issue 29, pp 23351–23362. DOI: 10.1007/s11356-017-9956-7- **Springer.**

3. **Venkatesh T. Lamani**, Ajay Kumar Yadav, Kumar G.N, Combustion, performance and tail pipe emissions of common rail diesel engine fuelled with waste plastic oil-diesel blends, journal of thermal science and engineering applications, **ASME (Accepted**).

4. **Venkatesh T. Lamani**, Aditya U. Baliga M, Ajay Kumar Yadav, G. N. Kumar, Effect of bioethanol-diesel blends, exhaust gas recirculation rate and injection timing on performance, emission and combustion characteristics of common rail diesel engine, Biofuels, DOI: 10.1080/17597269.2017.1329493,**Taylor and Francis.**

5. **Venkatesh T. Lamani**, Ajay Kumar Yadav, G. N. Kumar, Effect of exhaust gas recirculation rate on performance, emission and combustion characteristics of common rail diesel engine fuelled with n-butanol-diesel blends, Biofuels, http://dx.doi.org/10.1080/17597269.2017.1369631. **Taylor and Francis.**

6. **Venkatesh T. Lamani**, Adithya U. Baliga M, Ajay Kumar Yadav, Kumar G.N, Optimum injection timings for bioethanol - diesel blends and its effect on tail pipe emission in common rail diesel engine, Renewable energy focus, **Elsevier (Under**

review).

Book Chapters:

7. **Venkatesh T. Lamani**, Ajay Kumar Yadav, G. N. Kumar, Spray and Combustion Characterization in CRDI Engine- a Review, **Fire research and Engineering**, **Narosa publishing house**, ISBN: 978-81-8487-395-5, page no 451-466.

8. **Venkatesh T. Lamani**, Ajay Kumar Yadav, Kumar G.N, CFD simulation of a common rail diesel engine with biobutanol-diesel blends for various injection timings, **Springer Proceedings in Energy**, Biofuels and Bioenergy (BICE2016), ISBN:978-3-319-47255-3, 337951_1_En, (14).

CONFERENCE PAPERS BOOK CHAPTERS

International / National:

9. **Venkatesh T. Lamani**, Ajay Kumar Yadav, G. N. Kumar, Effect of exhaust gas recirculation rate and injection timing on emission and combustion characteristics of CRDI engine using biodiesel blends- a CFD approach" International Conference on Environment and Energy (ICEE - 2014) , JNTU Hyderabad , December 15th - 17th , 2014.

10. **Venkatesh T. Lamani**, Ajay Kumar Yadav, G. N. Kumar, "Effect of fuel temperature on spray characteristics - a CFD approach", 7th International Congress of Environmental Research (ICER2014), Dept. of Mechanical Engineering, R.V.College of Engineering, Bangalore, December 26th -28th , 2014.

11. **Venkatesh T. Lamani**, Ajay Kumar Yadav, G.N. Kumar, Performance and exhaust characteristics of CRDI engine operating on Dimethyl ether for various engine speed and exhaust gas recirculation rates, International Conference on Polygeneration (ICP2015), Anna University/IIT Madras, Chennai, February 18th - 20th , 2015.

12. **Venkatesh T. Lamani**, Ajay Kumar Yadav, G.N. Kumar, Effect of exhaust gas recirculation rate on a single cylinder four stroke CRDI engine using CFD

modeling, 4th International Engineering Symposium (IES2015), Kumamoto University, Japan, March 4th-6th , 2015.

13. **Venkatesh T. Lamani**, Ajay Kumar Yadav, Kumar G.N, Effect of EGR rate and diesel-DME blends on in-cylinder combustion and emissions of CRDI engine by CFD modeling, 23rdNational and 1st International ISHMT-ASTFE Heat and Mass Transfer Conference scheduled from 17th to 20th December, 2015 in Trivandrum, Kerala.

14. **Venkatesh T. Lamani**, Ajay Kumar Yadav, Kumar G.N, CFD simulation of a common rail diesel engine with biobutanol-diesel blends for various injection timings, Biofuels and Bioenergy: International conference and Exhibition, 23rd - 25th February, 2016 in MANIT, Bhopal, Madhya Pradesh.

15. **Venkatesh T. Lamani**, Adithya U Baliga M, Ajay Kumar Yadav, Kumar G.N, Effect of bioethanol-diesel blends, pilot injection timing on performance, emission and combustion characteristics of diesel engine, World congress on Engineering and applications (WCEA- 2016), 16th-17th December 2016, organized by Asian Society for Research in Engineering Sciences (ASRES) Bangkok, Thailand.

16. **Venkatesh T. Lamani**, Nuthan Prasad B.S., Archit. S. Ayodhya, Prakash Kumar Deep, Ajay Kumar Yadav, Kumar G. N., Computational investigation of n-butanol diesel blends and low temperature combustion in common rail diesel engine, International Conference on New and Renewable (ICONRER 2017), February 2nd-4th , 2017 at SKIT, Jaipur.

17. **Venkatesh T. Lamani**, Parashuram Bedar, Nuthan Prasad B.S., Archit S. Ayodhya, Prakash Kumar Deep, Ajay Kumar Yadav, Kumar G.N., Effect of n-butanol-diesel blends and injection timing on performance, emission and combustion characteristics of common rail diesel engine, International Conference on New and Renewable (ICONRER 2017), February 2nd-4th , 2017 at SKIT, Jaipur.

18. **Venkatesh T. Lamani**, Shambhu Kumar Tati, Ajay Kumar Yadav, Kumar G.N., Numerical Investigation of Effect of Intake Valve Closing Time on Common Rail Diesel Engine Fuelled with Butanol-Diesel Blends, 24th National and 2nd International ISHMT-ASTFE Heat and Mass Transfer Conference scheduled from 27th to 30th December, 2017 in BITS-Pilani, Hyderabad.*(Submitted).*

19. **Venkatesh T. Lamani**, Ajay Kumar Yadav, G.N. Kumar, Spray and combustion characterization in common rail direct injection (CRDI) engine - a review, National Conference on Fire Research and Engineering (FiRE), IIT Roorkee, India, March 01st -02nd , 2014.

20. **Venkatesh T. Lamani**, Ajay Kumar Yadav, Kumar G.N, CFD analysis on performance and exhaust characteristics of CRDI diesel engine for various engine speeds and EGR rates, 24th National conference on I.C. Engines and Combustion (NCICEC-2015), University of Petroleum and Energy Studies (UPES), Dehradun, India, India, 30th October-01st November 2015.

BIO-DATA

Name	**: VENKATESH T. LAMANI**
Date of Birth	: 10-05-1984
Residence Address	: S/o Tavareppa. G. Lamani
	: At: Katamalli Tanda, Tq: Savadatti
	: Dist: Belgaum, Karnataka, 591116.
Phone Number	: +91 - 9886898607
E-mail ID	: venkateshtlnitk@yahoo.com

Education :

Programme	Department /Specialization	Institute	University
B.E	Mechanical Engg	BEC, Bagalkot	VTU, Belgaum
M.E	Thermal Science and Engineering	UVCE, Bangalore	Bangalore University, Bangalore

Research interest

Combustion, I.C Engines, CFD, Fluid Mechanics

Soft Skills : AVL- FIRE, ANSYS, OPENFOAM

Awards And Recognition :

Best paper award received in an International Conference on Biofuels and Bio energy 2016

Reviewer for journals :

Society of Automotive Engineers (SAE), Biofuels- Taylor and Francis, Heat Transfer Research-Begell house

Publications :

International journal 08

Book Chapters: 02

Conference papers:

International/ National conference papers - 18

Memberships in professional societies:

International Association of Engineering